Rotationally Moulded Polyethylene Reinforced with Alkali Treated Hemp Fibre

A thesis

submitted in partial fulfilment

of the requirements for the degree

of

Doctor of Philosophy in Materials and Processing

at

The University of Waikato

by

MARIA OLIVEIRA

THE UNIVERSITY OF
WAIKATO
Te Whare Wānanga o Waikato

2022

Abstract

The increasing demand for rotationally moulded products highlights the necessity to develop cost-effective and sustainable materials to expand the application of such products. Natural fibres are a potential reinforcement for rotationally moulded products due to their high specific strength and stiffness. However, few attempts have been reported using natural fibres in rotational moulding. The most-reported challenges in incorporating natural fibres in this process are poor adhesion between fibre and matrix, fibre agglomeration and porosity, which require improvement. Accordingly, this research proposes methods to address these issues to increase rotationally moulded composites' tensile properties.

Initially, hemp fibres were alkali-treated to improve the fibre-matrix interface along with the coupling agent, maleic anhydride polyethylene (MAPE). The effect of alkali treatment on hemp fibre was assessed by single fibre tensile testing, X-ray diffraction, scanning electron microscopy (SEM), Fourier transform infrared spectroscopy (FT-IR) and thermogravimetric analysis (TGA).

Subsequently, materials were melt-compounded and chopped into pellets of different sizes to produce rotationally moulded composites with increased fibre length and uniform fibre distribution. The porosity within the final composites was assessed using optical microscopy, Archimedes density tests and micro-CT. To mitigate porosity within these composites, additives including mineral oil, stearic acid and recycled carbon fibre were tested. Fibre orientation in optical microscopy cross-sectional images of composites produced with pellets of aspect ratio larger than 1 were assessed using ImageJ.

The results showed that the alkali treatment removed the non-cellulosic components from hemp fibre, improving fibre separation, fibre resistance to thermal degradation, and fibre-matrix adhesion along with MAPE. In addition, composite pellets of up to 1.5 mm size were found suitable to produce rotationally moulded composites with increased fibre length and moderate porosity, with the addition of 3 wt.% of stearic acid. It was also observed that using pellets with an aspect ratio higher than 1 improved fibre orientation parallel to the composite mould wall, resulting in higher tensile properties than pure polyethylene.

Finally, the addition of recycled carbon fibre improved the melting of composite pellets of hemp-PE which reduced the void size in the final hybrid composites. This reduction in composite porosity, combined with the high stiffness of RCF, resulted in higher tensile properties with increasing RCF content. In conclusion, this research showed innovative methods and materials to produce reinforced rotationally moulded polyethylene composites with superior strength and stiffness, and moderate porosity.

Publications

Oliveira, M., Pickering, K., Sunny, T., & Lin, R. (2021). Treatment of hemp fibres for use in rotational moulding. Journal of Polymer Research, 28(2). https://doi.org/10.1007/s10965-021-02414-3

Oliveira, M. A. S., Pickering, K. L., Sunny, T., & Lin, R. J. T. (2018). Rotational Moulding of polyethylene reinforced with alkali-treated hemp fibre, in CHEMECA 2018. Conference held Queenstown, New Zealand.

Acknowledgements

My gratitude to my Chief Supervisor, Professor Kim Pickering, for giving me this opportunity, sharing her knowledge and guiding me during my research.

My thanks to my co-supervisor, Dr Richard Lin for his support.

My special thanks to Dr Christian Gauss for supporting my work and encouraging me to complete this PhD.

My deepest gratitude for the support of my friends: Safiya, Anuradha, Felipe, Eduardo, Mary, Zac, Mafalda, Silke, Mariana and Wagner. Your friendship made this journey brighter.

My love and appreciation to my family who endured my absence from their lives during all these years.

My appreciation to the composite research group at University of Waikato, especially Tom Sunny, Tim Ng and John McDonald, for their constant encouragement and contributions to my studies.

I would like to thank all the great professionals at the University of Waikato who helped me complete my research: Anne Ferrier-Watson, Cheryl Ward, Duncan Barnard, Jonathan Van Harselaar, Mary Dalbeth, Natalie Shaw, Andrea Haines and Dr. Chloe Wall.

My appreciation to Judy MacDonald for proof-reading this thesis.

My deep appreciation goes to my previous colleagues and always friends from the chemical division (AQI) of DCTA in Brazil, who inspired me to pursue a PhD.

Last but not least, I would also like to thank all the brave women who have inspired me to become who I am, starting with my sister Elaine.

“It’s your road, and yours alone; others may walk it with you, but no one can walk it for you.”

Rumi

Table of Contents

List of Tables

List of Figures

Abbreviations and Symbols

ASTM: American Society for Testing and Materials

CBD: Cannabidiol

CFRC: Carbon Fibre Reinforced Composite

DTG: Differential Thermal Gravimetry

DSF: Dynamic Sheet Forming

FT-IR: Fourier Transform Infrared Spectroscopy

HF: Hemp Fibre

HNO_3: Nitric Acid

IFSS: Interfacial Shear Strength

MO: Mineral Oil

MAPE: Maleic Anhydride Polyethylene

MFI: Melt Flow Index

NaOH: Sodium Hydroxide

Na_2SO_3: Sodium Sulphite

NF: Natural Fibre

NFC: Natural Fibre Composite

PE: Polyethylene

PIAT: Peak Internal Air Temperature

PAN: Polyacrylonitrile

RCF: Recycled Carbon Fibre

SEM: Scanning Electron Microscopy

SA: Stearic Acid

THC: Tetrahydrocannabinol

TGA: Thermogravimetric Analysis

TTS: Transversal Tensile Strength

LTS: Longitudinal Tensile Strength

XRD: X-ray Diffraction

σf: Fibre's Tensile Strength

τ: Interfacial Shear Strength

Chapter 1
Introduction

Rotational moulding is used to manufacture hollow or double-walled plastic products without external pressure. The main advantages of this process are the low cost of moulds and the flexibility of product sizes and thicknesses [1; 2]. Nowadays, the most typical applications of rotationally moulded products include chemical tanks, playground equipment and leisure boats [2, 5].

The rotational moulding industry has advanced in the past decade with new machines, moulds and materials. However, polyethylene (PE) is still the most used polymer in the rotational moulding industry due to its advantages: low melting point, low cost and good thermal stability [3; 4]. Despite its advantages, polyethylene has a low Young`s modulus and strength, which prevent its use in many applications.

Therefore, reinforcements such as natural and synthetic fibres have been suggested to modify the physical and mechanical properties of rotationally moulded products, thus expanding the application of this process [5]. This research suggested industrial hemp fibre as a reinforcement for rotationally moulded products due to its high specific Young's modulus, tensile strength and local availability in New Zealand [2; 6]. Other advantages of fibres are low cost, low density, CO_2 neutrality, and good mechanical and recyclable properties [7; 8]. This is because thermoplastic composites reinforced with natural fibre can be recycled several times, with slightly reduced strength and stiffness [9].

However, natural fibres have a hydrophilic nature, which results in poor interfacial bonding with non-polar thermoplastic matrices such as polyethylene. A high interfacial bond is required for efficient stress transfer from the matrix to the fibres, thus increasing the tensile properties of the material [2; 10]. Previous approaches, including chemical, physical and biological treatments and the use of coupling agents, have aimed to improve interfacial bonding in polymer-natural fibre composites [11; 12]. Among the available chemical treatments, alkali has been reported as the most efficient method to remove amorphous components from lignocellulosic fibres. The removal of these materials improves fibre separation and exposes hydroxyl (OH) groups on the crystalline cellulose on the fibre surface for improved interfacial strength with the matrix [12-14]. These cellulose OH groups can react with coupling agents such as maleic anhydride via covalent or hydrogen bonds, while

the polyethylene chain on MAPE entangles with the polyethylene matrix, thus improving the bonding between fibre and matrix [15-18].

Other common issues reported with the addition of natural fibres in rotational moulding are fibre agglomeration and reduction of polymer processability, due to the absence of external pressure and the low-speed rotation applied in this process. The combination of those factors results in an increase in porosity in the final composites and consequently reduces tensile properties [19-21].

Melt compounding of materials before processing is reported to prevent fibre agglomeration and phase segregation [22]. This method is usually followed by a grinding step to convert the material into fine particles of about 500 μm in size, which are considered ideal for producing void-free products by rotational moulding [2]. This additional step in the process leads to a significant reduction in fibre length and adds an extra cost.

Alternatively, using large composite pellets in rotational moulding would reduce processing cost and maintain fibre length, thus obtaining maximum reinforcement from it [17]. This is because the load is transferred from the matrix to the fibre by shear at the fibre/matrix interface, whereas tensile stress is zero at the fibre's end and increases along the length of the fibre [23].

However, the use of large particles in rotational moulding results in high porosity within composites. The most common method used by the rotational moulding industry to minimize porosity is increased processing time. However, this method is detrimental to mechanical properties due to polymer thermal degradation, which reduces tensile strength [24; 25]. Additionally, this method results in longer cycle times, reducing process efficiency [26]. Alternatively, previous studies have reported positive results on reducing porosity in rotationally moulded composites by using low molecular weight additives to improve polymer flow [27; 28].

This innovative research proposes methods to address to address the main factors that affect the mechanical properties of natural fibre-reinforced composites, such as fibre-matrix interface, fibre dispersion, orientation, aspect ratio and porosity. The aim of these improvements is to produce hemp fibre reinforced rotationally moulded polyethylene composites with enhanced strength and stiffness compared to neat polyethylene.

1.1 Research Objectives

The overall aim of this thesis was to improve the stiffness and strength of rotationally moulded polyethylene composites using alkali-treated hemp fibre as reinforcement. The primary objectives of this thesis were to:

1. Evaluate the benefits of pre-treating hemp fibre to improve fibre separation and fibre-matrix adhesion in rotationally moulded composites.
2. Assess the potential of using composite pellets to produce rotationally moulded composites with increased fibre length.
3. Evaluate the performance of low molecular weight additives to reduce porosity in rotationally moulded composites.
4. Assess the effect of the aspect ratio of composite pellets to improve fibre orientation in rotationally moulded composites.
5. Assess the benefit of the hybridisation of hemp-PE composites with recycled carbon fibre to produce rotationally moulded composites with low porosity and superior tensile properties.

1.2 Thesis Organisation

Chapter 1: gives an introduction to the research topic developed in this thesis.

Chapter 2: provides a literature review of all the topics discussed in this research.

Chapter 3: assesses the benefit of using alkali-treated hemp fibres and MAPE to improve fibre-matrix bonding in rotationally moulded composites.

Chapter 4: reports on the potential use of large composite pellets to produce rotationally moulded composites with increased fibre length and mitigated porosity.

Chapter 5: reports on the fibre orientation assessment in rotationally moulded composites produced with pellets of composites with an aspect ratio larger than 1.

Chapter 6: describes the benefits of using recycled carbon fibre along with hemp fibre in rotational moulding to produce hybrid composites.

Chapter 7: provides the main conclusions of each chapter and correlates them.

Chapter 8: presents recommendations for future work based on the findings of this research.

Chapter 2

Literature Review

2.1 Natural Fibres

Natural fibres can be derived from either mineral, animal or plant sources. However, cellulose fibres tend to have higher tensile properties than those derived from animal sources and are more suitable for composite materials. Lignocellulose fibres are grouped into three different types: seed/hair, bast and leaf fibres. Some examples are cotton (seed and hair); jute, flax, hemp and kenaf (bast fibres); and sisal (leaf fibres). Bast fibres exhibit superior flexural strength and modulus of elasticity, whereas leaf fibres show superior impact properties [29].

2.2 Chemical Composition of Natural Fibres

The chemical components of lignocellulosic fibres are cellulose, hemicellulose, lignin and pectin; each of these components contributes to the overall properties of the fibre. The structure of a lignocellulose fibre and a brief description of each of its components are provided below.

2.2.1 Cellulose

Cellulose is the primary component in lignocellulosic fibres and it provides fibre strength, stiffness and structural stability [10] . The chemical structure of cellulose consists of a linear polymer of D-anhydroglucose units joined by ß-1,4-glycosidic linkages and many hydroxyl groups (OH), as shown in Figure 2-1.

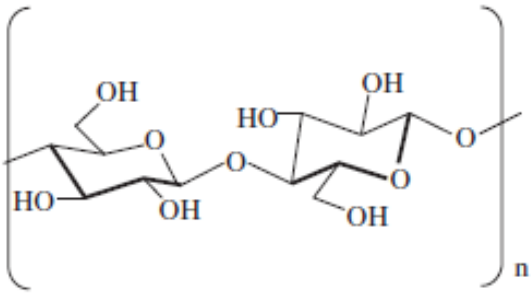

Figure 2-1: Chemical structure of cellulose [10].

Cellulose may be either crystalline or amorphous (non-crystalline), as shown in Figure 2-2. The amorphous cellulose regions have fewer interchain hydrogen bonds and chains, with a relatively large specific volume, which makes reactive hydroxyl groups (OH) more exposed for bonding with water molecules. In contrast, chains are closely packed and strongly hydrogen bonded to each other in the crystalline cellulose region, and therefore far less hydrophilic than amorphous cellulose.

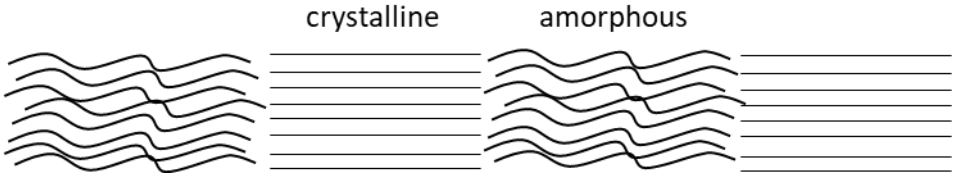

Figure 2-2: Schematic representation of the crystalline structure of cellulose. Source: adapted from [30].

Each fibre cell wall consists of a primary and secondary layer of cellulose microfibrils (Figure 2-3). At a nanoscale, microfibrils consist of cellulose chains (crystalline zones) embedded in a matrix of polysaccharides mainly comprised of pectin and hemicellulose. Crystalline microfibrils consist of tightly packed cellulose chains with accessible hydroxyl groups present on the surface of the structure, as shown in Figure 2-4.

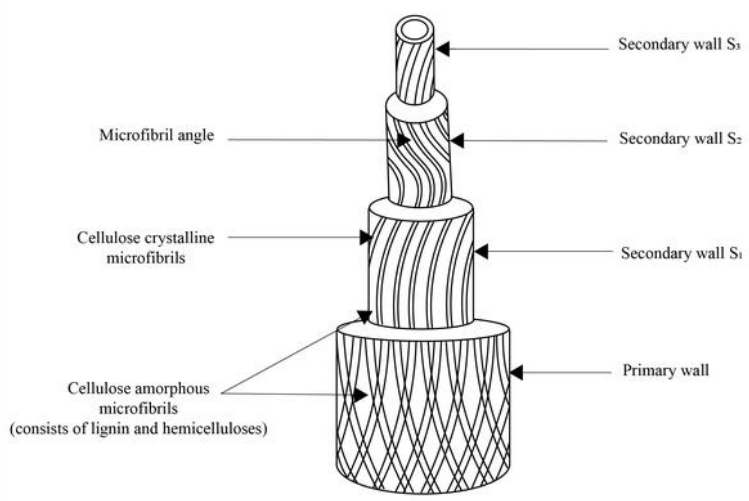

Figure 2-3: Structure of natural fibre. Source: adapted from [10] .

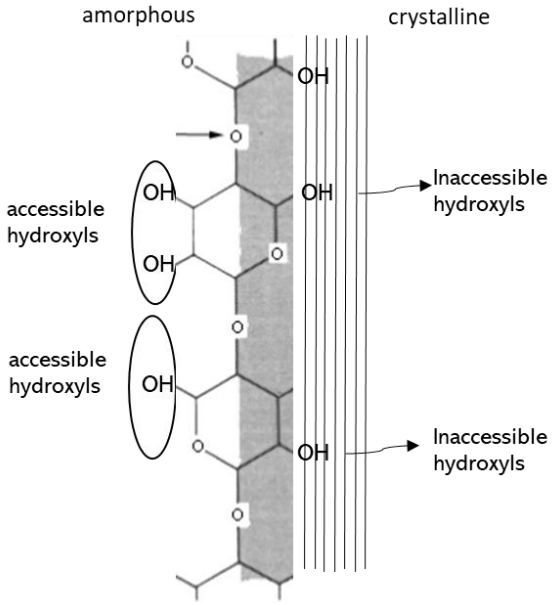

Figure 2-4: Microfibril surface. Source: adapted from [31].

2.2.2 Hemicellulose

Hemicellulose consists of a group of polysaccharides, which contain several different sugar units as shown in Figure 2-5; In comparison with cellulose, hemicellulose exhibits an amorphous structure, a considerable degree of chain branching and a lower degree of polymerisation [32].

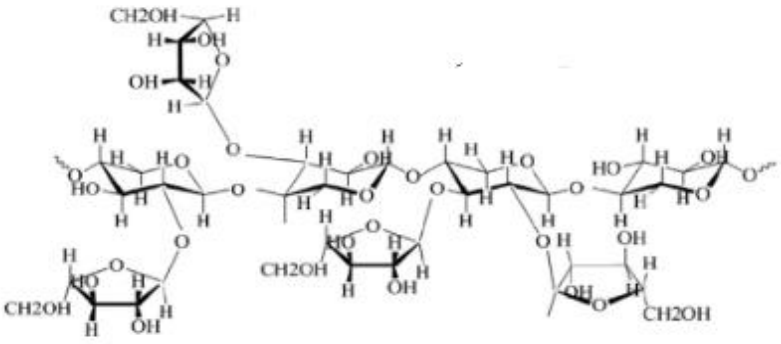

Figure 2-5: Chemical structure of hemicellulose [33].

2.2.3 Lignin

Lignin is the encrusting substance gluing the fibre cells together and providing rigidity to the cell wall. It is amorphous, with an aromatic structure, as shown in Figure 2-6.

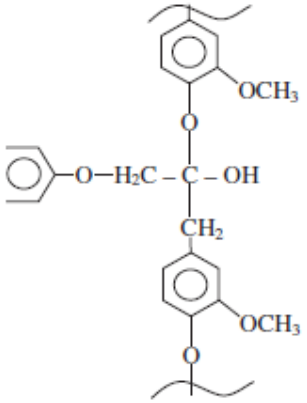

Figure 2-6: Chemical structure of lignin [10] .

Pectin is comprised of complex polysaccharides whose side chains are cross-linked with calcium ions and arabinose sugars [10].

2.3 Industrial Hemp Fibre

Hemp is native to central Asia and has been grown for more than 12,000 years [34]. Hemp is the common name for plants belonging to the genus *Cannabis, species sativa.* Industrial hemp fibre (*Cannabis sativa subsp. Sativa L*) differs from recreational cannabis (*C. sativa)* as it has low levels of DELTA9-tetrahydrocannabinol (THC) (about 0.6%) and higher levels of cannabidiol (CBD) [35]. Industrial hemp has been largely used in textile, paper, biofuel, automotive industry and building applications [36]. Indeed, hemp fibre has great potential to be used as reinforcement for plastic materials due to its high specific strength and stiffness, light weight and carbon storage capacity. The main drawback of natural fibres is the variability in composition from plant to plant. This means that the relative amount of hemp fibre principal constituents, such as cellulose, hemicellulose, lignin, and pectin, may vary from one fibre to another. As a result, the physical and mechanical properties of the fibre depend on factors such as source, age, retting, separating techniques, geographic origin, rainfall during growth and constituent content [34]. Figure 2-7 shows a hemp crop, leaves and stem. Fibres from the stem are used as reinforcement for thermoplastics.

2.4 Natural Fibre Reinforced Composites

Nowadays, glass fibre is the most commonly used synthetic fibre for the manufacturing of composites due to its relatively low cost and high strength. However, inhaling fibre glass particles can cause irritation and potentially a life-threatening condition. In addition to the health risks, its brittle nature can cause fibre length reductions during processing, leading to lower mechanical properties. Recent environmental concerns have increased research and applications for natural reinforced composites as a sustainable alternative to their synthetic fibre counterparts. Cellulosic-based fibres are durable enough to withstand the shear forces involved in reprocessing. This means composites can be recycled several times without significant reductions in strength and stiffness [37; 38]. Table 2-1 shows the advantages of natural fibres in comparison with glass fibre.

Table 2-1: Comparison of natural and glass fibre` properties [39].

Properties	***Natural fibres***	***Glass fibre***
Density	Low	Twice that of natural fibre
Cost	Low	Higher than natural fibre
Renewability	Yes	No
Recyclability	Yes	No
Energy Consumption	Low	High
CO_2 neutral	Yes	No
Abrasion to machines	No	Yes
Health risk when inhaled	No	Yes
Disposal	Biodegradable	Not Biodegradable

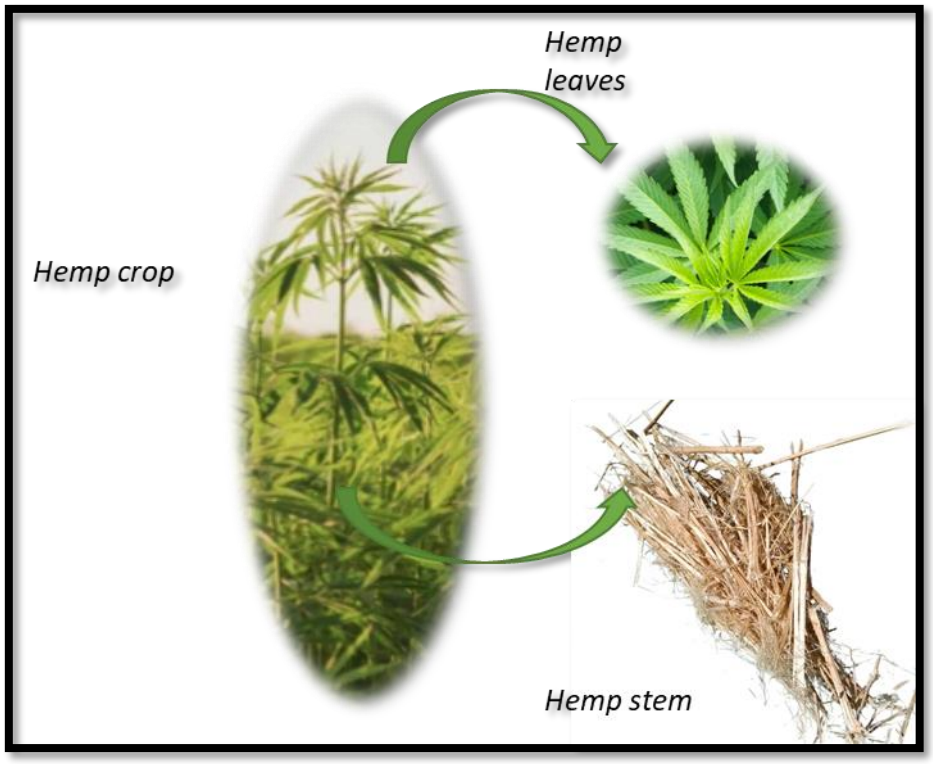

Figure 2-7: Hemp crop, leaves and stem. Source: Author.

2.5 Factors Influencing the Performance of Natural Fibre Composites

2.5.1 Thermal Stability

Natural fibres are not thermally stable and tend to degrade at 240 °C due to their lignocellulosic components [40]. For this reason, only thermoplastics with a low melting point, such as polyethylene, polypropylene, polyvinyl chloride, polystyrene and PLA, are used as a matrix for natural fibre composites [41]. However, these thermoplastics are the most consumed in the plastics industry.

2.5.2 Fibre Dispersion

Natural fibres tend to agglomerate during mixing with polymer due to their hydrogen bonds (fibre-fibre interactions) and fibre length. It is known that good fibre dispersion promotes interfacial bonding by ensuring that fibres are completely wetted by the matrix [6]. Therefore, poor fibre dispersion leads to poor mechanical properties in composite materials. For this reason, chemical approaches, such as coupling agents and stearic acid, have been applied to improve the fibre dispersion in the matrix. Stearic acid improves fibre dispersion by reducing the fibre-fibre interaction, whereas coupling agents increase fibre/matrix compatibility and thus improve fibre dispersion [42].

2.5.3 Fibre Orientation

Fibre orientation is another important parameter that influences the mechanical properties of fibre-reinforced composites. The best composite performance is obtained when the fibres are aligned parallel to the direction of the applied load [6]. Complex fibre orientation changes occur during polymer processing such as extrusion, compounding, and injection moulding. This behaviour depends on factors such as size and fibre concentration, the viscoelastic properties of the polymer matrix, mould cavity and processing conditions [43]. For example, the molten polymer is subjected to both extensional and shear flow during extrusion, leading to fibre alignment in the flow direction.

During injection moulding, the fibre and molten polymer are also subjected to complex and variable flow conditions that result in some level of fibre orientation within the final composite. Another technique for improving the fibre alignment in short-fibre thermoplastics is compression moulding. In this technique, the polymer is combined with a pre-fabricated aligned-fibre mat and consolidated at elevated temperatures and pressures in a hot press [31].

Another alternative, used by the paper industry and recently adopted by the textile industry, is Dynamic Sheet Forming (DSF). In this method, short fibres are suspended in water and sprayed through a nozzle into a rotating drum with a mesh through which water is removed. Consequently, the fibres are aligned in the direction of spraying and rotation [6].

2.5.4 Fibre Aspect Ratio

The fibre aspect ratio (length/diameter) is a critical parameter in composite materials. A critical fibre aspect ratio for a short-fibre composite system is defined as the minimum aspect

ratio in which the maximum fibre stress can be achieved for a given load. The critical aspect ratio of a composite can be calculated using the following Equation (2-1).

$$\frac{L_C}{D} = \frac{\sigma_f}{2\tau} \quad 2\text{-}1$$

where Lc is the critical fibre length, D is the fibre diameter, σf is the fibre's tensile strength, and τ is the interfacial shear strength.

The critical fibre length depends mainly on the fibre-matrix interface as the load is transferred from the matrix to the fibre at the interface by shear. The tensile stress increases along the fibre length until the stress in the fibre reaches the fibre fracture tensile stress (σf) [94]. Therefore, fibre reinforcement becomes more effective if the fibre length (L) > Lc so that the fibre can be fully loaded before fracture [6]. The value of the critical length defines whether the fibre is long enough to act as reinforcement or is only an incorporated load. A sub-critical length fibre will not significantly contribute to composite strength, as it will be pulled out of the matrix before it can be fully stressed. On the other hand, very long fibres may get entangled during composite processing, resulting in poor fibre dispersion.

2.5.5 Interfacial Bonding

Interfacial bonding plays an important role in the mechanical properties of composites since the stress is transferred from the matrix to the fibres across the interface [6]. As a non-polar matrix, polyethylene has limited interaction with polar natural fibres, which results in poor adhesion. To achieve maximum reinforcement from natural fibres, their incorporation into a polymer matrix requires overcoming this interfacial incompatibility, which requires an improvement of fibre/matrix interfacial bonding. Thus, modifications can be made to the fibres, the matrix, or both. For example, interfacial strength can be engineered by modifying the fibre surface with fibre treatments, along with using coupling agents [10; 44; 45]. Fibre treatments are performed to achieve the following objectives [31]:

- Removal of undesirable fibre constituents.
- Roughening of the fibre surface.
- Separation of individual fibres from their fibre bundles.
- Modification of the chemical nature of the fibre surface.
- Reduction of fibre hydrophilicity.

One or more of the following interfacial bonding mechanisms can occur when the fibre-matrix interface is improved: mechanical interlocking, electrostatic bonding, chemical bonding and reaction, or interdiffusion bonding.

2.5.5.1 Mechanical Interlocking

A representation of mechanical interlocking between fibre and matrix interface is shown in Figure 2-8. A rougher fibre surface provides more spots for anchoring the matrix, thus increasing the possibility of mechanical bonding [46].

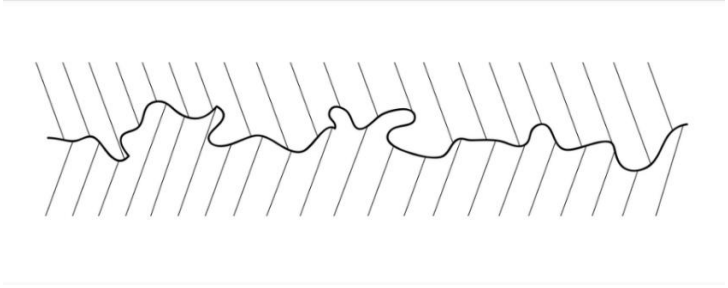

Figure 2-8: Schematic mechanical interlocking. Source: author.

2.5.5.2 Electrostatic Bonding

Electrostatic bonding occurs when either the fibre or the matrix is positively charged and the other is negatively charged, as shown in Figure 2-9. This type of bonding requires a difference in charge and intimate contact between the composite components [46].

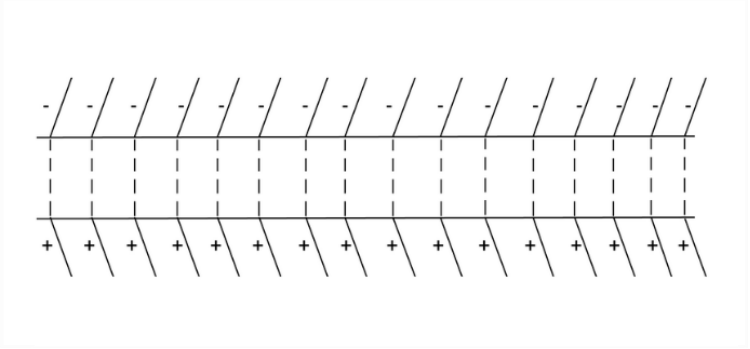

Figure 2-9: Schematic electrostatic bonding. Source: author.

2.5.5.3 Chemical Bonding

Chemical bonding occurs when a reaction takes place between reactive chemical groups present on the fibre surface and compatible groups in the matrix. The strength of the chemical bond depends on the type and number of bonds per unit area. The most common chemical bonds and their relative strengths are described in Table 2-2 [47]:

Table 2-2: Type of chemical bonding and their related energy.

Type of bond	*Energy (kJ mol^{-1})*
Covalent Bond	200 – 800
Hydrogen Bond	10 – 40
Van der Waals	1 – 10

2.5.5.4 Interdiffusion Bonding

Atoms or molecules of the fibre and matrix may interact at the interface to create reaction or interdiffusion bonding. For interfaces involving polymers, reaction bonding occurs when polymer chains from each component entangle together, as shown in Figure 2-10. The strength of this bonding mechanism depends on the distance over which the chains are intertwined, the degree of entanglement and the number of chains per unit area [46].

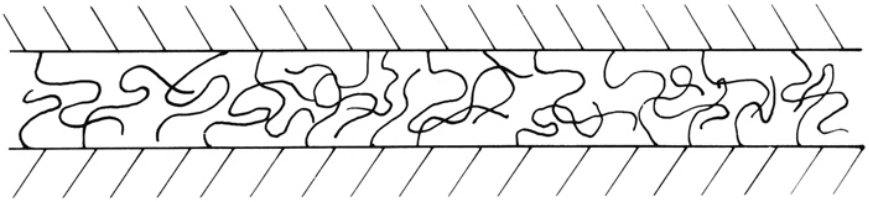

Figure 2-10: Schematic of reaction bonding involving polymers. Source: author.

2.6 Fibre Treatments

2.6.1 Biological Treatments

Many bacteria and fungi have been used produce enzymes that work synergically to degrade lignin and hemicellulose, which contributes to fibre separation [48]. These microorganisms can also roughen the fibre surface, thus improving interfacial bonding. However, biological treatments occur in an aqueous environment and tend to be time-consuming and water-polluting, thus not suitable for industrial processes [31].

2.6.2 Physical Treatments

Physical approaches include plasma, corona, ultraviolet, heat treatments, electron radiation and fibre beating [6]. The most popular techniques use electric discharge, such as plasma and

corona. Plasma is a partially ionised gas composed of photons, electrons, ions, radicals, and excited species [35]. Very high temperatures and strong electric or magnetic fields are employed to form these states. In addition, plasma treatment is performed in a vacuum chamber with gas continuously supplied to maintain the appropriate pressure and gas composition [6; 35]. Corona involves applying the plasma generated by high voltage to sharp electrode tips separated by quartz at low gas temperature and atmospheric pressure and commonly includes oxygen-containing species [6; 49]. These treatments have been reported to improve fibre-matrix interfacial adhesion by changing fibre surface polarity and increasing fibre surface roughness [50].

2.6.3 Chemical Treatments

Chemical modification of natural fibres is suggested to improve the fibre-matrix interface and can be classified as fibre pre-treatments, coupling agents, or dispersing agents such as surfactants [51]. The most popular chemical treatments are alkali, acetyl, silane and grafted anhydride [6]. Pre-treatments, such as alkali treatment, modify the surface of natural fibres by removing non-cellulosic components and exposing functional groups. Coupling agents act as a bridge between the fibres and the polymer matrix, reacting with the fibres by covalent or hydrogen bonding and with the polymer by chain entanglement [52]. In contrast, surfactants are chemicals that can lower fibre surface energy, thus improving fibre wettability. All bonding agents and surfactants have been grouped together as chemical treatments for simplicity [31].

2.6.3.1 Alkali Treatment

Alkali treatment consists of using sodium hydroxide (NaOH) to modify the cellulosic molecular structure of natural fibre by partially removing amorphous materials such as hemicellulose, lignin, wax and oils covering the external surface of the fibre cell wall, as shown in Figure 2-11, The removal of these cementing materials exposes reactive OH groups on the fibre surface that can react with coupling agents, thus enabling better bonding between fibre and matrix [20].

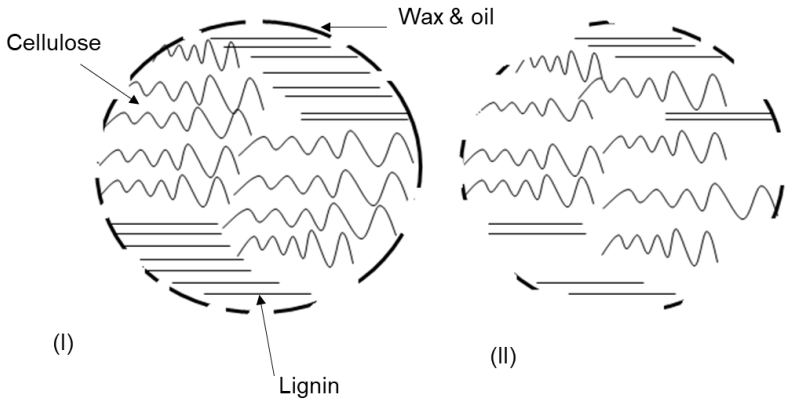

Figure 2-11: (i) Before alkali treatment and (ii) after alkali treatment. Source: author.

Additionally, fibres are separated from their bundles during alkali treatment, increasing the effective surface area for bonding with the polymer matrix. Furthermore, the alkali treatment usually results in a rougher fibre topography, improving fibre adhesion by providing additional sites for mechanical interlocking [10; 53; 54]. Consequently, it improves fibre strength, contributing to developing a composite material with superior tensile properties. Finally, removing those amorphous compounds can lead to an increase in the fibre crystallinity index [55]. This research has adopted from a study of the optimization of the alkaline treatment which showed that the $NaOH/Na_2SO_3$ treatment resulted in fibres with the highest tensile properties and good level of fibre separation [31].

2.6.3.2 Maleic Anhydride Grafted Polyethylene (MAPE)

The coupling agent MAPE has been extensively reported as an efficient bonding promoter for natural fibre-polyethylene composites [53; 56]. MAPE has anhydride groups that react with the hydroxyl groups present on natural fibres, improving their adhesion and reducing water absorption [56]. Some authors suggest there is a broader interfacial bonding consisting of covalent bonds and secondary bonding (such as hydrogen bonding and van der Waals forces) and mechanical interlocking [15; 53; 57]. Figure 2-12 shows the reaction between maleic anhydride polypropylene (MAPE) and natural fibres.

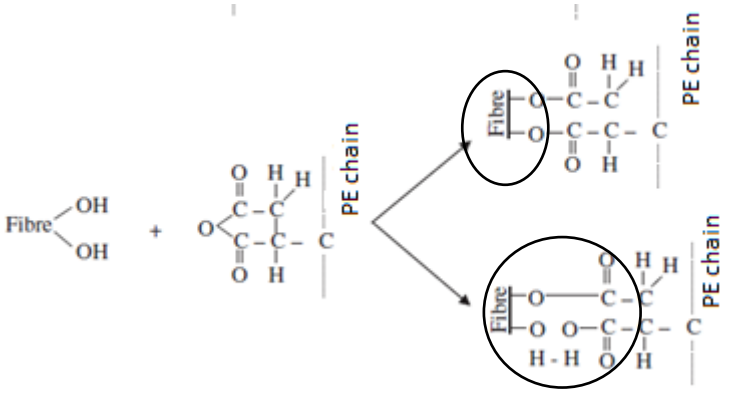

Figure 2-12: MAPE reaction with natural fibre.

Two critical factors have to be considered when selecting a coupling agent. Firstly, sufficient functional groups should be present, and secondly, the coupling agent polymer chains should be long enough to permit entanglements with the polymer matrix. Long chains are essential to maximise the effectiveness of the "physical crosslink" [44; 57]. The long hydrocarbon chains of MAPE become involved in interchain entanglement with the polymer matrix. Considering these factors, the acid number (which represents the amount of functionality in a coupling agent), and the molecular weight are two important properties influencing the coupling agent's effectiveness. Therefore, a malleated coupling agent with a correct balance of molecular weight and anhydride groups can achieve the best performance on natural fibre composites [15].

2.6.3.3 Stearic Acid

Stearic acids (fatty acids) are commonly used in cosmetics, pharmaceutics and bio-medicals, lubricants and the rubber industry [58; 59]. They can behave as dispersing agents, activators, surfactants, softening agents, lubricants and surface modifiers. In composite materials, stearic acid has been the most common processing aid used to improve the flow behaviour of filled polymers by lowering the mixture's viscosity [60]. This improvement in fibre wetting by the polymer matrix allows an intimate molecular contact between their interfaces, which is crucial for achieving strong fibre-matrix bonding. For this reason, in this research stearic acid was used as a processing aid in rotationally moulded composites reinforced with hemp fibre.

Fatty acids are amphiphile molecules with a hydrophobic carbon tail and hydrophilic carboxyl head. These molecules are absorbed on the surface of the particles through hydrogen bond with the polar groups, resulting in lower surface energy and reduced interfacial tension, as shown in Figure 2-13. The reduction of particle agglomeration results from a higher

stabilization of particles due to steric effects, where repulsive forces are high enough to overcome the attractive van der Waals forces [61; 62].

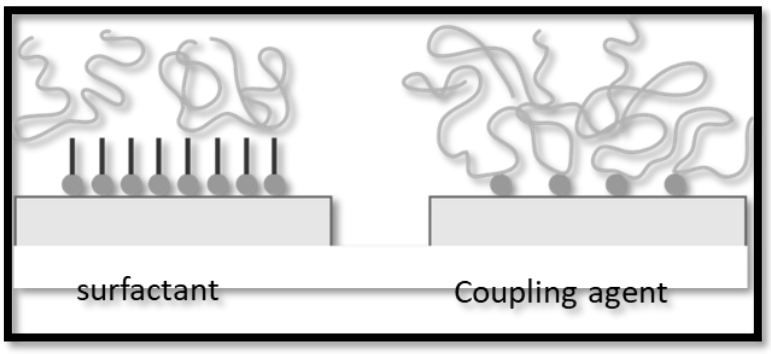

Figure 2-13: Schematic of interaction between fibre and matrix using a surfactant and a coupling agent. Source: author.

2.6.3.4 Mineral Oil

Mineral oils, also known as "white oils", are refined petroleum-based hydrocarbons such as paraffin, naphthene, and aromatic oils. Mineral oils are used in various applications depending on their purity, from the rubber industry to cosmetics and food [63]. For example, they are largely used as processing aids in carbon black filled natural rubber. In addition, a previous study with processing enhancers in rotational moulding reported that mineral oil efficiently reduced the viscosity of the molten polymer, which resulted in much faster densification and bubble removal [27].

2.7 Synthetic Fibres

Synthetic fibres are made from raw materials, such as petroleum, based on chemicals or petrochemicals. These materials are polymerised into long, linear chains with different chemical compounds and are used to produce various types of fibres, such as carbon and glass fibres.

2.7.1 Carbon Fibre

Carbon fibre is a lightweight graphitic material with higher tensile strength than steel and lower density than aluminium. Due to these characteristics, woven or non-woven carbon fibres can be combined with polymeric materials to produce high-performance carbon fibre reinforced composites (CFRCs) [64]. Carbon has two crystalline forms (diamond and graphite), but it also exists in quasicrystalline and glassy states. Its graphitic structure consists

of hexagonal layers with covalent bonds (525 kJ/mol); these layers, which are called the basal planes, are stacked in an ABAB sequence with an inter-layer of van der Waals bonds (<10kJ/mol). This difference in the intra-layer and inter-layer bonding strength results in very anisotropic properties [46].

The most common types of carbon fibres available have as precursors polyacrylonitrile (PAN) or pitch. PAN-based fibres can be subdivided into high Young's modulus (Type I) and high strength (Type II). These are usually used as continuous fibres in polymer matrices. Pitch fibres are generally stiffer than PAN-based fibres, but they have lower strength and strain to failure. PAN-based carbon fibres are the most commercially used. The process to produce PAN-based carbon fibres starts with the polymerisation of the acrylonitrile monomer, followed by spinning PAN from this polymer solution.

2.7.2 Recycled Carbon Fibre

Carbon fibre reinforced composites (CFRCs) have been applied mainly in the aerospace and automotive industries due to their superior combination of stiffness, strength, low density and durability. However, as a consequence of the increasing use of carbon fibre composites, much waste is generated. For example, commercial airplanes have up to 50% of their weight in CFRCs, and after 25-30 years of service, they are deactivated, generating tons of waste [65].

Other sources of CFRCs waste include out-of-date pre-pregs, manufacturing cut-offs, testing materials and production tools [66; 67]. Therefore, there are several reasons for CFRCs being recycled, including environmental impact from the waste material, production cost and economic opportunity, as recycling could convert expensive waste disposal into a profitable reusable material. However, recycling thermoset composites has a few challenges to overcome, as thermosets cannot be remoulded through heating, due to their cross-linked bonds. In addition, CFRCs have a complex composition of fibres, polymer and sometimes fillers, and often they are combined with other materials, such as metal inserts, to facilitate fastening to other components [66]. Fibre reclamation processes are particularly suitable for CFRCs because carbon fibres have high thermal and chemical stability, so their mechanical properties are not significantly degraded (especially stiffness) [68].

The first step for recycling CFRCs is a mechanical process involving breaking down the composite into smaller pieces. The resulting scrap pieces are then segregated by sieving into powdered products (rich in resin) and fibrous products (rich in fibres).

The next step is fibre reclamation by applying chemical or thermal methods to break down the matrix (typically a thermoset). Chemical processes use solvent solutions to remove the polymeric matrix from the composites. This method is reported to maintain about 90% of the tensile strength of carbon fibres, but it is a long process and uses large amounts of hazardous solvents.

Thermal methods include pyrolysis and a fluidised bed process. During pyrolysis, CFRCs are heated above 300°C in the near-absence of oxygen. Then, the polymeric matrix is volatilised into lower-weight molecules, while the fibres remain inert and are eventually recovered [69; 70]. The recovered fibres can be contaminated by pyrolytic carbon remaining from the degradation of the thermoset. The amount of this pyrolytic carbon and the mechanical properties of these reclaimed fibres depend on the process parameters, such as oven atmosphere, temperature, and heating rate [69].

During the fluidised bed process, composite scrap is introduced into a bed of silica sand, and hot steam is passed through the bed. In the silica bed, the polymer matrix is volatilised, and fibres and fillers are released to be carried out suspended in the air stream. Fibres and fillers are then separated from the gas stream in a cyclone chamber where the polymer is fully oxidised [68; 71]. The recovered fibres are clean and show very little contamination. However, this process results in some degradation of fibre properties. Tensile strength is reduced to around 50–75% of the virgin fibre strength while Young's modulus is practically unchanged [71]. The advantages and disadvantages of each of these processes are depicted in Table 2-3.

Table 2-3: Advantages and drawbacks of different recycling processes [66] .

Type of Process	*Advantages*	*Drawbacks*
Mechanical	Simple process Recovery of both fibre and polymer No use or production of hazardous chemicals	Modest mechanical performance Unstructured, coarse and variable fibre architecture Limited remanufacturing possibilities
Pyrolysis	High retention of fibre properties for optimised processes Existing commercial implementations	Possible deposition of residual matrix/char on the fibre surface Quality of fibres is sensitive to processing parameters Need for off-gas treatment unit
Fluidised Bed	No residual products on fibre surface Well-established process	Quality of the fibres is sensitive to processing parameters Need for off-gas treatment unit
Chemical	Very high retention of fibre properties	Environmental impact if using hazardous solvents Reduced scalability of most processes

Another challenge of recycling carbon fibre is finding profitable applications for it. Recycled carbon fibre can be cheaper than virgin carbon fibre, opening new markets and new opportunities in different industries. A typical application for mechanically recycled composites includes their re-incorporation in new composites as fillers or reinforcement. For example, these are used in the construction industry as fillers for asphalt or as mineral sources for cement [60].

Recycled carbon fibre also has the potential to be used as a thermal conductor, as it has a high intrinsic thermal conductivity and even a small load can significantly increase the thermal conductivity of composites. Many research efforts have been focused on using mesophase pitch-based carbon fibres as thermally conductive reinforcements [72].

2.8 Surface Modification of Carbon Fibre

Carbon fibre has a crystallised graphitic basal plane structure with a non-polar surface. For example, PAN-based carbon fibres have an inert surface due to the high temperature applied during the carbonisation/graphitisation process. Different fibre treatments have been

suggested to overcome carbon fibre surface inertness and improve carbon fibre-matrix adhesion by the following means [73; 74]:

- Increasing fibre surface roughness to enhance polymer/fibre contact and improve mechanical interlocking between them.
- Increasing fibre wettability by the polymer matrix.
- Increasing the number of chemically active sites on the fibre surface for subsequent chemical bonding with the polymer matrix.
- Using a coupling agent to chemically bond fibre and matrix.
- Commercial carbon fibres are usually coated with polymeric sizing, which not only protects them in transportation but improves the compatibility between carbon fibre and polymer matrices [36].

2.8.1 Chemical Treatment with HNO_3

Acid solutions are used to corrode the carbon fibre surface to increase roughness, thus improving fibre-matrix interlocking [75; 76]. Adversely, this treatment also induces pits, expanded micro-voids and flaws on the fibre surface, which reduces single fibre strength [76]. The extent of this adverse effect depends on factors such as treatment time and acid concentration [77]. Oxidation with nitric acid also increases fibres' surface activity by introducing polar groups such as hydroxyl (OH). These -OH groups can react with chemical groups present on coupling agents, such as maleic anhydride grafted PE, while the main PE constituent of PE-g-MAH can diffuse in the polymeric matrix to improve the interfacial bonding between the fibre and matrix [78].

Coupling agents have been reported in the literature to improve the adhesion between acidic treated carbon fibres and thermoplastic matrices, resulting in significantly enhanced mechanical properties [78-80]. The addition of MAPE has also been reported to increase the tensile strength of hybrid composites with untreated carbon/wood fibre and PE by about 113% [81]. Wong et al. [82] also showed a significant improvement in interfacial shear, tensile and flexural strength of recycled carbon fibre and PP with MAPP coupling agents, while maximum strength was achieved with the highest molecular weight MAPP.

2.9 Hybrid Composites

Hybrid composites are systems where one type of reinforcement is incorporated into a mixture of different matrices, or two or more types of reinforcements are incorporated into a

common matrix [83]. Hybrid composites offer more flexibility in manipulating composite properties, as the drawbacks of one fibre can be alleviated while keeping the benefits of the other. For example, carbon fibre has higher strength and stiffness than glass fibre, but it is relatively expensive and brittle, while glass fibre is cheaper and tougher.

Carbon and glass fibres can be combined in the same polymeric matrix to create a hybrid composite with a balance between their properties and, at the same time, reduce materials costs [84; 85]. The hybridisation of natural fibre composites with synthetic fibres, such as glass and carbon, has been reported to improve stiffness, strength, and moisture resistance [86-90].

2.10 Rotational Moulding

Rotational moulding is used to produce hollow plastic products without using applied pressure. The result is a product that is almost free of residual stress. Nowadays, the most common applications for rotationally moulded products are recreational boats (such as kayaks), large storage tanks for water or chemicals, and playground equipment.

This process basically consists of adding a polymer powder into a mould which rotates slowly (up to 12 rpm) about one or two perpendicular axes. This mould is heated until the polymer melts and then cooled until polymer solidification occurs, as shown in Figure 2-14 [1; 91].

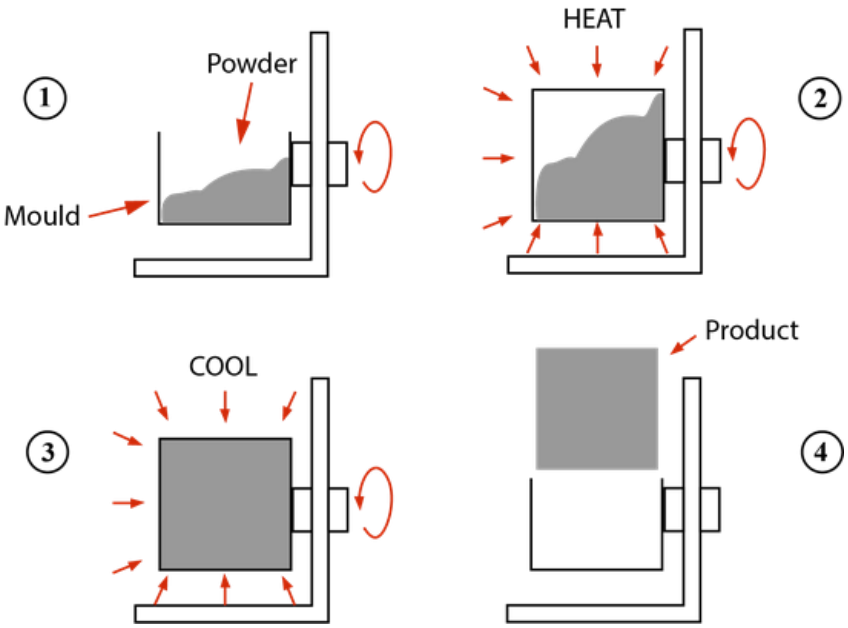

Figure 2-14: Schematic of rotational moulding. Source: author.

The most critical processing parameters influencing the properties of rotationally moulded products are oven time and temperature. As an example, short heating cycles or low temperatures may result in poor polymer consolidation, and resulting products with low strength, stiffness and toughness. On the other hand, very high oven temperatures or long processing periods can cause polymer oxidation, which results in a brittle material.

The optimum processing time and temperature in rotational moulding industry are commonly established by trial and error, and the best condition is usually considered to be where the products show only a small number of pinholes on their inner surface [3]. However, this approach is wasteful and imprecise, as many external variables can influence the amount of heating applied to a polymer charge within a fixed period.

Another method of controlling the rotational moulding cycle is to monitor the temperatures of the moulding process, particularly the Peak Internal Air Temperature (PIAT). As the internal mould temperature determines the polymer's melting inside the mould, the PIAT typically fixes the point when the molten polymer starts to cool down. However, there is always a delay between turning off the heating, starting the cooling step, and reaching the PIAT. The reason for that is that the thermocouple used to read the internal air temperature is in the centre of the mould, and it reads the convective temperature inside. Therefore, monitoring and controlling the PIAT is vital for ensuring good product quality and reproducibility.

A typical internal temperature curve obtained during the rotational moulding is shown in Figure 2-15. Initially, the temperature inside the mould rises slowly as the polymer absorbs the heat input. At this point, the polymer particles start melting (sintering). The polymer has melted during the densification phase, so the internal temperature rises quickly, while the molten polymer coats the mould wall. Once the internal temperature reaches the desired temperature, the heat input stops (peak temperature). There is a well-defined ‘kink’ in the air temperature curve at this final phase, which indicates that the solidification phase has begun. The air temperature inside the mould reduces due to the thermal energy being released during cooling. Once solidification is complete, the internal air temperature continues to decrease until it reaches room temperature. A water spray or gentle air cooling is usually used to assist cooling (demoulding) [91].

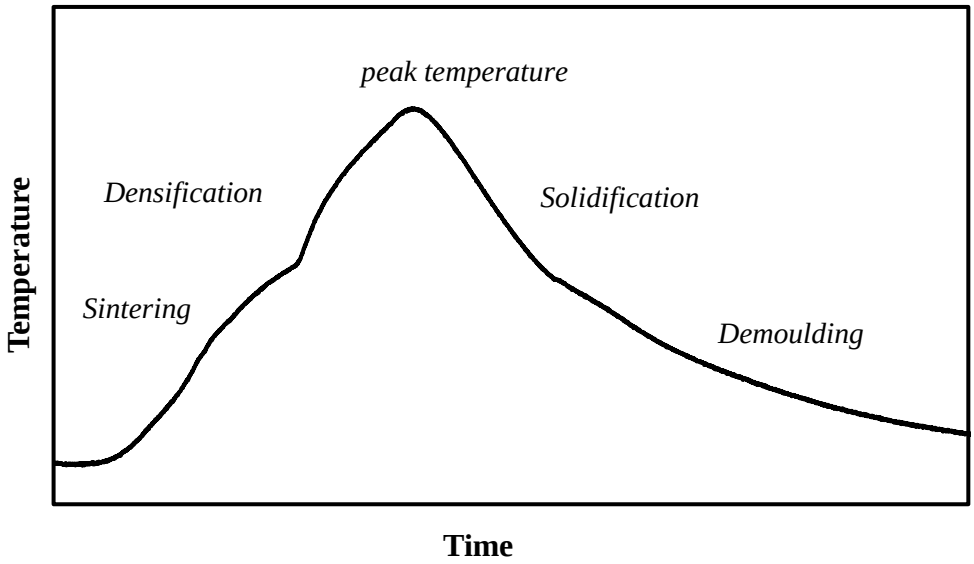

Figure 2-15: Typical oven temperature curve during rotational moulding. Source: author.

Rotational moulding is considered a potential alternative to processes such as blow moulding and thermoforming as it can produce stress-free products, with uniform wall thickness and potentially complex shapes. Further advantages of rotational moulding include the ability to produce multi-layered and foamed parts as well as parts with metal or plastic inserts.

The main advantage of rotational moulding over other processing methods is its capacity for producing large hollow parts with a high degree of complexity and a uniform wall thickness once using the correct process control and mould geometry [14]. The main drawback of rotational moulding is its long cycle times, which means a few hours for very large products. This drawback makes this process unsuitable for extensive product runs. However, it is ideal for short product runs and bulky parts, such as water tanks, boats or playground equipment. Other advantages and disadvantages of rotational moulding are described in Table 2-4.

Table 2-4: Advantages and disadvantages of rotational moulding [1].

Advantages	***Disadvantages***
Moulds of different sizes and shapes can run simultaneously in the same equipment.	Materials suited to rotational moulding are limited. Polyethylene accounts for over 90% of the materials used currently.
Moulds are simple and relatively inexpensive. As it is a low-pressure process, high-strength moulds are not required.	The process is not suited for large-scale production of small parts because of its long temperature cycle times.
Articles with undercuts and complex shapes can be moulded easily.	Materials cost can be relatively high since most plastics are available as pellets and must be reduced to powder.
Parts have good wall thickness uniformity compared to those produced by blow-moulding and thermoforming.	Bosses and solid ribs cannot be easily moulded.
It is possible to have control over the polymer distribution inside the mould by altering the rotational speed.	The presence of small bubbles or pinholes within the wall thickness and/or at the outside surface is common.

2.11 Thermoplastic Matrices for Rotational Moulding

Nowadays about 90% of rotationally moulded products are made of polyethylene due to its characteristics, which include low viscosity, good thermal resistance and relatively low cost [26]. Other materials that have been used in rotational moulding are polyvinyl chloride, polycarbonate, nylon, polypropylene and, occasionally, unsaturated polyesters, ABS, acrylics, cellulosic, epoxies, fluorocarbons, phenolic, polybutylenes, polystyrenes, polyurethanes and silicones [1].

There are some characteristics that a material needs to be used in rotational moulding, such as low viscosity and melting point. Rotationally moulded products tend to be very porous due to the typical characteristics of this process, such as low-speed rotation and the absence of external pressure. Therefore, highly viscous polymers impede the flow of air between the particles, so the air gets trapped between the polymer particles, increasing porosity. In

addition, materials for rotational moulding must withstand the prolonged time-temperature environment of the process to avoid polymer thermal degradation.

Polyethylene is usually subdivided into three categories, as shown in Table 2-5, according to density [3].

Table 2-5: Density of different grades of polyethylene.

Material	***Material Density (kg/m^3)***
Low-density polyethylene (LDPE)	915–929
Medium-density polyethylene (MDPE)	930–939
High-density polyethylene (HDPE)	940–965

Composite properties, such as hardness, stiffness and chemical resistance, tend to increase with polymer density, whereas impact strength and stress crack resistance decrease. The fundamental differences between low and high-density grades of polyethylene are structural. For example, LDPE has a random long-branching structure, with branches on branches. The molecular mass distribution is moderately broad. The forces of attraction between them are not strong because the branches prevent the polyethylene molecules from packing closely together. As a result, it has good flow behaviour and displays excellent resistance to chemicals, flexibility and toughness at low temperatures [3; 92].

In contrast, in the high-density grades of polyethylene, the molecular chains are mostly linear, with few side branches, so the chains can pack closely together to provide more material per unit volume. This material is stronger and stiffer than LDPE, but its impact strength is not so good at low temperatures, and it is also prone to warpage due to high crystallinity [3].

The development of linear low-density grades of polyethylene (LLDPEs) has resulted in an inherently stronger and stiffer structure than LDPE at the same density, while retaining toughness and stress crack resistance. This material has side branches, which keep its density low, but the branches are short, and their occurrence can be well controlled. LLDPEs differ from HDPE because they have many more relatively longer branches off the main molecular chain. This prevents the molecules from packing closely together as they do in the high-density material [3; 92]. LLDPE has proved to be very popular in the rotational moulding industry due to its excellent chemical resistance.

2.12 Mixing Methods prior Rotational Moulding

2.12.1 Dry Mixing

Two different methods have been used to incorporate reinforcements, such as fibres, in rotational moulding: dry mixing and melt compounding. The dry mixing method is the most straightforward approach, whereby the additives or reinforcements are dispersed throughout the polymer powder and moulded directly. The major problem with this method is fibre agglomeration and phase segregation due to the slow speed rotation of this process. This can result in poor fibre wetting by the molten polymer, which can significantly compromise the fibre-polymer interface as well as the mechanical properties of the composite material [93].

2.12.2 Melt Compounding

This technique is used to compound thermoplastic polymers (usually obtained in pellet or powder form) with short reinforcing fibres via extrusion. It has been reported to be more effective than dry mixing for optimum fibre distribution during rotational moulding [94]. During melt compounding, the composition is drawn into a heated extrusion barrel employing a single screw or two co-rotating screws, depending on the extruder used to form the composite melt. This composite melt exits the barrel through a die, which determines the shape of the extruded composite [95]. Then, this extruded material must be re-ground or pelletised into a form suitable for rotational moulding.

Some extruder processing variables must be optimised to produce composites with high mechanical performance, such as barrel length, temperature profile, screw configuration and screw speed. Incorrect extruder set-up can result in poor dispersion and wetting of the fibres with the polymer matrix [31]. Another issue with melt compounding fibre-polymers into particles suitable for rotational moulding is that the following powder-grinding step may cause a reduction in fibre length, which can severely restrict their reinforcing efficiency [96].

2.13 Void Formation in Rotationally Moulded Products

The formation of voids and pinholes on rotationally moulded products has been a challenge for manufacturers. The occurrence of voids in composites is generally associated with a reduction of strength and stiffness, and also impairs the surface aesthetics of the final product. In rotational moulding, polymers with low viscosity and produced as fine powders are

reported to improve the efficiency of polymer sintering and hence the manufacture of void-free products [3]. The standard particle size for achieving proper polymer sintering and coalescence in rotational moulding has been reported to be around 500 μm or less [1].

Nowadays, the most common strategy used by industry to reduce porosity in rotationally moulded composites is prolonging the heating cycle. However, this procedure can result in polymer oxidation, which can be detrimental to the mechanical properties of the final product. A few studies have succeeded in reducing porosity by changing the internal mould pressure during or after the process [97; 98]. However, using external pressure would be an additional cost in the process, as high-strength moulds are required. The use of vacuum has also shown some benefit in decreasing the void content in rotationally moulded products [99].

Previous research [27] has shown that the addition of mineral oil and glycerol monostearate in rotational moulding reduces polymer viscosity, thus improving polymer flow. As a consequence, the porosity of the final product was reduced without reducing impact strength. Similarly, another study used additives such as silica fume, vinyl-silanes and stearates to improve the flow of polyethylene micro-pellets during the rotational moulding process [28].

2.14 Evaluation of Fibre Orientation

Orientation analysis in NPFCs is challenging due to the innate variability in the cross-section of natural fibres. Image analysis is considered a relatively quick way to assess and quantify fibre orientation. In general, it consists of cutting and polishing a sample from the composite and analysing the elliptical shape of the fibres using image analysis software [51]. The angle between the fibre axis and the direction perpendicular to the cutting plane can be measured from the eccentricity of the ellipse. The disadvantage of this technique is that these measurements can be inaccurate due to difficulties associated with distinguishing ellipses of low eccentricity.

The ImageJ plugin “directionality” indicates the fibre orientation by the predominant peak of an orientation distribution profile. This plugin calculates the spatial frequencies within an image given a set of radial directions. Then, the method generates normalised histograms revealing the amount of fibres present between 0° and 180° with a bin size of 1 [100].

An effective assessment of fibre orientation using XRD has also been reported in the literature [101]. X-ray diffraction (XRD) can provide mean diffraction patterns for samples, from which the preferred orientation of the crystalline cellulose component can be determined to quantify fibre alignment within composites. The disadvantage of this technique

is that it only allows the determination of the planar fibre orientation; fibre orientation along the thickness of the sample cannot be measured. In addition, the low absorption rate of polymers makes the identification of fibre orientation more difficult.

Micro-CT technology provides the means to acquire 3D images of samples in a non-destructive way, visualising the internal architecture of the material at the microscopic level [102]. However, this method is very costly and requires high-resolution scans and high computational resources and analysis time [103].

Chapter 3

Alkali Treatment of Hemp Fibres Applied to Rotational Moulding

This chapter provides an assessment of alkali-treated hemp fibre as a reinforcement for rotationally moulded polyethylene composites. Firstly, untreated and alkali-treated hemp fibres were characterised using the following techniques: scanning electron microscopy (SEM), thermal gravimetric analyses (TGA), Fourier transform infrared spectroscopy (FT-IR) and X-ray diffraction (XRD). Secondly, the effect of using maleic anhydride grafted polyethylene (MAPE) as a coupling agent was investigated by tensile testing composites produced with and without MAPE. In addition, the effect of different levels of fibre content in rotationally moulded composites was investigated.

The results showed that the alkali treatment removed non-cellulosic components from hemp fibres, which improved their separation, thermal resistance and increased their fibre crystallinity index. Also, alkali-treated fibre composites resisted exposure to elevated temperatures for prolonged periods (characteristic of the rotational moulding process) with no apparent signs of thermal degradation, unlike untreated fibre composites. The addition of 3 wt.% MAPE improved the tensile strength and Young's modulus of alkali-treated fibre composites due to better fibre-matrix adhesion. In general, a poor fibre distribution within all the rotationally moulded composites was observed. This behaviour tended to worsen above 5 wt.% fibre content, which reduced the composite's tensile strength and Young's modulus. The reduction in mechanical properties with the addition of fibres in comparison with polyethylene was attributed to poor fibre distribution and high porosity in the final composites.

3.1 Materials

The industrial hemp fibre (*Cannabis Sativa L.*), used as reinforcement, was grown in New Zealand. Hemp fibre was treated with an alkali solution of NaOH and Na_2SO_3; both were 98% purity and obtained from Merck. The coupling agent, polyethylene-grafted maleic anhydride, code 456632, with viscosity 1,700–4,500 cP (140°C) and a saponification value of 30–40 mg KOH/g, was obtained from Sigma Aldrich in powder form. A rotational moulding grade of low-medium-density polyethylene, VX567, with a melt flow index of 6.0 g/10 min (ASTM D 1238), and a density of 0.935 g/cm^3 (ASTM D 1505), was obtained from Vision Plastics (VPLAS) in powder form.

3.2 Methods

3.2.1 Alkali Treatment of Hemp Fibres

Hemp fibre was treated with a solution of 5 wt.% NaOH and 2 wt.% Na_2SO_3 with a fibre/solution ratio of 1:8 (by weight) in a lab-scale pulp digester, according to the schedule in Figure 3-1. These conditions were adopted from previous research on the optimisation of alkaline treatment [31]. The alkali-treated fibres were washed in running water and then dried at 80 ℃ for 24 h. Figure 3-2 shows the hemp fibre before and after the treatment.

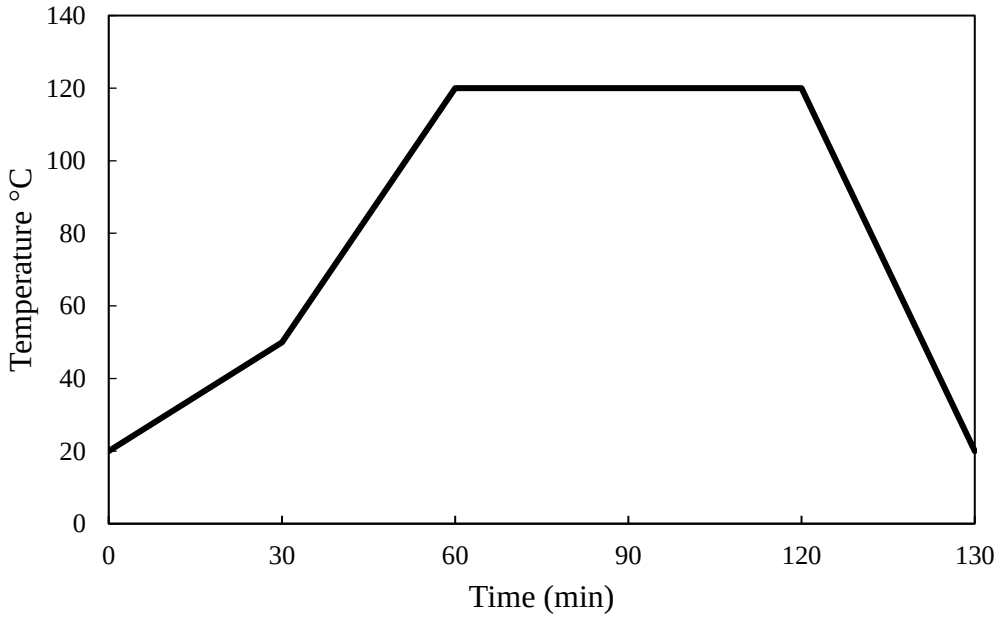

Figure 3-1 Digestion profile of the alkali treatment.

Figure 3-2: Untreated (left) and alkali-treated hemp fibre (right).

3.2.2 Dry Mixing

Rotationally moulded composites were prepared according to the compositions shown in Table 3-1. Hemp fibres were chopped using a granulator fitted with a 4 mm aperture screen sieve and dried at 80 ℃ for 24 h. They were then dry mixed with the other materials using a laboratory blender, for 5 min, prior to rotational moulding.

Table 3-1: Composition of rotationally moulded composites.

Sample code	***Composition***
2.5TM	2.5 wt.% Treated hemp fibre – 3 wt.% MAPE - 94.5 wt.% PE powder
5TM	5 wt.% Treated hemp fibre – 3 wt.% MAPE - 92 wt.% PE powder
7TM	7 wt.% Treated hemp fibre – 3 wt.% MAPE - 90 wt.% PE powder
5UM	5 wt.% Untreated hemp fibre – 3 wt.% MAPE - 92 wt.% PE powder
5T	5 wt.% Treated hemp fibre – 95 wt.% PE powder
5U	5 wt.% Untreated hemp fibre – 95 wt.% PE powder
PE	100 wt.% Polyethylene powder
The samples were named according to the following scheme: Fibre content (wt.%), T = treated hemp; U= untreated hemp, M = MAPE, PE = pure polyethylene	

3.2.3 Rotational Moulding

Figure 3-3 shows the set-up of the rotational moulder equipment based on a small, electrically heated oven. The oven was modified to allow closed-loop computer control of the oven temperature and the speed of rotation of a monoaxial square cross-section mould with internal dimensions of 100 mm x 100 mm x 140 mm.

Figure 3-3: Monoaxial rotational moulder set-up.

The moulding procedure used with the monoaxial rotational moulding is as follows:

- The mould was coated with 808 silicone mould release, according to the manufacturer's application instructions.
- The mould was charged with 350 g of material and then threaded into the drive-spindle inside the rotational moulding. The equipment was at room temperature at this stage.
- The oven temperature was set to 240 °C (maximum temperature available in this oven), and mould rotation started as soon as heating began. During moulding, the internal air temperature was monitored with a hand-held digital thermometer and thermocouple probe. A typical rotational moulding curve was obtained as a Temperature versus Time graph.

- When the mould internal air temperature reached 180 ℃, the heating was turned off. The oven door was opened, and a fan was placed in front of the oven to assist the cooling process. The temperature of the air inside the mould continued to rise for a short period, reaching a peak internal air temperature (PIAT) of 190 ℃. The product was demoulded when the internal temperature dropped to 40 ℃.

3.2.4 Thickness Adjustment

Rotationally moulded composites were produced in a box-shaped mould and machined into individual sheets using a bandsaw. A Carbatec TH BX330P benchtop thicknesser (Figure 3-4) was used to adjust the thickness of these sheets to about 3 mm. This material was later converted into specimens suitable for tensile testing (Section 3.2.5).

Figure 3-4: Carbatec TH BX330P benchtop thicknesser with sample on the bed before (left) and after (right) the process.

3.2.5 Tensile Testing of Single Fibres

Initially, hemp fibres were separated from their bundles by hand. Then, a single fibre was glued (both ends) onto 2 mm thick cardboard with a 2 mm fibre gauge length, as shown in Figure 3-5. An Olympus BX60 metallurgical microscope was used to ensure that only a single fibre was present on each piece of cardboard. Finally, the supporting sides of the mounting cards were carefully cut once the cardboard was griped in the tensile machine, using a hot-wire cutter. These fibres were tensile tested according to the ASTM D3379-75

"Standard Test Method for Tensile Strength and Young's Modulus for High-Modulus Single Filament Materials". A total of 30 single fibres were tensile tested to failure at a rate of 0.5 mm/min using a 10 N load cell and an Instron-4204 tensile testing machine. The average fibre diameter was obtained by measuring the diameter at four locations along the fibre length.

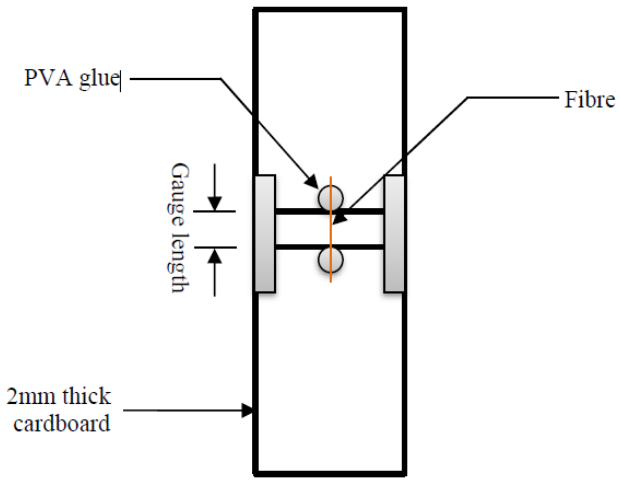

Figure 3-5: Schematic diagram of the cardboard used to tensile testing single fibres [31].

3.2.6 Scanning Electron Microscopy

Scanning electron microscopy (SEM) was used to investigate the effect of the alkali treatment on the separation of the fibres from their bundles. In addition, SEM images of the fractured composite surfaces with and without the coupling agent MAPE were used to analyse the interface between fibre and matrix. In both cases, the samples were mounted on aluminium stubs and coated with platinum plasma sputtering. SEM micrographs were obtained using a Hitachi S-4100 field at 5 kV.

3.2.7 Thermal Analysis

Thermogravimetry analysis (TGA and DTG) was used to analyse the thermal behaviour of untreated and alkali-treated hemp fibre. Five samples of about 2–3 mg were analysed using a PerkinElmer STA 8000 analyser. This analysis was performed in a dynamic mode by heating the samples from 40 °C to 800 °C at 10 °C/min in oxidant atmosphere purged at 50 ml/min with an empty pan used as a reference.

3.2.8 X-ray Diffraction

In order to assess the influence of alkali treatment on the crystallinity of hemp fibre, a Philips X'Pert diffractometer was used. Three samples were prepared with untreated and treated hemp fibres granulated into fine particles and compressed into disks using a cylindrical steel mould (θ = 15 mm) with an applied pressure of 32 MPa. The diffracted intensity of CuKα radiation (λ = 1.54 nm) was recorded between 10º and 40º (2Θ- angle range) using a current and voltage of 40 mA and 40 mV with a scanning speed of 0.02 degrees/second. The crystalline index (CI) of untreated and treated fibre, which measures the relative degree of the cellulose crystallinity, was evaluated using the Segal empiric model [104] according to Equation 3-1.

$$CI\ (\%) = \frac{I_{002} - I_{am}}{I_{002}}\ x\ 100 \qquad 3\text{-}1$$

where I_{002} represents the maximum intensity of the 002-lattice reflection of cellulose I, and I_{am} is the maximum intensity of X-ray scattering broadband due to the amorphous part of the sample.

3.2.9 Fourier Transform Infrared Spectroscopy

Fourier Transform Infrared Spectroscopy (FT-IR) was used to investigate the removal of chemical groups corresponding to non-cellulosic components on hemp fibres after the alkali treatment. A PerkinElmer Spectrum with transmission mode 4000 to 400 cm^{-1} was used with a total of 20 scans for each sample and a resolution of 4 cm^{-1}. The three samples used consisted of ground dried fibre and KBr (0.8 mg fibre per 400 mg KBr) pressed into pellets.

3.2.10 Tensile Testing of Rotationally Moulded Composites

Samples for tensile testing were cut from the composites with adjusted thickness (Section 3.2.4) according to "sample V" described in ASTM D638-14 "Standard method for tensile properties of plastics". These samples were placed in a conditioning chamber at 23 ℃ ± 3 ℃ and 50 % ± 5 % relative humidity for 48 hours. An INSTRON-4204 tensile testing machine fitted with a 10 KN load cell operated at a 1 mm/min crosshead speed was used. An Instron extensometer was used to measure the composite strain. Seven specimens of each composite were tested to failure.

3.2.11 Filament Fabrication

To evaluate the effect of using MAPE at different contents to improve fibre-matrix adhesion, filaments of composites were produced using a Labtech 1201-LTE20-44 20mm diameter co-rotating twin-screw extruder with a 3 mm die. A filament winder (see Figure 3-6) was used to improve the diameter consistency of these filaments to about 2 mm. The temperature control on the extruder was separated into five zones set at T_1:130 ℃ (barrel entrance), T_2:140 ℃, T_3:140 ℃, T_4:140 ℃ and T_5:125 ℃ (barrel exit). These temperatures were based on the polymer melting point. The twin co-rotating screws were operated at 80 rpm.

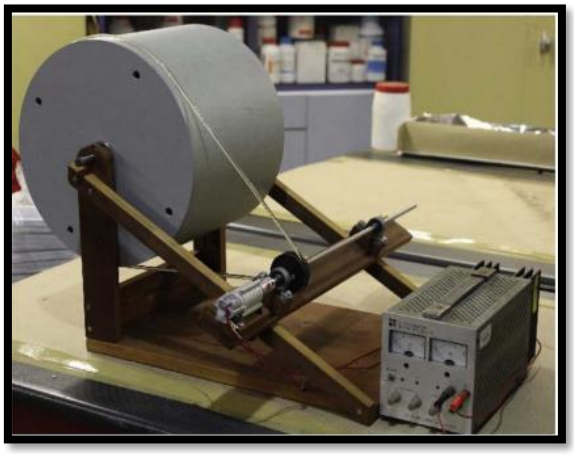

Figure 3-6: Filament winder [105].

3.2.12 Tensile Testing of the Composites' Filaments

Filaments of composites with a length of 200 mm and diameter of 2 mm were tensile tested using an Instron-4204 machine fitted with a 5 KN load cell at a crosshead speed of 1 mm/min. The strain was measured using an Intron 2630-112 extensometer with 50 mm length fitted to the samples, and a gauge length of 120 mm was assigned to each sample. This test method was adapted from previous research [105]. All five composite specimens were tested to the point of maximum stress due to excessive necking. The average of five measurements was taken as the experimental value.

3.3 Statistical Analysis

The software MINITAB version 18 was used for the statistical analysis of the results of tensile testing. First, the values of different parameters were expressed as mean values with standard deviation and coefficient of variation. Then, one-way ANOVA was applied to

compare the differences in the mean values with a 95% simultaneous confidence level. A hypothesis test that evaluates two mutually exclusive statements about two or more population was used to determine whether to reject the null hypothesis [106].

3.4 Results and Discussion

3.4.1 Single Fibre Tensile Properties

Alkali treatment was used to remove non-cellulosic material such as lignin, pectin and hemicellulose from hemp fibres. It is well known that the rate of lignin removal is dependent on NaOH concentration. However, overtreatment with alkali solution has been shown to reduce fibre properties [107]. Sodium sulphite (Na_2SO_3) is reported to assist NaOH in removing lignin from lignocellulosic fibres, and to shorten the treatment time. The introduction of sulphite groups (SO_3^{2-}) into the lignin side chains through sulphonation enables lignin to be rapidly dissolved in alkali solution [108]. The treatment parameters adopted in this research have been optimised in previous research, which showed that a combination of NaOH and Na_2SO_3 results in fibres with the highest strength and with a good level of fibre separation [31]. It was observed that alkali treatment reduced fibre diameter by nearly 24% (Table 3-2); fibre diameter reduction is consistent with the removal of non-cellulosic materials. Table 3-2 also shows that the tensile strength remained approximately the same after the treatment, suggesting no degradation in the cellulose microfibrils during the alkali treatment.

Table 3-2: Mean and median of diameter and tensile strength of untreated and treated hemp fibre.

Fibre treatment	***Sample Size***	***Fibre diameter (µm)*** ***Mean***	***Fibre diameter (µm)*** ***Median***	***Tensile Strength (MPa)*** ***Median***	***Tensile Strength (MPa)*** ***Mean***
Untreated	30	29 ± 11	24	545	715 ± 471
$NaOH/Na_2SO_3$	30	22 ± 8	22	521	703 ± 412

3.4.2 Scanning Electron Microscopy (SEM)

SEM images showed that hemp fibres were initially in bundles (Figure 3-7a), which were separated by the alkali treatment (Figure 3-7b). Alkali treatment has been reported as the most efficient method for removing lignin and other cementing materials from lignocellulose fibres, thus improving fibre separation from bundles [10; 53]. In addition, the alkali treatment

breaks the OH bonding in the fibre network structure, resulting in the separation of the interfibrillar regions from the cellulose fibres [109].

Fibre separation enables good fibre wetting by the polymer, which promotes interfacial bonding between fibre and matrix. Consequently, there is a void reduction within composites as the fibres are fully surrounded by the matrix. The combination of these factors can improve the tensile properties of short-fibre composites.

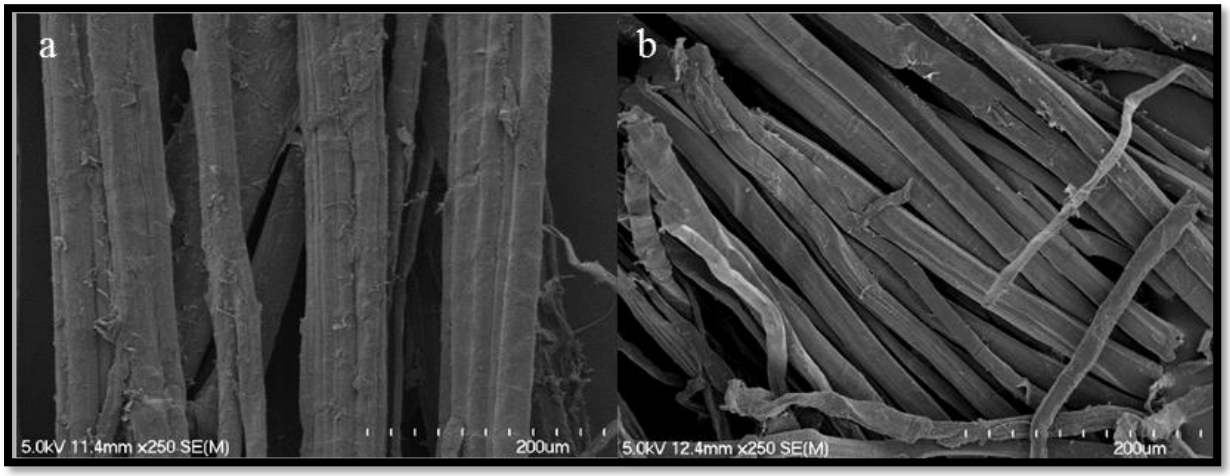

Figure 3-7 SEM micrograph of (a) untreated and (b) alkali-treated hemp fibre.

3.4.3 Fourier Transform Infrared Spectroscopy (FT-IR)

FT-IR was used to assess the variation in hemp fibre chemical composition after the alkali treatment. Figure 3-8 shows that the peak at 1740 cm^{-1}, which is related to the C=O stretching of acetyl or carboxylic acid groups, has fully disappeared after the alkali treatment due to the removal of hemicellulose from the hemp fibres [44; 110].

Another noticeable difference was that the peak at 1232 cm^{-1} corresponding to the C-O stretching vibration in lignin, disappeared after the treatment [110]. These results support the reduction of hemicellulose and lignin content in hemp fibre after alkali treatment. A summary of the main functional groups in hemp fibre spectra is presented in Table 3-3.

.

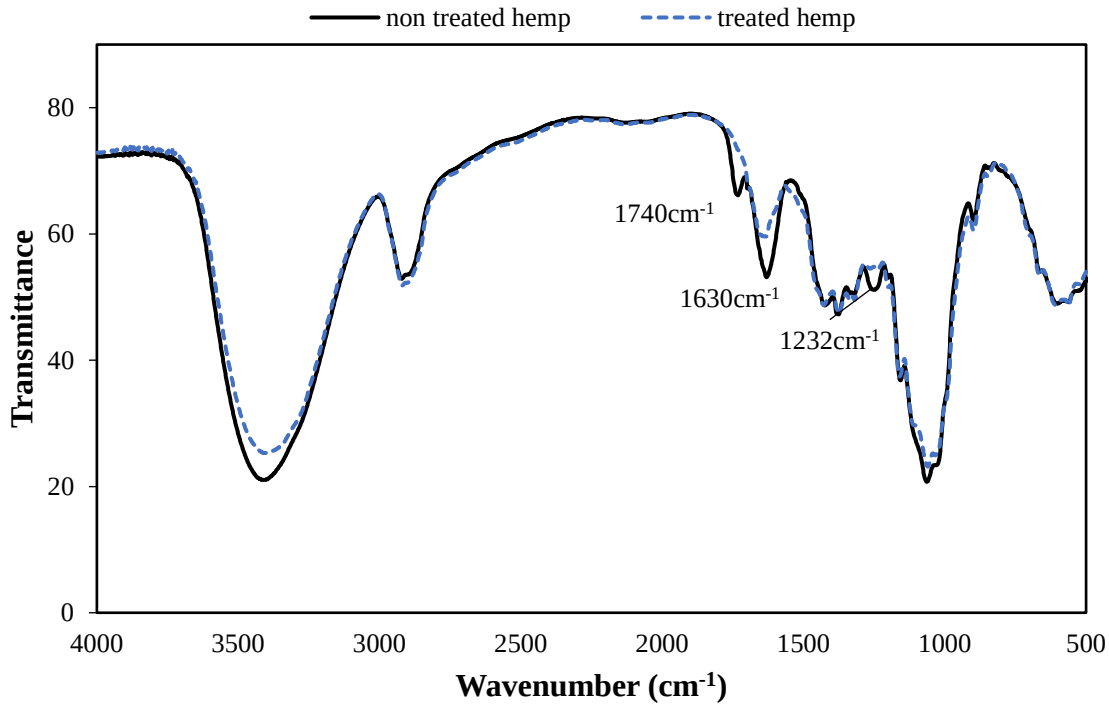

Figure 3-8: FT-IR spectra of untreated and treated hemp fibre.

Table 3-3: Band assignment of the main functional groups found in the untreated hemp fibre spectrum.

Wavelength (cm^{-1})	***Functional Group***	***Band Assignment***
3397	OH	Water absorption and OH groups in hemp fibre components
2900	C=H, CH_2	Stretching of the methyl and methylene groups, hydrocarbon chains
1740	COOH (C=O)	Free carbonyl groups, stretching of acetyl or carboxylic acid (hemicellulose)
1630	C=C and C = O	Stretching vibration in conjugated carbonyl of lignin (lignin)
1428	CH_2	Aromatic skeletal vibrations (lignin) and CH deformation in-plane (cellulose)
1374	C-H	Aliphatic C-H stretching in methyl and phenol OH (cellulose and hemicellulose)
1318	O-H	Phenol group (cellulose)
1232	CO	Aromatic C-O stretching vibrations (C-O stretching are those of the methoxyl and phenol groups)- lignin
1063	CO	C-O deformation in secondary alcohols and aliphatic ethers
890	C-H	CH deformation in cellulose

3.4.4 X-ray Diffraction (XRD)

The X-ray diffractograms of untreated and treated hemp fibre are shown in Figure 3-9. Typical crystalline peaks assigned to the cellulose Iβ structure are observed around 2Θ = 15º (110), 17º (1$\bar{1}$0) and 22º (002) [111]. However, the plane peaks of (110) and (1$\bar{1}$0) overlap and appear as one broad peak. According to previous research, the amorphous phase is at the lowest point between the peaks corresponding to the planes (1$\bar{1}$0) and (002) at 2Θ =18º [112].

Figure 3-9 shows that the intensity of the peaks 2Θ = 15º, 17º and 22º increased after the alkali treatment, suggesting removal of amorphous materials from the hemp fibres [11; 45]. As previously showed by FT-IR analysis, amorphous materials such as hemicellulose and lignin were partially removed from treated fibres, which was reflected in the proportion of crystalline cellulose.

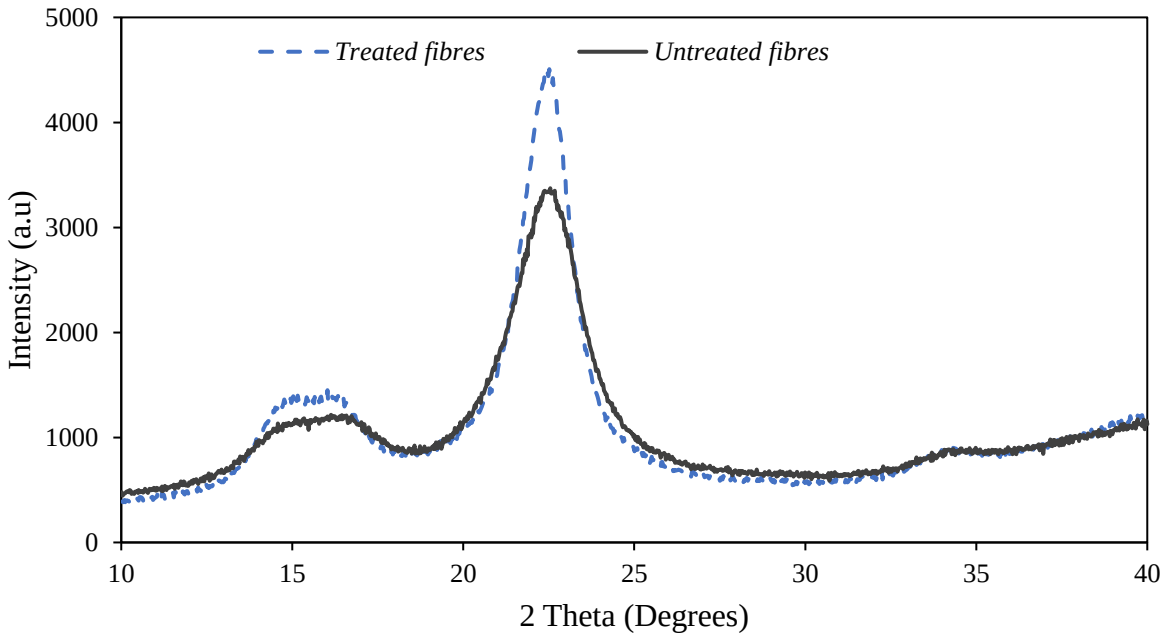

Figure 3-9: X-ray diffraction patterns for untreated and treated hemp fibre.

The crystalline index (CI) of untreated and treated fibre, which measures the relative degree of cellulose crystallinity, was evaluated using the Segal empiric model [104]. The results shown in Table 3-4 indicate an increase of about 9% in the crystallinity index after the treatment. This increased crystallinity index suggests removal of amorphous cellulose or conversion of it to crystalline cellulose. The crystallinity index is useful on a comparison basis; it should be noted that it indicates the order of crystallinity rather than the absolute crystallinity [113].

Table 3-4: Cellulose crystallinity index of untreated and treated hemp fibre.

Hemp Fibre	$I_{am}(2\Theta = 18^{o})$	I_{002} $(2\Theta = 22^{o})$	*Crystallinity Index (%)*
Untreated	873	3251	73.15
Treated	874	4434	80.29

3.4.5 Thermogravimetric Analysis

Figure 3-10 shows three weight-loss stages in the TGA thermograms of both treated and untreated fibre. The first stage of weight loss from 30 to 100 ℃ is due to the release of moisture content from the fibre. The second stage of weight loss, from about 200 to 360 ℃, is due to the thermal degradation of amorphous materials such as hemicellulose, lignin and pectin, followed by cellulose [45; 114]. Finally, the third stage of weight loss, from 360 to 500 ℃, is due to the thermal degradation of cellulose and the remaining lignin.

The DTG (Differential Thermal Gravimetry) curves shown in Figure 3-10 confirmed that untreated fibres initiated thermal degradation at lower temperatures than the treated fibres as they have more thermally unstable components. On the other hand, the thermal decomposition in treated fibres mainly occurs in the amorphous and crystalline cellulose [45; 115]. The crystalline cellulose contain strong hydrogen bonds and thus requires high levels of energy to be broken [54].

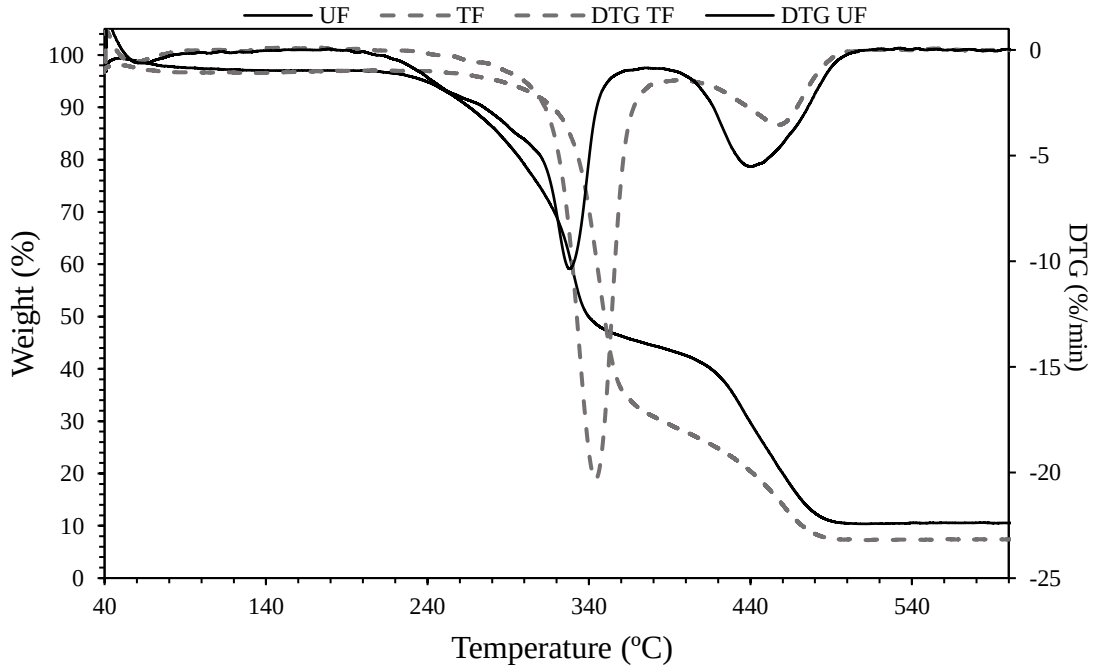

Figure 3-10: Thermogravimetric analysis curves of untreated (UF) and treated hemp fibre (TF).

Table 3-5: Summary of TGA results for untreated and treated hemp fibre.

Hemp Fibre	T_{10} (℃)	T_{50}(℃)	T_{70}(℃)
Untreated	275	340	385
Treated	315	348	440

T_{10}(℃), T_{50}(℃) and T_{70}(℃) mean temperature at 10%, 50% and 70% weight loss.

3.4.6 The effect of MAPE Content on Composites' Mechanical Properties

3.4.6.1 Tensile Testing of Extruded Filaments

Treated hemp fibre was extruded with polyethylene and different levels of MAPE to produce filaments of composites for tensile testing. Figure 3-11 shows that the best-performing composite was produced with 3 wt.% of MAPE content. This result was confirmed to be statistically significant by two-way ANOVA (Figure 3-12). Coupling agents such as maleic grafted anhydride polyethylene (MAPE) react with hydroxyl groups exposed on the fibre surface via covalent and secondary bonds (such as hydrogen and Van der Wales's forces) and with the polymer matrix by mechanical interlocking, hence improving the interfacial bonding [15]. This improvement in interfacial bonding allows efficient stress propagation from the matrix to the fibre, thus increasing tensile strength.

A slight reduction in tensile strength was also observed above 3 wt.% of MAPE, which indicates that there was enough content to saturate most of the OH groups available on the surface of the alkali-treated fibres (Figure 3-11). An excess of MAPE has been reported to cause polyethylene chains to entangle with each other rather than with the polymer matrix, resulting in slippage [116; 117]. In addition, Figure 3-11 shows no particular trend relating MAPE content to Young's modulus, which was confirmed by statistical analysis (Figure 3-13). Similarly, previous research [31] observed no link between increased MAPP content and Young's modulus in hemp fibre-MAPP composites.

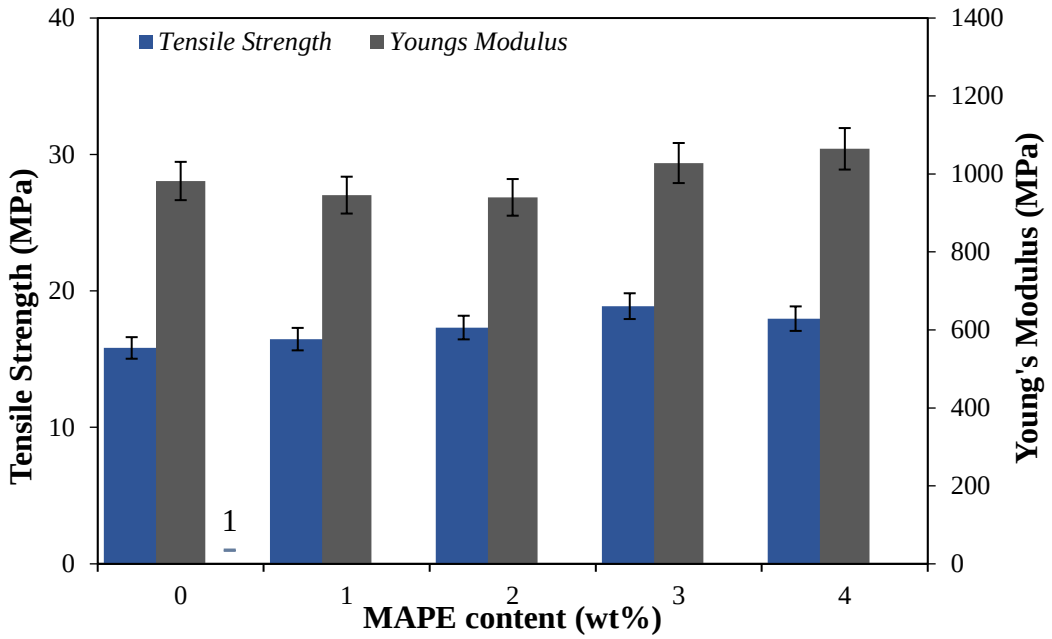

Figure 3-11: Effect of MAPE content on the tensile strength and Young's modulus of filaments of composites with 10wt.% alkali-treated fibre.

Table 3-6: Statistical analysis of the tensile strength and Young's modulus of filaments of composites with different MAPE content (0-4% by weight). P>0.05 (Gaussian distribution)

MAPE content (%)	*Sample Size*	*Tensile Strength (MPa)*	*SD*	*CV*	*Young's modulus (MPa)*	*SD*	*CV*
0	5	15.82	1.18	07.44	982.0	107.6	10.95
1	5	16.47	0.91	10.84	945.7	123.2	13.00
2	5	17.32	0.94	08.97	940.0	160.5	20.18
3	5	18.89	0.50	06.30	1028.1	346.0	41.12
4	5	17.97	2.04	06.74	1064.6	353.0	38.20

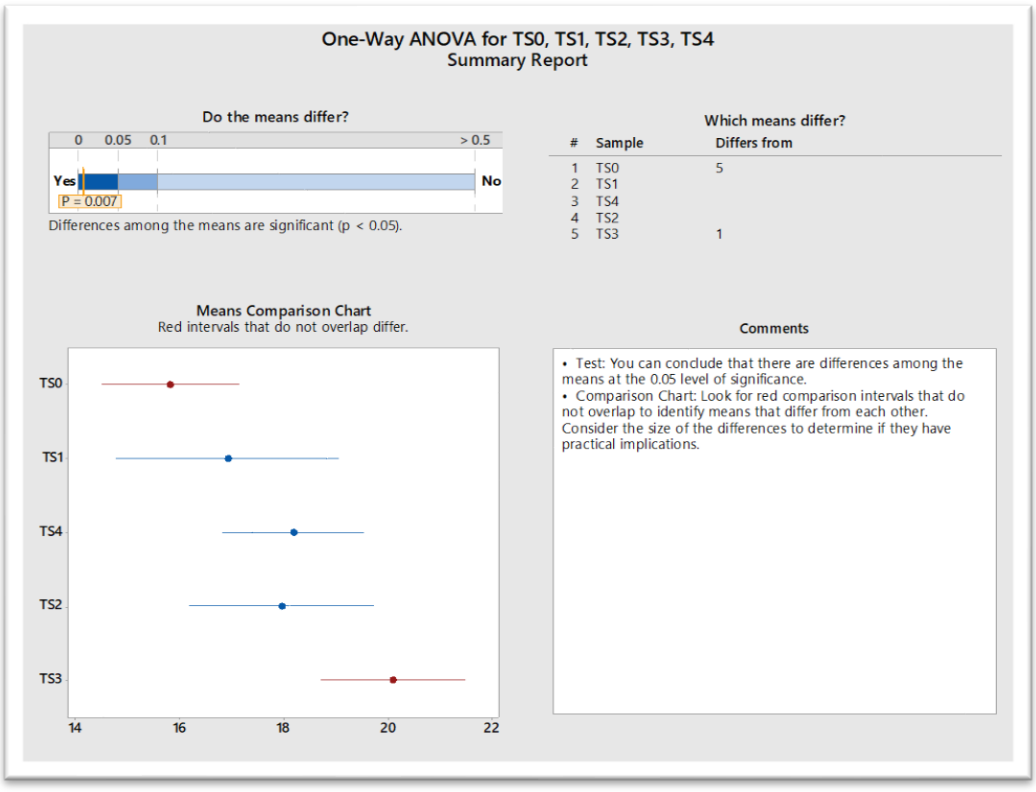

Figure 3-12: Result of one-way ANOVA hypothesis test of tensile strength of composite filaments with different MAPE content (0-4% by weight).

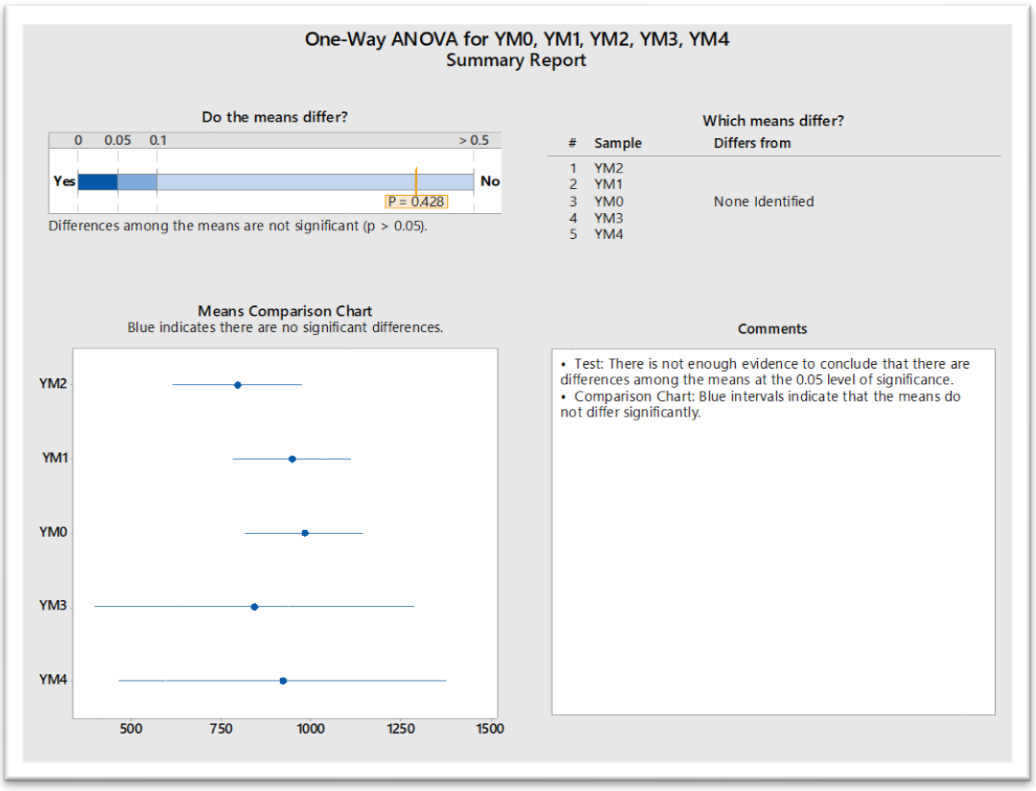

Figure 3-13: Result of one-way ANOVA hypothesis test of Young's modulus of composite filaments with different MAPE content (0-4% by weight).

3.4.7 Reinforced Rotationally Moulded Polyethylene Composites

Figure 3-14 shows the optical microscope images of the external surfaces of rotationally moulded composites produced with untreated and treated hemp fibre (5 wt.% content). It was observed that composites with untreated fibre were dark brown due to fibre thermal degradation. In contrast, thermal degradation was not evident for composites produced with alkali-treated fibre (Figure 3-14). In addition, a higher number of pores were observed on the surface of untreated fibre composites (Figure 3-14b and Figure 3-14d) compared to alkali-treated fibre composites (Figure 3-14a and Figure 3-14c). This behaviour is probably due to the release of volatiles during the thermal degradation of amorphous components present in untreated hemp fibre, such as hemicellulose and lignin, which together represent about 20% of the chemical composition of hemp fibres [34]. Previously in this research, TGA and FT-IR analyses confirmed that after the alkali treatment these amorphous components were partially removed.

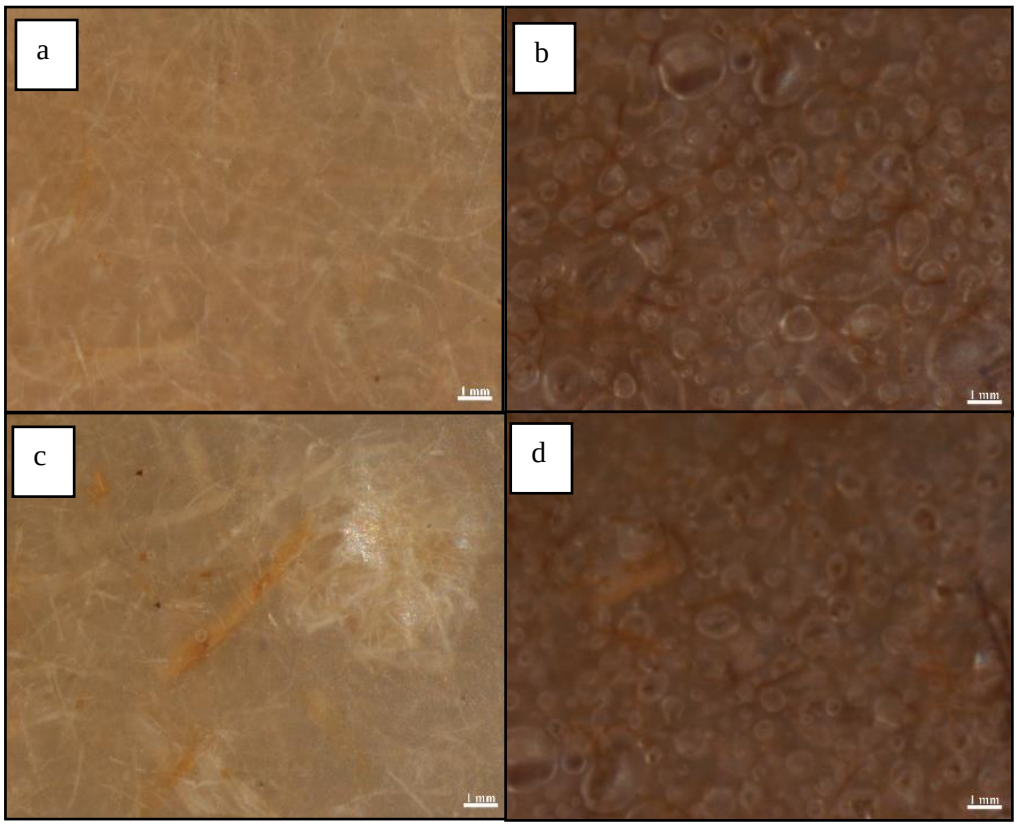

Figure 3-14: Optical microscopy images of the external surface of rotationally moulded hemp-PE composites, samples: 5TM (a), 5U (b), 5T(c) and 5UM (d). Sample code: T = treated hemp; U= untreated hemp, M = MAPE.

Rotationally moulded composites produced with untreated and treated hemp fibre were tensile tested, as shown in Figure 3-15. Composites produced with treated fibre showed higher tensile properties than composites with untreated fibre, regardless of the MAPE addition. This result is probably due to treated hemp fibres having a better fibre separation than untreated fibres, as previously shown by SEM. It is already known that an efficient fibre separation increases the effective fibre surface area available for wetting by the matrix, allowing efficient stress propagation from the matrix to the fibre.

Figure 3-15 also shows that the addition of MAPE in composites with 5 wt.% treated fibre increased their tensile properties (see Figure 3-16 and Figure 3-17). Previous studies in rotational moulding also reported an improvement in tensile properties using coupling agents such as MAPE [18; 118]. This is because the mechanical performance of short fibre-reinforced composites depends, amongst other factors, on an effective interfacial stress transfer between fibre and matrix [114; 119].

It was also observed that the addition of fibre in rotationally moulded composite did not improve its tensile properties compared to pure polyethylene. This was probably due to the increased porosity observed with the addition of fibre in rotationally moulded PE composites.

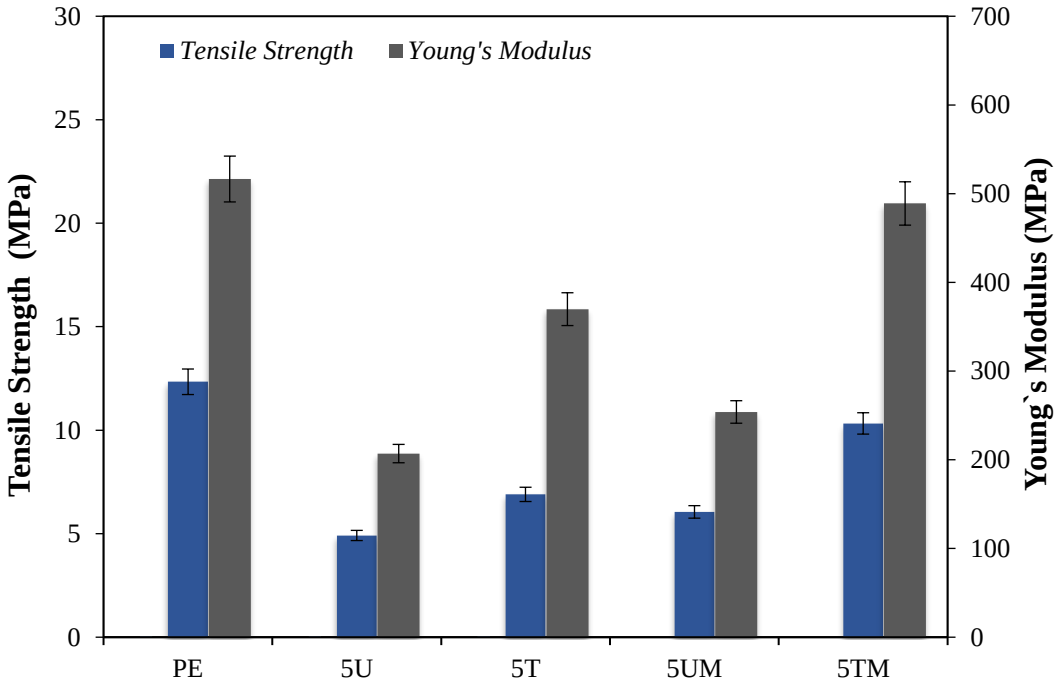

Figure 3-15: Tensile strength and Young's modulus of rotationally moulded composites. Sample code: fibre content (wt.%), T = treated hemp; U= untreated hemp, M = MAPE, PE = pure polyethylene.

Table 3-7: Statistical analysis of the tensile strength and Young's modulus of rotationally moulded composites. P>0.05 (Gaussian distribution).

Sample	*Sample size*	*Tensile Strength (MPa)*	*SD*	*CV*	*Young's modulus (MPa)*	*SD*	*CV*
PE	5	12.3	1.2	9.8	516.5	62.7	12.4
5U	5	4.9	0.6	11.8	207.2	48.7	24.7
5T	5	6.9	1.7	25.0	369.8	111.3	30.1
5UM	5	6.0	0.8	12.9	253.9	60.0	23.6
5TM	5	10.3	0.6	3.6	488.9	102.6	20.2

Sample code: Fibre content (wt.%), T = treated hemp; U= untreated hemp, M = MAPE, PE = pure polyethylene.

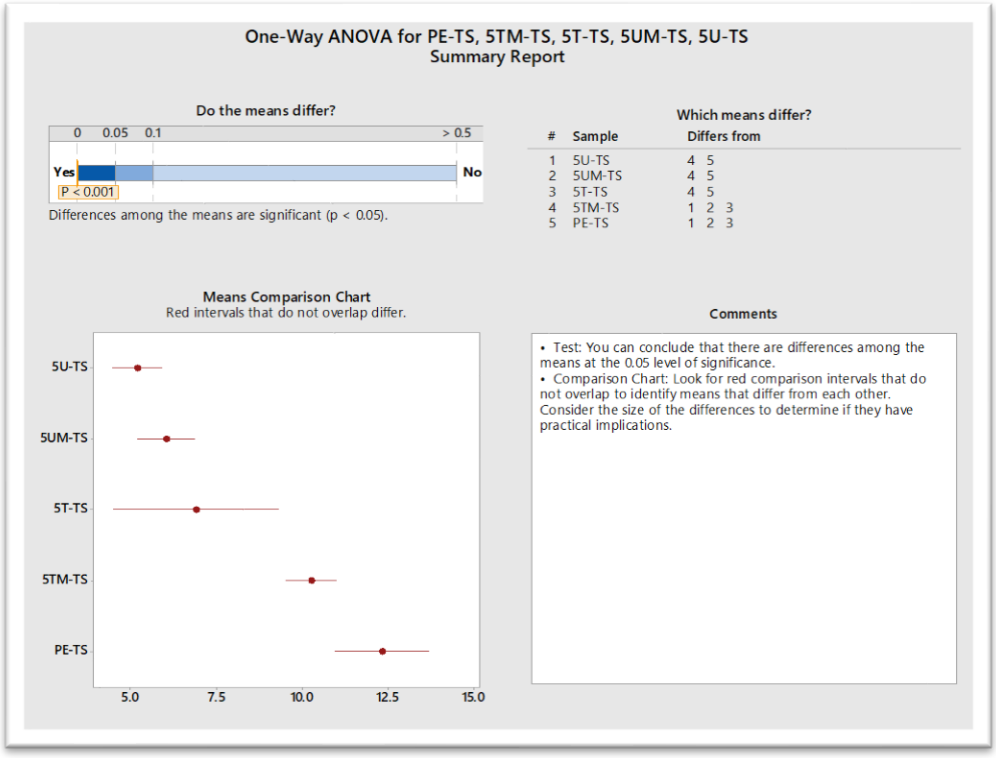

Figure 3-16: Result of one-way ANOVA hypothesis test of tensile strength (TS) of rotationally moulded composites with 5wt.% untreated (U) or treated (T) fibre with MAPE (M).

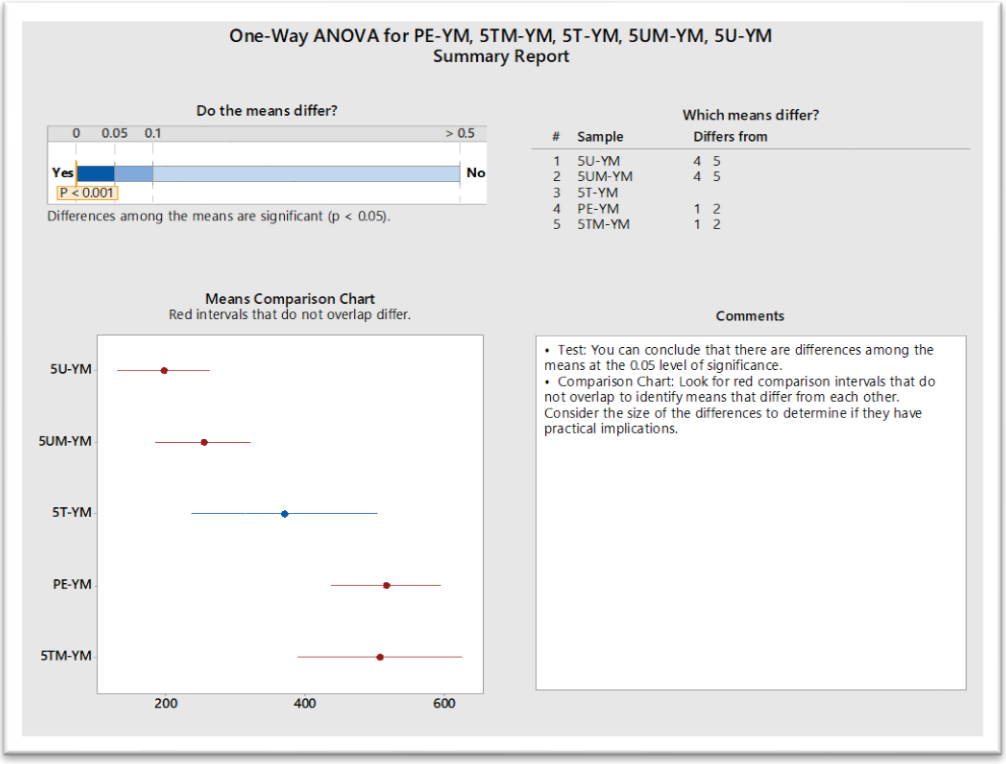

Figure 3-17: Result of one-way ANOVA hypothesis test of Young's modulus (YM) of rotationally moulded composites with 5wt.% untreated (U) or treated (T) fibre with MAPE (M).

Figure 3-18 shows photographs of rotationally moulded composites produced with 2.5, 5, 7.5 and 10 wt.% fibre content (composition described in Table 3-1). Fibre agglomeration increased considerably above 5 wt.% fibre content, as can be seen in Figure 3-18. Natural fibres tend to agglomerate due to their hydrophilic nature. In addition, achieving a good fibre distribution in rotational moulding is a challenge due to the absence of external pressure in this process. Composites with 10 wt.% fibre had insufficient consolidation for tensile testing due to poor fibre wetting by the matrix.

Figure 3-18: Rotationally moulded PE composites reinforced with different contents of treated hemp fibre.

All successfully rotationally moulded composites' tensile strength and Young's modulus were assessed (Figure 3-19). Composites with 2.5 and 5 wt.% of alkali-treated fibre maintained the same tensile strength as polyethylene. A reduction of about 9% in tensile strength was observed as the fibre content increased from 5 wt.% to 7.5 wt.% (Figure 3-20). This reduction was probably due to the increase in fibre agglomeration seen above 5 wt.% fibre content (Figure 3-18), reducing fibre wetting by the polymer, and hence the interface between them. This poor fibre distribution also explains the lower tensile properties of composites with 7.5 wt.% fibre compared to pure polyethylene.

The low-shear and pressure characteristics of rotational moulding limit the amount of reinforcement incorporated into rotationally moulded composites. In fact, fibre agglomeration/segregation and void formation are commonly associated with low mechanical properties in fibre-reinforced composites produced by rotational moulding [5; 120; 121]. There was no difference in Young's modulus with the addition of fibre, compared to PE (Figure 3-21).

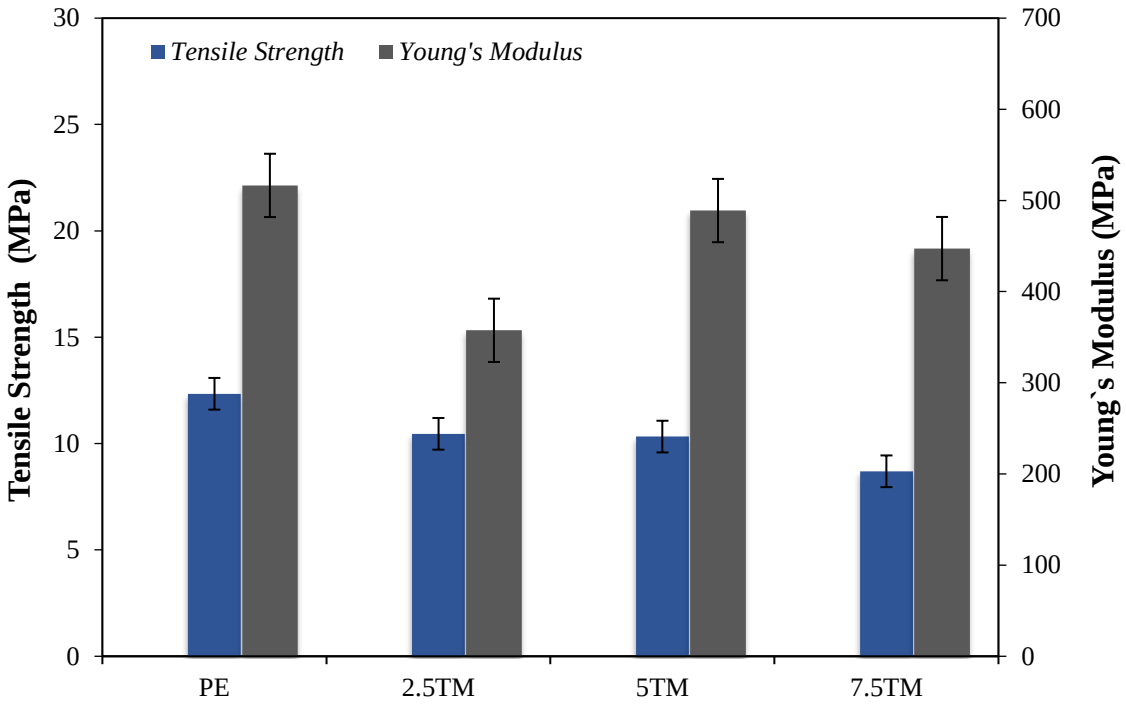

Figure 3-19: Tensile strength and Young`s modulus of rotationally moulded composites. Sample code: fibre content (wt.%), T = treated hemp, M = MAPE, PE = polyethylene.

Table 3-8: Statistical analysis of tensile strength and Young's modulus of rotationally moulded composites. P>0.05 (Gaussian distribution).

Samples	*Sample size*	*Tensile Strength (MPa)*	*SD*	*CV*	*Young's modulus (MPa)*	*SD*	*CV*
PE	5	12.3	1.2	9.8	516.5	62.7	12.4
2.5TM	5	10.4	1	9.5	375.5	57.3	9.5
5TM	5	10.2	0.4	3.6	490.2	48.7	3.6
7.5TM	5	8.9	1.0	11.6	447.2	60.0	11.6

Sample code: Fibre content, T = treated hemp, M = MAPE, PE = polyethylene.

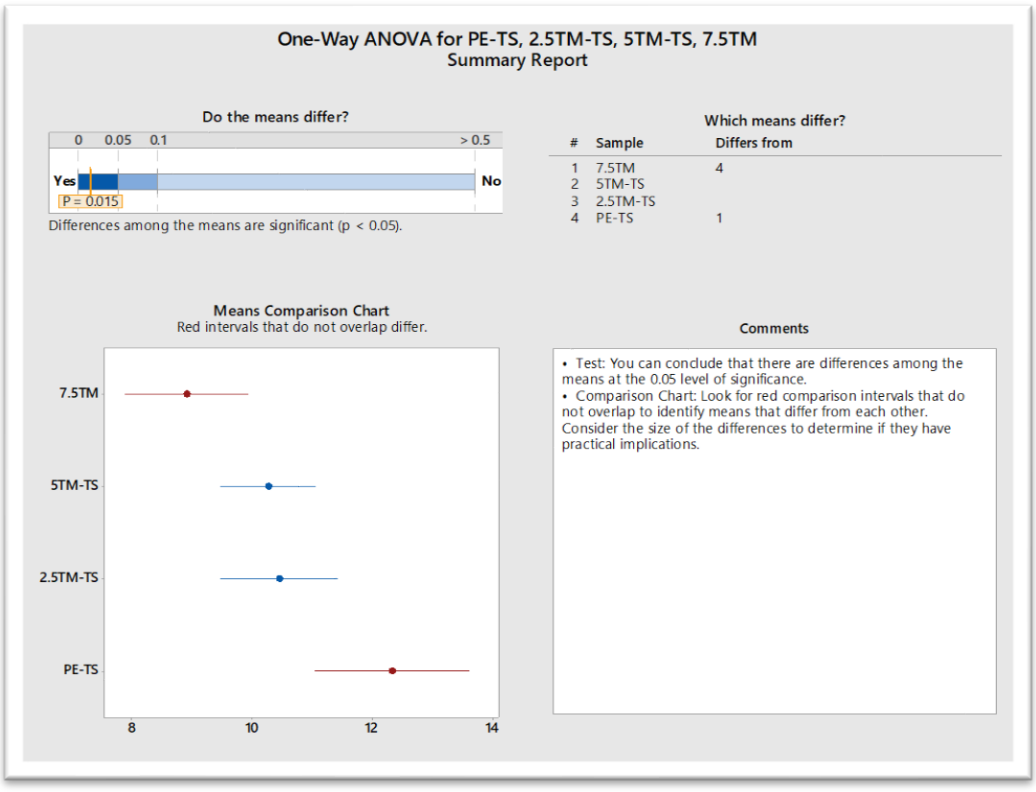

Figure 3-20: Result of one-way ANOVA hypothesis test of tensile strength of rotationally moulded composites with different content of treated fibre (T) and 3wt.% MAPE (M).

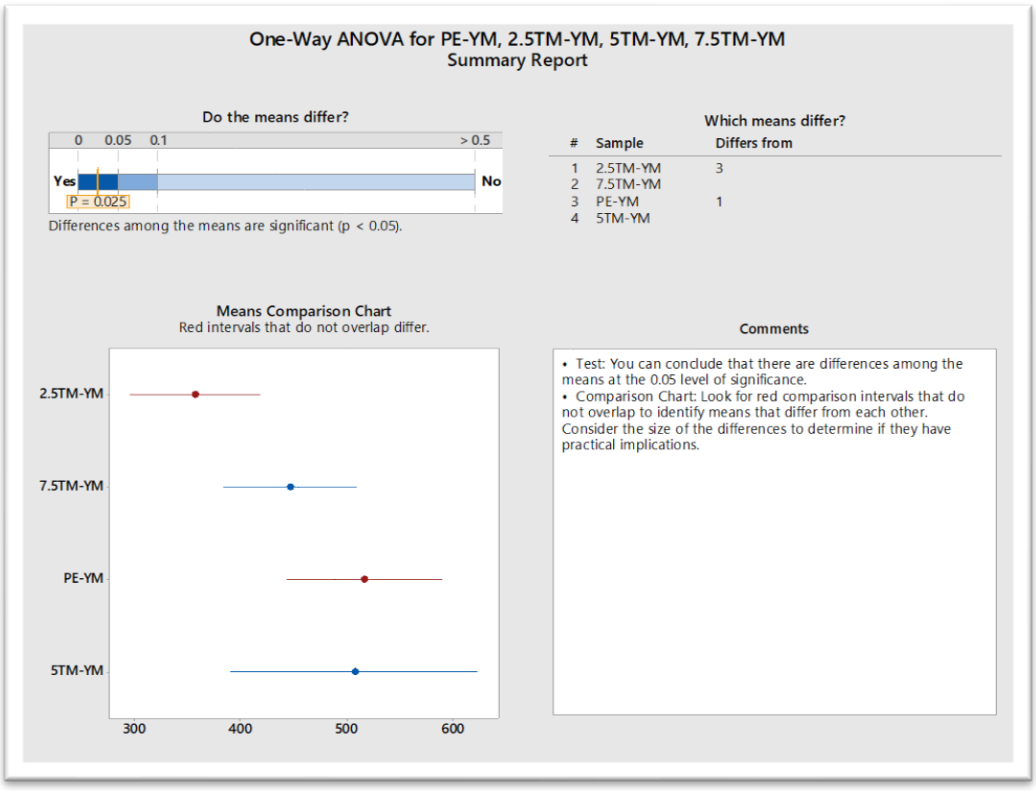

Figure 3-21: Result of one-way ANOVA hypothesis test of Young's modulus of rotationally moulded composites with different content of treated fibre (T) and 3wt.% MAPE (M).

SEM micrographs of the fracture surfaces of the highest performing composite, 5TM, were compared with those for 5T. Fewer fibre pull-outs (circles) and signs of fibre-matrix debonding (arrows) were observed for 5TM samples (Figure 3-22) compared with 5T samples (Figure 3-23). This behaviour indicates a weak interfacial adhesion between fibre and matrix without MAPE, since the fibres cannot support the applied load and are extracted mechanically. Furthermore, hemp fibres were attached to the polymer matrix in sample 5TM, which indicates a good interface between them (Figure 3-24). In contrast, there was a poor interface between the fibre surface and matrix for sample 5T (Figure 3-25). This result can be explained by the addition of MAPE, with which the carbonyl groups react by chemical bonding with the hydroxyl groups exposed after alkali treatment of the fibre surface, whereas the MAPE polymer chain entangles with the polymer matrix, thus improving interfacial bonding [15; 122].

Figure 3-22: Fracture surface image of sample 5TM (5wt.% treated fibre and MAPE).

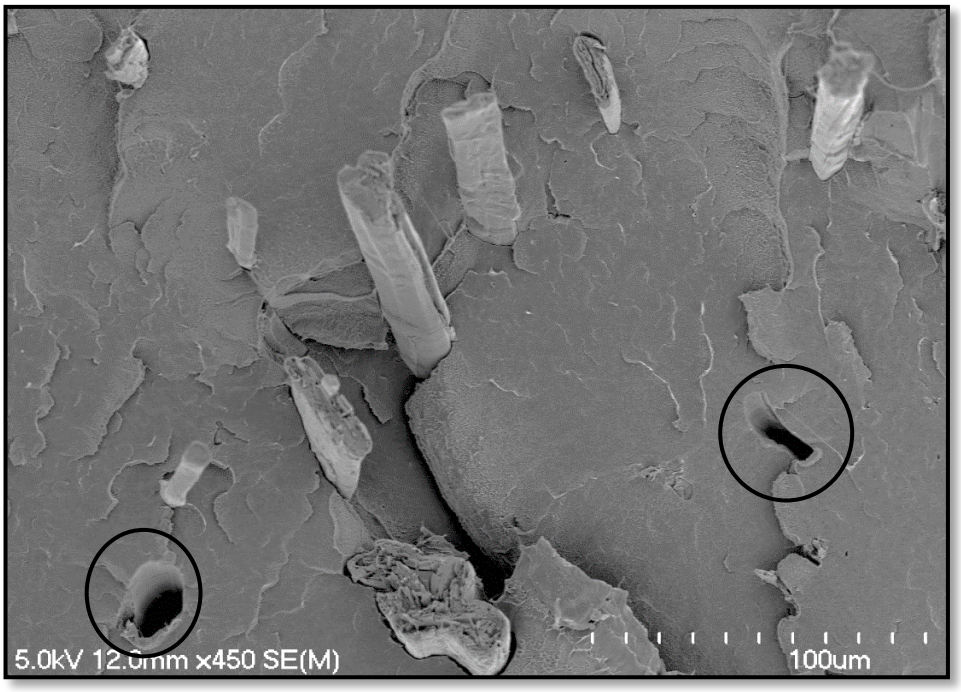

Figure 3-23: Fracture surface image of sample 5T (5wt.% treated fibre).

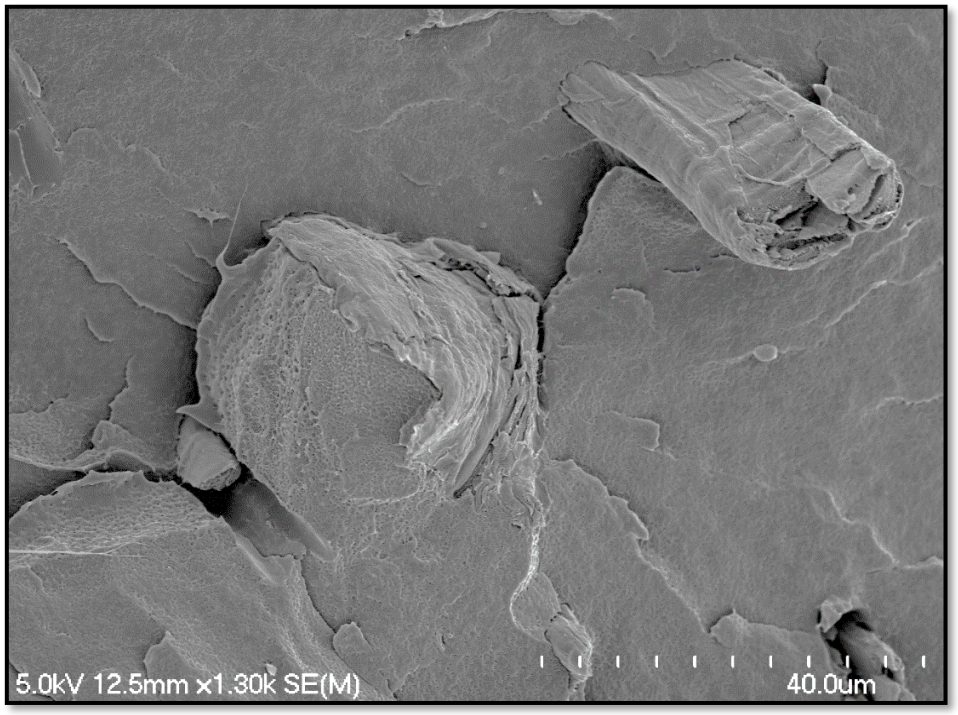

Figure 3-24: Fracture surface image of sample 5TM (5wt.% treated fibre and MAPE).

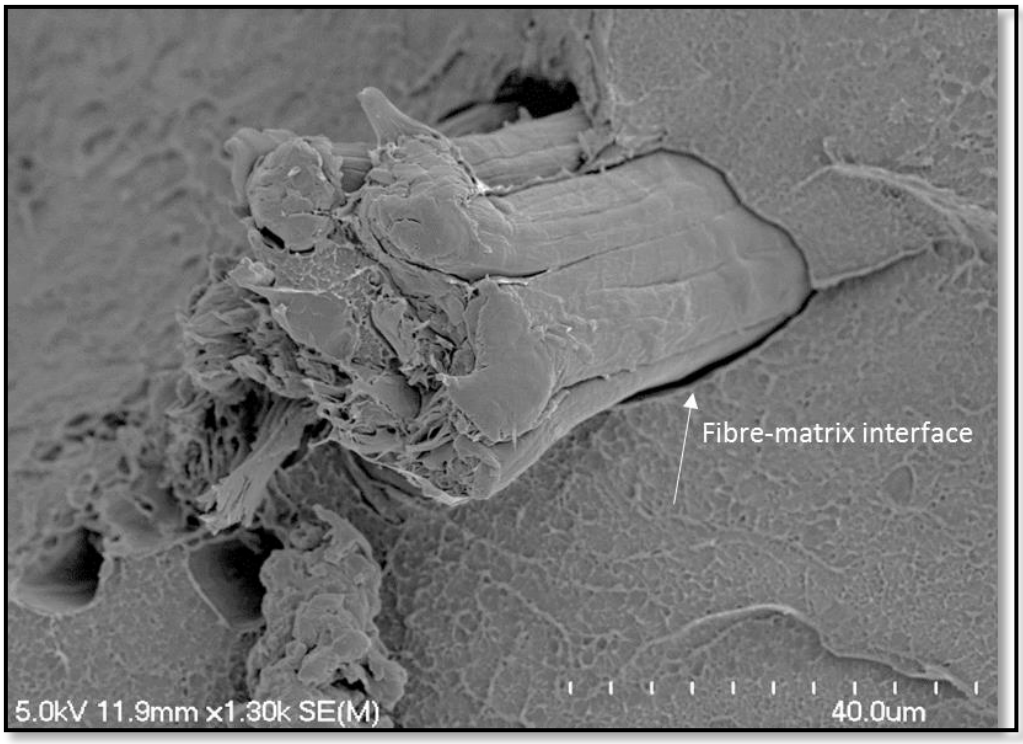

Figure 3-25: Fracture surface image of sample 5T (5 wt.% treated fibre).

3.5 Chapter Conclusions

As seen in previous research, alkali treatment removes non-cellulosic material such as lignin and hemicellulose, as supported by the FT-IR results. The removal of these non-cellulosic components is consistent with the reduction of fibre diameter and the improvement in fibre separation observed with SEM. Their removal also improved fibre resistance to thermal degradation, as shown by thermal analysis. It was observed that composites produced with alkali-treated fibre were more resistant to thermal degradation during the rotational moulding process. In contrast, composites with untreated fibre showed signs of thermal degradation, which resulted in low tensile strength and Young's modulus.

Filaments of composite with 3 wt.% MAPE showed the highest tensile strength, while no difference in Young's modulus was observed. For this reason, 3 wt.% was considered the optimum content of MAPE to bond PE with treated hemp fibres. Consequently, rotationally moulded composites with 5 wt.% alkali-treated fibre and 3 wt.% MAPE had superior tensile properties compared with samples without MAPE. However, above 5% by weight of fibre content, there was a reduction in the composites' tensile properties due to an increase in observed fibre agglomeration.

It was also observed that the addition of hemp fibre did not increase the tensile properties of the rotationally moulded composites compared to pure polyethylene, regardless of the use of MAPE. This result is likely due to a poor fibre-matrix interface resulting from a combination of fibre agglomeration and high porosity within the composites, caused by the absence of external pressure characteristic of rotational moulding. This highlights the importance of researching methods to improve fibre distribution and reduce porosity in rotationally moulded composites.

Chapter 4

The Use of Composite Pellets and Processing Aids to Produce Rotationally Moulded Hemp Fibre-Reinforced Polyethylene Composites

This chapter describes the use of composite pellets to produce reinforced rotationally moulded PE composites with increased fibre length. Alkali-treated fibre, MAPE and PE were compounded by extrusion, then randomly chopped into different sizes of pellet to be used in rotational moulding. The use of large pellets of composites in rotational moulding would be advantageous since large pellets would maintain the fibre length and eliminate costs associated with grinding. However, it was expected that porosity in rotationally moulded composites would increase with particle size. For these reasons, composites produced had their porosity assessed by optical microscopy, an Archimedes' density test and micro-CT.

The results showed that the size of voids within rotationally moulded composites increased with composite pellet size, reducing tensile strength and Young's modulus. However, composites produced with 1.5 mm pellet size had a higher fibre aspect ratio than composites produced with 0.5 mm pellet size, which can be favourable in improving mechanical performance. Therefore, processing aids (mineral oil and stearic acid) were tested to mitigate the composites' porosity when produced using a 1.5 mm pellet size.

The addition of 3 wt.% stearic acid reduced polymer viscosity during the process, which decreased composite porosity. Consequently, Young's modulus increased by about 18% compared to composites without stearic acid. This reduction in the mixture's viscosity allowed the fibre content to be increased from 10 to 12.5% in composites produced with 1.5 mm pellets, improving Young's modulus by about 24% compared to pure polyethylene. Above 12.5 wt.% fibre content, the composite produced lacked adequate consolidation for testing due to poor fibre wetting by the polymer.

4.1 Materials and Methods

4.1.1 Materials

Stearic acid with a molecular weight of 284.48 g/mol was obtained from Merck, and mineral oil, code 0707026, with a density of 0.87−0.89 g/mL was supplied by Ajax Finechem. The other materials for the production of the composites are described in Chapter 3.

4.2 Methods

4.2.1 Melt Compounding

A Labtech twin-screw extruder (Figure 4-1), L/D ratio 44:1, was used for compounding fibres with additives and polyethylene (Table 4-1). The temperature control on the extruder was separated into five zones, which were set at T_1:130 °C (barrel entrance), T_2:140 °C, T_3:140 °C, T_4:140 °C and T_5:125 °C (barrel exit).

Treated hemp fibre, MAPE, PE and the processing aids at different concentrations (see Table 4-1) were mixed by hand for 5 min prior extrusion. The composite material was drawn forward through the extruder barrel and further mixed and compressed to improve the melt homogeneity before extrusion through a 3 mm diameter circular die. The twin co-rotating screws were operated at 80 rpm.

Figure 4-1: Labtech twin-screw extruder.

Table 4-1: Details of the composition of rotationally moulded composites.

Sample code	***Fibre Content (wt%)***	***MAPE (wt%)***	***Additives (wt%)***	***Pellet size (mm)***
H10P0.5	10	3	--------	0.2-0.5
H10P1.5	10	3	--------	1.2-1.5
H10P1.5(MO1) H10P1.5(MO3)	10	3	1 3	1.2-1.5
H10P1.5(SA1) H10P1.5(SA3) H10P1.5(SA5)	10	3	1 3 5	1.2-1.5
H12.5P1.5(SA3)	12.5	3	3	1.2-1.5
H15P1.5(SA3)	15	3	3	1.2-1.5
H10P4	10	3	--------	3-4
Sample code: type of fibre (H = Hemp), fibre content (wt.%), (P=pellet) followed by their size and (SA = Stearic acid and MO= Mineral oil) and its concentration.				

4.2.2 Pelletising and Grinding

Extruded filaments were randomly chopped by granulation to convert this material into a suitable form for rotational moulding. The granulators (Figure 4-2 and Figure 4-3-left) - were fitted with a 4 mm and 1.5 mm aperture screen sieve, respectively, to provide control of the

size of the pellet produced. This material was further ground with a Power King microniser, as shown in Figure 4-3-right.

Figure 4-2: Moreto granulator, model CM20/20.

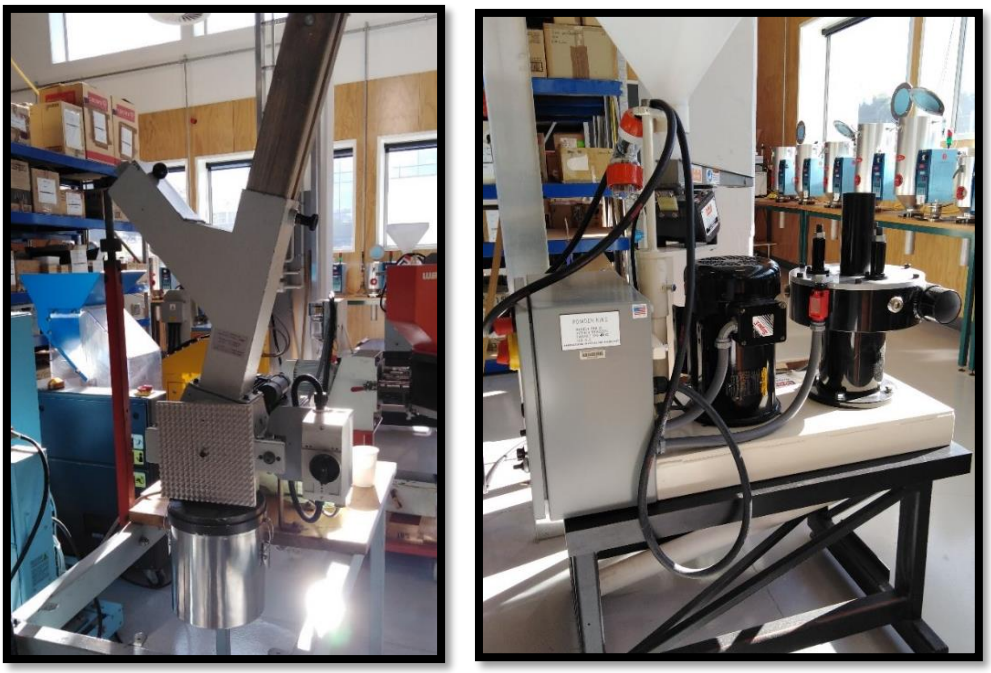

Figure 4-3: Retsch granulator, model SM 100 (left) and Power King microniser, model PKA 18 (right).

4.2.3 Thickness Adjustment of Rotationally Moulded Composites

Rotationally moulded composites were produced in a box-shaped mould and machined into individual sheets using a bandsaw. A Carbatec TH BX330P benchtop thicknesser was used to adjust the thickness of these sheets to about 3 mm. This material was later converted into specimens suitable for tensile testing.

4.2.4 Analysis of Fibre Length Distribution

Approximately 2 g of each sample of the composite was dissolved in 200 ml of boiling xylene (135 °C) for 30 min and then filtered through a mesh with aperture dimensions of 120 µm x 120 µm to separate the fibres from the xylene filtrate. These fibres were then dried and immersed in water with a small amount of dishwashing detergent to assist with fibre dispersal. An FQA-360 electronic sequential fibre length analyser was used to obtain a mean fibre length and fibre distribution for each composite.

4.2.5 Porosity by Optical Microscopy

Optical microscopy images of the surface of rotationally moulded composites were taken with 6.5x magnification, using a WILD M3B stereomicroscope fitted with a Nikon camera (Digital Sight DSU1). These images were used for porosity analyses by ImageJ. Twelve optical microscopy images were taken from an area of 400 cm^2 for each composite.

Porosity analysis was adapted from a previous study [123], whereas the porosity percentage was calculated according to Equation 4-1.

$$\text{Porosity (\%)} = \Sigma\text{pore area} / \Sigma\text{analysed area} \quad 4\text{-}1$$

4.2.6 Porosity by the Archimedes Density Test

The void content of rotationally moulded composites was determined according to ASTM D2734-16 (Standard Test Methods for Void Content of Reinforced Plastics). First, the density of the sample was measured using the Archimedes principle, where the specimen is weighed in air ($W_{specimen}$) and then weighed while submerged ($W_{submerged}$). Next, the sample volume ($V_{specimen}$) was calculated in conjunction with the submerging liquid density (Equation 4-2), which in this case was distilled water (ρ_{water}). The actual density of the five sample specimens was then calculated using Equation 4-3.

$$V_{specimen} = \frac{W_{specimen} - W_{submerged}}{\rho_{water}} \quad 4\text{-}2$$

$$\rho_{specimen} = \frac{W_{specimen}}{V_{specimen}} \quad 4\text{-}3$$

The void volume fraction (V_v) was calculated using Equation 4-4, with the mass fraction (%m) and density (ρ) of the primary constituents required. It is critical that the material properties are accurately known, as minor variations can significantly affect the accuracy of the calculated void volume fraction (V_v).

$$V_v = 100 - \rho_{specimen}\left(\frac{\%m_{matrix}}{\rho_{matrix}} + \frac{\%m_{fibre}}{\rho_{fibre}}\right) \quad 4\text{-}4$$

4.2.7 Porosity by Micro-CT

Micro-CT imaging was carried out using a Bruker SkyScan 1272 instrument (Bruker micro-CT, Kontich, Belgium) in the Auckland Bioengineering Institute's Micro-CT facility. Two rectangular samples cut to 4 x 4 x 3 mm from rotationally moulded hemp-PE composites produced with 0.5 and 1.5 mm pellet size were mounted in a 6 mm diameter straw; the device limits the sample size. Imaging parameters at 1 µm pixel size were: 48 kV, 200 µA, 1200 mS, no filter using a 4904-pixel wide camera selection. Scanning parameters were: 0.15 deg rotational step, 2x frame averaging, 4x random movement for 180 degrees rotation resulting in a 2 h and 6 min scan time. Reconstructions were carried out using InstaRecon®. Bruker DataView software was used to re-orientate the samples. Bruker CTAn v1.18.4.0 was used for the analysis. Datasets were downsized by 4 to reduce the file sizes for analysis.

4.2.8 Tensile Testing

Tensile testing specimens were cut on the orientation of the polymer flow during processing with the dimensions of sample V described in ASTM D638-14 "Standard Method for Tensile Properties of Plastics" due to the limited composite area available. These samples were placed in a conditioning chamber at 23 ± 3 °C and 50 ± 5 % relative humidity for 48 hours. The specimens were then tested according to ASTM D638-14 using an INSTRON-4204 universal testing machine fitted with a 10 KN load cell at a 1 mm/min crosshead speed. An extensometer was used to measure the composite strain. Five specimens of each composite were tested to failure.

4.2.9 Melt Flow Index

The melt flow indices (MFI) of the composites were determined according to ASTM D 1238-04 “Melt Flow Rates of Thermoplastics by Extrusion Plastometer”, using a moderated strain rate of 2.16 kg of static mass at 190 ℃ in a Pantech MFI400E device (Figure 4-4).

Figure 4-4: Pantech MFI400E.

4.2.10 Rheology Analysis

Rheology analysis of composites with different concentrations of processing aids was carried out using a parallel plate rheometer (TA instruments DHR-1). The tests were conducted on a 40 mm parallel plate at 190 ℃, shear rate from 0.1 to 100/s, and 1000 µm gap. The samples were cut from rotationally moulded HF-PE composites, 20 mm diameter and 3 mm thickness. Three samples of each composite were tested.

4.3 Statistical Analysis

The software MINITAB version 18.1 was used for the statistical analysis of the results of tensile testing. First, the values of different parameters were expressed as mean values with standard deviation and coefficient of variation. Then, one-way ANOVA was applied to

compare the differences in the mean values, with a 95% simultaneous confidence level. A hypothesis test evaluates two mutually exclusive statements about two or more population means to determine whether to reject the null hypothesis [106].

4.4 Results and Discussion

4.4.1 Rotationally Moulded Composites Produced with Different Composite Pellet Size

Treated fibre and polyethylene were melt compounded by extrusion and randomly chopped into pellets of 4, 1.5 and 0.5 mm size to be used in rotational moulding. Melt compounding fibre and matrix by extrusion before rotational moulding has been reported to improve fibre distribution and segregation [22]. Actually, melt compounding materials prior rotational moulding allowed the incorporation of 10 wt.% fibre content with apparent uniform fibre distribution. The previous chapter showed a high increase in fibre agglomeration above 5 wt.% in composites prepared using the dry-mixing technique.

Figure 4-5c shows that the surface aesthetics of rotationally moulded composites was greatly affected by using 4 mm composite pellet size. The large size of these pellets combined with the low thermal conductivity of natural fibres increased polymer melting time, which means that these pellets did not fully melt during the process. For this reason, no further experiments were performed with composites produced using a 4 mm pellet size.

In contrast, rotationally moulded composites produced with 0.5 and 1.5 mm pellet sizes presented satisfactory surface aesthetics (Figure 4-5a and Figure 4-5b). It was observed that larger particles tended to migrate to the mould's inner surface during the process, whereas a higher fraction of finer particles were located on the outer surface of the moulding. This natural sieving behaviour during rotational moulding has been previously reported in the literature [124].

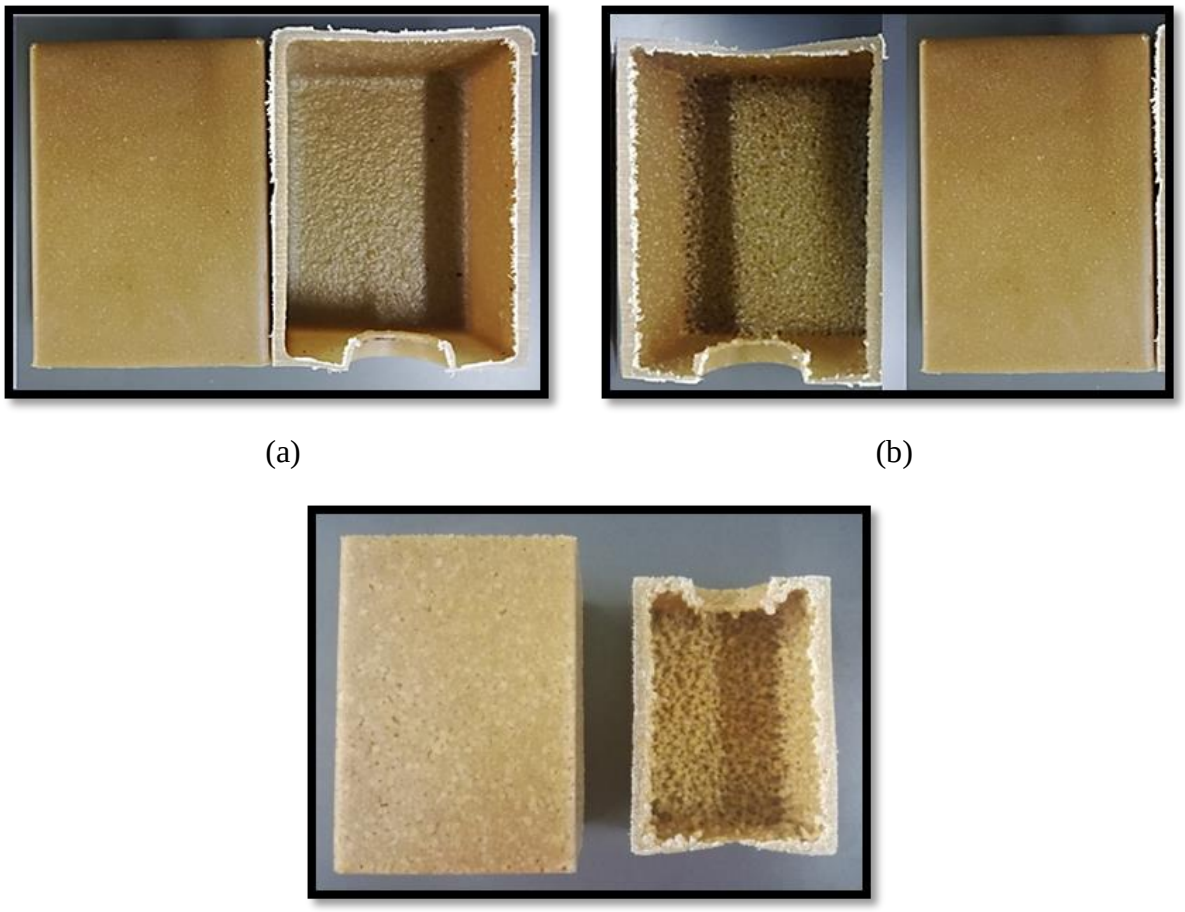

(a) (b)

(c)

Figure 4-5: Photographic images of the following samples: H10P0.5(a), H10P1.5(b) and H10P4(c). Sample code: (H = Hemp), fibre concentration, (P= pellet) followed by pellet size.

4.4.2 Porosity Analysis by Optical Microscopy

Optical microscopy images of the external surface of rotationally moulded composites produced with 1.5 and 0.5 mm pellet size are shown in Figure 4.6. As the pellet size increased from 0.5 to 1.5 mm, fewer but larger voids were more evident on the composite surface. Porosity analysis showed that the size of the voids ranged from 100–400 µm in composites with 0.5 mm pellet size and from about 100–900 µm in composites with 1.5 mm pellet size (Figure 4-7). The occurrence of larger voids was associated with the higher porosity found in composites produced with 1.5 mm pellet size compared to composites with 0.5 mm pellet size (Table 4-2). Similarly, previous studies have reported heating rate and particle size as the two most significant variables affecting polymer densification in rotational moulding [125]. This is because the polymer flow and the heat transfer during the process are reduced by increasing the size of the pellets used in rotational moulding, which negatively

affect polymer sintering [126-128]. It must be noted that even though optical microscopy provides valuable information about the void size and porosity on the surface of composites, the accuracy of this technique is limited due to adjustments of the image analysis software threshold, which are subject to error.

Table 4-2 Porosity analysis of rotationally moulded composites with different pellet sizes

Sample	***Sample Size***	***Porosity per area (%)***	***Void size - median (µm)***
H10P0.5	12	2	211
H10P1.5	12	5	270

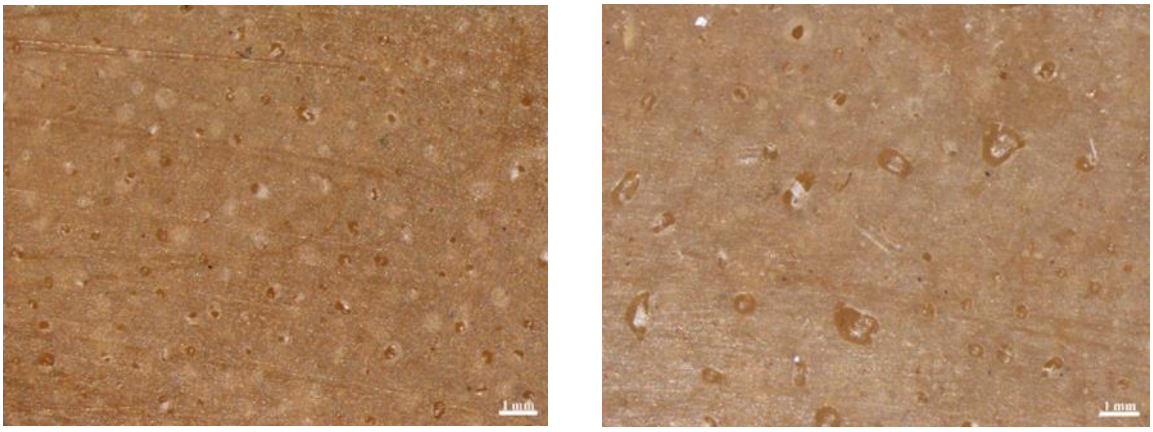

a) b)

Figure 4-6: Optical microscope images of rotationally moulded composites H10P0.5(a), and H10P1.5 (b). Sample code: (H = Hemp), fibre content (wt.%), (P= pellet) followed by pellet size.

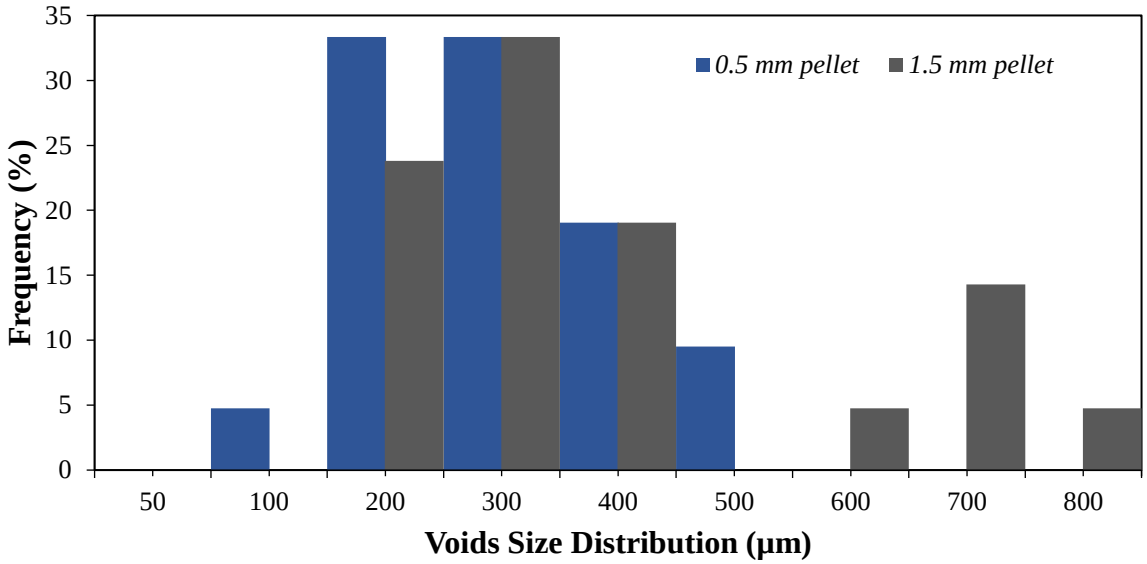

Figure 4-7: Void size and distribution in the composites: H10P0.5 (blue) and H10P1.5 (black). Sample code: H = Hemp, fibre content (wt.%), P= pellet followed by pellet size.

4.4.3 Porosity Analysis by the Archimedes Density Test

Porosity analysis using the Archimedes density test is suitable for qualitative purposes as it is inexpensive and can be performed relatively quickly. However, the accuracy of this method is limited by needing precise knowledge of the density and volume fraction of the materials, as minor variations can affect the calculated void volume fraction [124; 129]. Optical microscopy analysis also gives information about the apparent porosity in the composite. The results showed that composites produced with 1.5 mm pellet size were twice as porous as composites produced with a pellet size of 0.5 mm (see Table 4-3). Porosity in rotationally moulded composites is mainly associated with the inclusion of air during the process, which cannot be eliminated due to the absence of external pressure.

Table 4-3 Porosity analysis of rotationally moulded composites with different sizes of composite pellets by the Archimedes density test.

Sample	***Sample Size***	***Porosity (vol. %)***
H10P0.5	5	3.2
H10P1.5	5	6.2

4.4.4 Porosity Analysis by Micro-CT

The internal geometry of rotationally moulded composites was observed and analysed by X-ray micro-CT. This technique allows the reconstruction of images composed of several planes in a 3D spatial configuration (Figure 4-8) and provides information about void size and porosity. It was observed that the composite produced with a 1.5 mm pellet size (Figure 4-8b) had larger but fewer voids than the composite produced with a 0.5 mm pellet size (Figure 4-8a). Figure 4-9 shows that void sizes in the composite produced with 0.5 mm pellet size ranged from 170-414 µm, while void sizes in the composite with 1.5 mm pellet size ranged from 170-742 µm (Figure 4-10). This result was supported by image analysis performed using optical microscopy (Item 4.3.2).

Porosity analysis using micro-CT also showed that the composite produced with a 1.5 mm pellet size was twice as porous as the composite produced with a 0.5 mm pellet size (see Table 4-4). The same trend of increased porosity per volume with pellet size was observed in porosity analyses using the Archimedes density test. The challenge of comparing the results from these techniques lies in the different factors that limit the accuracy of each one. Also, it is not possible to comment on the accuracy of each method applied in this research, as the actual void content is unknown. The advantage of micro-CT is its ability to construct 3D images of the internal structure of a sample, and consequently provide information about void size, distribution and volume fraction. However, micro-CT is limited to small sample sizes (ideal size of 1 mm^3) and is a very expensive technique. Another limitation of micro-CT is that its accuracy relies on scan resolution and threshold adjustment. Micro-CT scans commonly visualise scanned objects by selecting a grey value threshold that separates solid material from air, and high variability due to threshold selection has been reported [130].

Table 4-4: Porosity analysis by micro-CT of rotationally moulded composites with different pellet sizes.

Sample	*Size range of voids (µm)*	*Porosity (vol. %)*
H10P0.5	100-400	0.469
H10P1.5	100-600	1.063

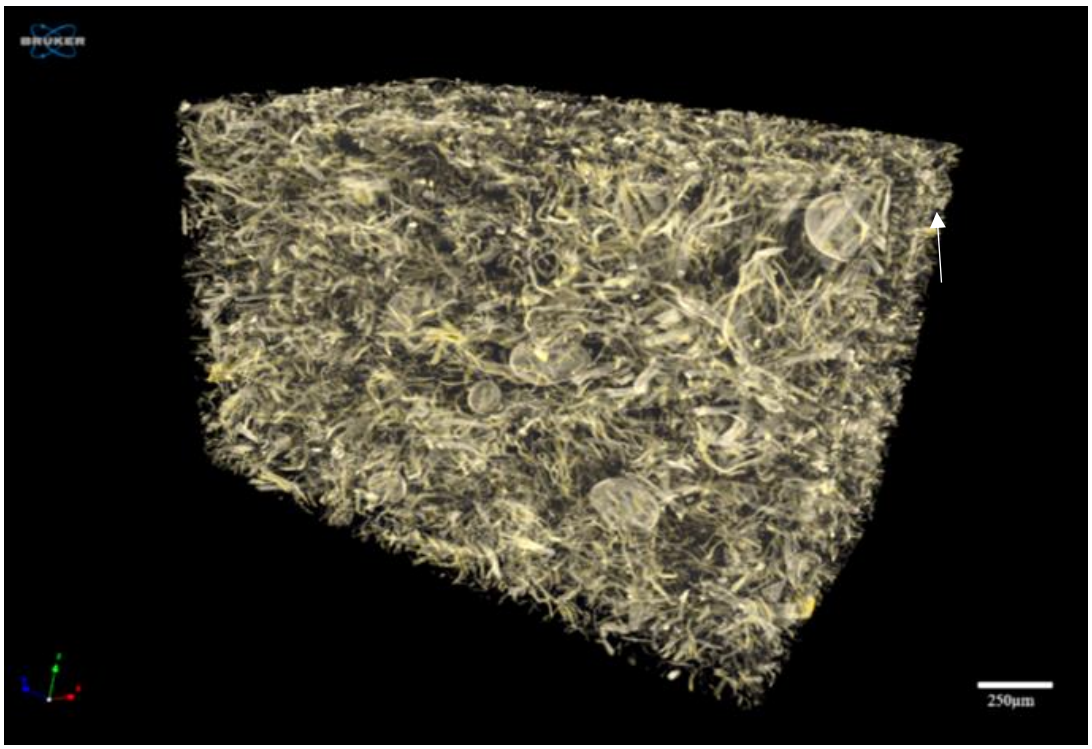

(a)

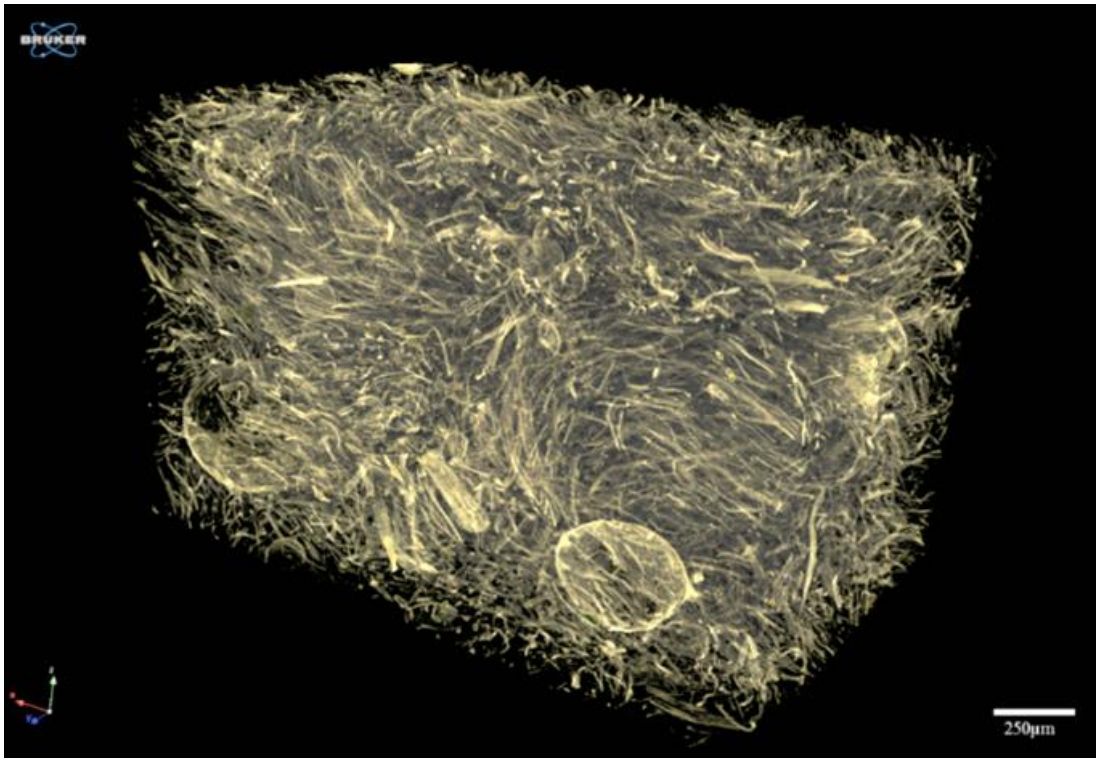

(b)

Figure 4-8: 3D images of the rotationally moulded composites produced with pellet sizes of 0.5 mm (a) and 1.5 mm (b).

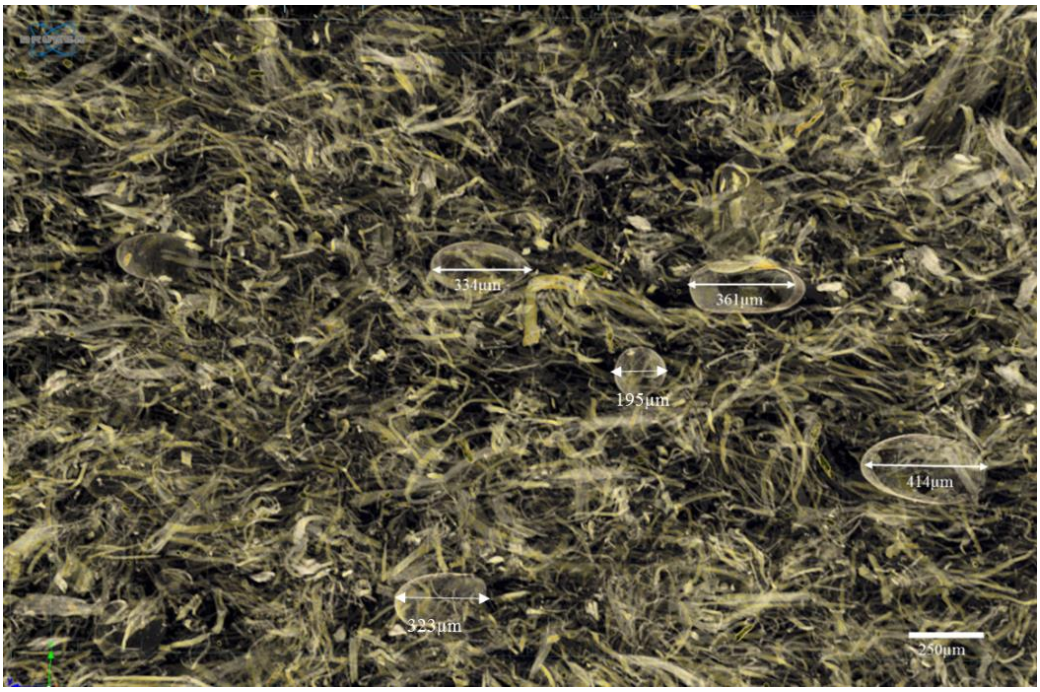

Figure 4-9: 2D image of the rotationally moulded composite produced with 0.5 mm pellet size.

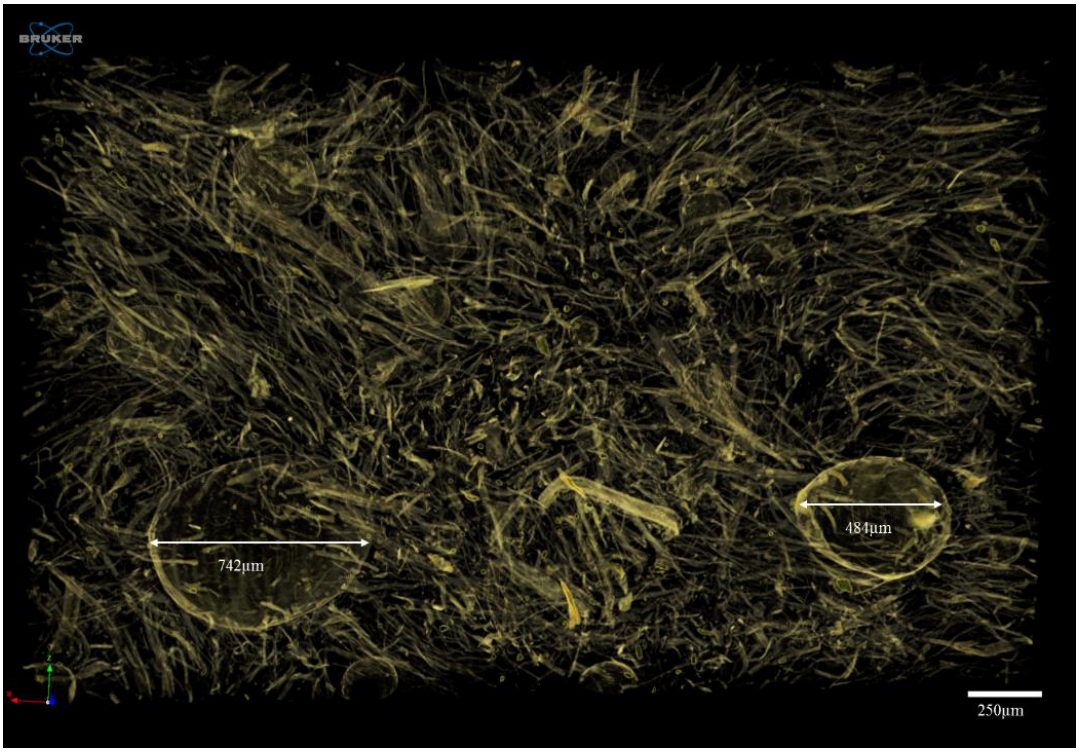

Figure 4-10: 2D image of the rotationally moulded composite produced with 1.5 mm pellet size.

4.4.5 Analysis of Fibre Length Distribution

Figure 4-11 shows the fibre length distribution in composites produced with 0.5 mm and 1.5 mm pellet sizes. Initially, the treated hemp fibres were 1.2 mm long, and after the extrusion, their length was about 500 µm. This reduction in fibre length was associated with fibre breakages induced by the extrusion, which occurs due to polymer interaction, fibre-fibre interaction, and fibre contact with the surfaces of the processing equipment [43]. Similarly, previous work reported a fibre length reduction of about 60% after the extrusion of hemp fibre [131].

Composites produced with 0.5 mm pellet size had a weighted fibre length of about 175 µm (aspect ratio of 7), while composites produced with 1.5 mm pellets had a weighted fibre length of 256 µm (aspect ratio of 11). This further fibre reduction in composites produced with 0.5 mm pellet size is due to multiple granulations and grinding. This result confirms that using larger pellets in rotational moulding would be beneficial in maintaining fibre length.

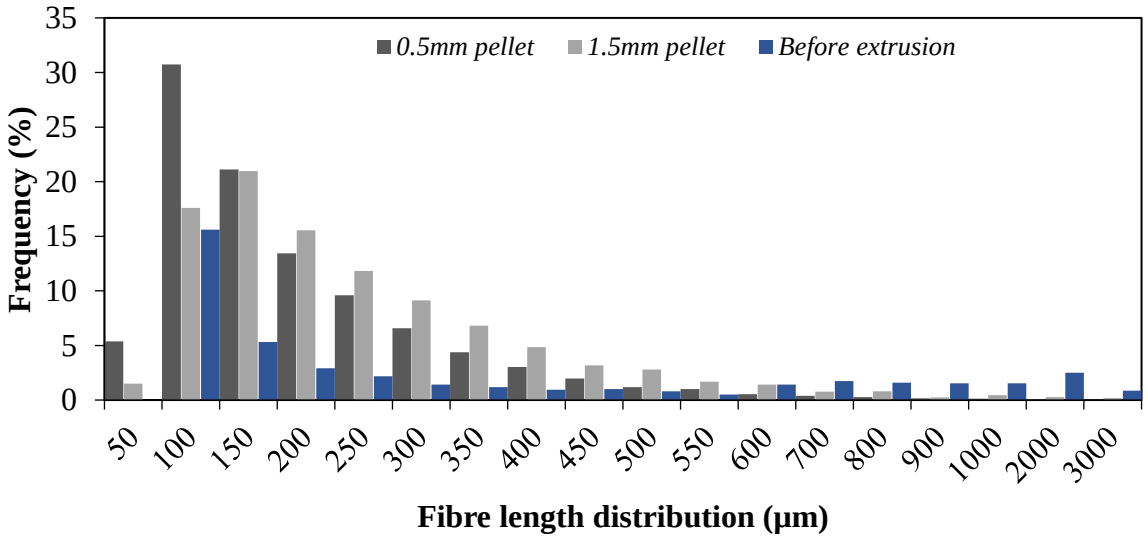

Figure 4-11: Fibre length distribution in composites produced with 0.5 and 1.5 mm pellet sizes, and fibre lengths before extrusion.

4.4.6 Tensile Testing of Rotationally Moulded Composites

Figure 4-12 shows the results of tensile testing of rotationally moulded composites produced with different pellet sizes. It was observed that the tensile properties of the composite produced with 0.5 mm pellet size were not statistically different from pure PE (Figure 4-13). The addition of fibres, which have higher strength and stiffness than the polymeric matrix, is

expected to improve the tensile properties of composites [6; 132]. However, this reinforcement depends on the interface between fibre and matrix as well as the fibre length. This result implies that the fibre length reduction, after extrusion and micronizing processes, led these fibres to act like fillers; therefore, no reinforcement was obtained.

In contrast, the composite produced with 1.5 mm pellet size had a lower tensile strength and Young's modulus than PE (Figure 4-12 and Table 4-5). This reduction in tensile properties compared to pure PE was attributed to the porosity in composites produced with 1.5 mm pellet size. It is well known that voids significantly affect the stress transfer from the matrix to the fibre, which is detrimental to the mechanical properties of composites. The stress concentration around the voids also facilitates crack initiation, which reduces tensile strength [129]. The results were subjected to statistical analysis by ANOVA with a 95% confidence interval (see Figure 4-13 and Figure 4-14). Composite pellets of 1.5 mm size were found to have potential for use in rotational moulding if the porosity in the final composite is addressed. This is because additional steps such as grinding require more time, add costs to the process, and lead to further fibre length reduction.

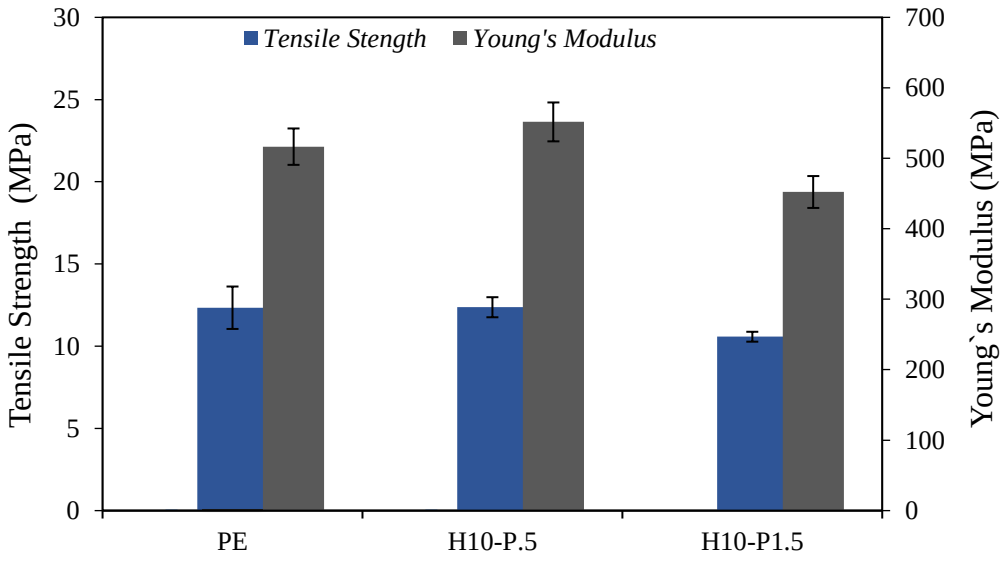

Figure 4-12: Tensile strength and Young's modulus of rotationally moulded composites and pure polyethylene powder. Sample code: (H = Hemp), fibre concentration, (P= pellet) followed by pellet size.

Table 4-5: Statistical analysis of the tensile strength and Young's modulus of rotationally moulded composites. P>0.05 (Gaussian distribution).

Sample code	***Sample Size***	***Tensile Strength (MPa)***	***SD***	***CV***	***Young's Modulus (MPa)***	***SD***	***CV***
PE	5	12.34	1.2	9.69	516.5	62.7	12.38
H10P0.5	5	12.37	0.7	5.58	551.6	24.3	4.41
H10P1.5	5	10.75	0.3	2.65	459.2	13.9	3.05
Sample code: H = Hemp, followed by fibre content (wt.%), P= pellet, followed by pellet size and PE = pure polyethylene.							

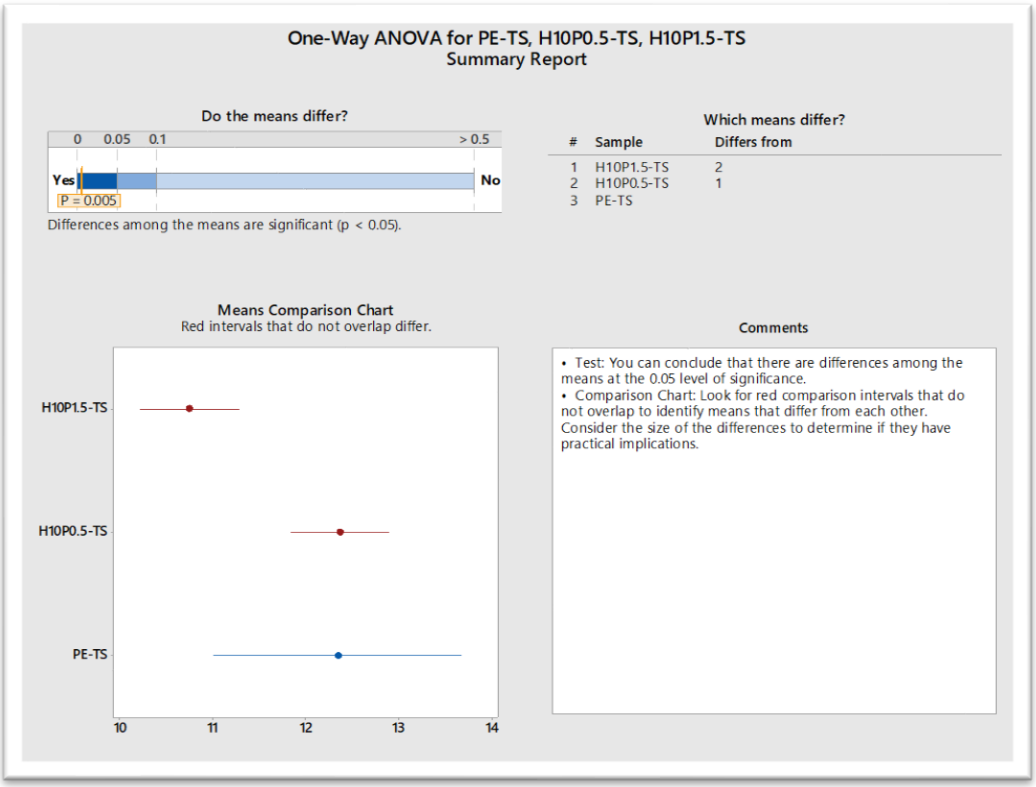

Figure 4-13 Result of one-way ANOVA hypothesis test of the tensile strength (TS) of rotationally moulded composites produced with composite pellets of 0.5 and 1.5 mm size, and pure PE.

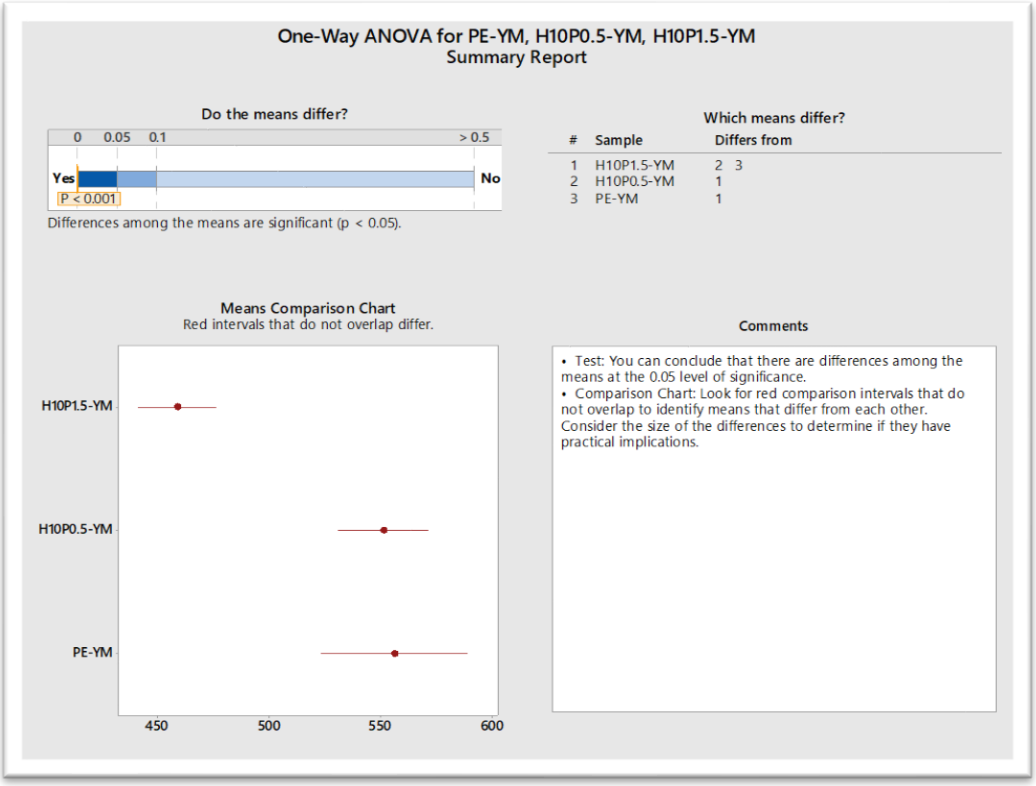

Figure 4-14: Result of one-way ANOVA hypothesis test of the Young's modulus (YM) of rotationally moulded composites produced with composite pellets of 0.5 and 1.5 mm size, and pure PE.

4.4.7 Use of Processing Aids in Composites Produced with 1.5 mm Pellet Size

4.4.7.1 Melt Flow Index (MFI)

In this study, mineral oil and stearic acid were tested at different concentrations in rotationally moulded composites produced with 1.5 mm pellet size to determine their ability to improve polymer flow during processing. The melt flow index (MFI) of composites is an important physical parameter, which indicates how easily the molten polymer flows during processing. However, MFI takes no account of the shear rate effect. Instead, it is a single-point viscosity measurement at a relatively low shear rate and a specific temperature.

Figure 4-15 shows that the addition of 1 wt.% of mineral oil did not change the viscosity of the polymer/fibre mixture. In contrast, a slight increase in MFI was observed in composites with mineral oil at 3 wt.% and stearic acid at 1 and 3 wt.%. This increase in MFI indicates a reduction in polymer viscosity. However, these results were not statistically significant at the 95% confidence level (P=0.07). In contrast, the addition of 5 wt.% stearic acid slightly reduced the MFI of this composition, indicating an increase in polymer viscosity.

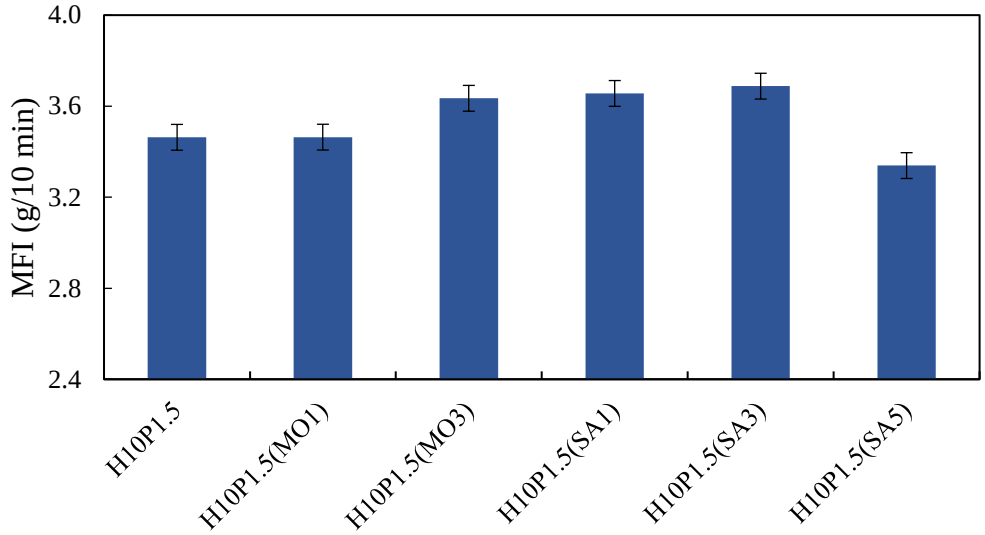

Figure 4-15: Melt flow index of rotationally moulded composites without and with processing aids. Sample code: H = Hemp, fibre content (wt.%), P= pellet, followed by pellet size, MO= mineral oil, SA=stearic acid and their respective concentration (wt.%).

4.4.7.2 Rheology Analysis

Rheology analysis was performed to investigate the effect of using processing aids on the mixture polymer/fibre viscosity (η) at low shear rates, simulating the conditions of rotational moulding (at low-speed rotation). Figure 4-16 shows that mineral oil at 1 wt.% content was not sufficient to change the viscosity of the molten polymer/fibres. However, the addition of 3 wt.% mineral oil reduced the mixture viscosity at low shear rates. This is because low molecular weight substances, such as mineral oils, act as lubricants, facilitating the movement of the polymer chains, thus improving the polymer flow.

Likewise, the addition of stearic acid at 1 and 3 wt.% reduced the polymer viscosity at low shear rates, as shown in Figure 4-16. Stearic acid lowers fibres' surface tension and their tendency to agglomerate, thus improving fibre wetting by the polymer matrix. Consequently, the fibre dispersion in the polymer matrix is enhanced, which reduces polymer/fibre viscosity during the process [62; 133-135]. Similar results have been reported by adding stearic acid in polypropylene/calcium carbonate nanoparticles [136].

The determination of the optimal content of surfactant is essential for an efficient treatment, as an insufficient amount might not cover evenly the particles, but an excess forms a core-shell structure leading to processing issues [60]. Likewise, previous research with EVA has reported the excess of stearic acid accumulates in the matrix, forming regions or networks inside it, which restrict polymer chain flexibility [137]. This restriction on polymer chain

flexibility explains the increased composition viscosity with 5 wt.% stearic acid, as shown in Figure 4-16.

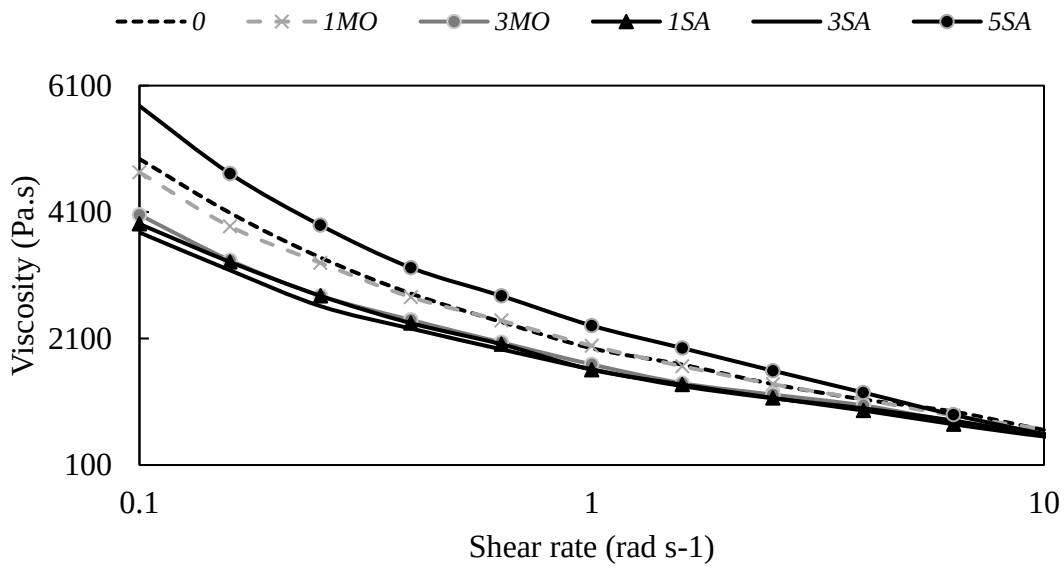

Figure 4-16: Viscosity of rotationally moulded composites (10 wt.% HF) produced with the processing aids: mineral oil (MO) at 1 and 3 wt.%, and stearic acid (SA) at 1, 3, and 5 wt.%.

4.4.7.3 Porosity measured using the Archimedes Density Test

The effect of processing aids on composite porosity was evaluated using the Archimedes density test. This method was chosen because it is easy to perform and provides valuable information about composite open porosity for qualitative analyses. A slight reduction in composite porosity was observed with the addition of mineral oil and stearic acid, as shown in Figure 4-17. The only exception was stearic acid at 5 wt.% content, which did not reduce the porosity of the composites.

The most significant reduction in porosity within the composite was with 3 wt.% stearic acid, due to the reduction of polymer viscosity, as previously reported by rheology analysis (Section 4.3.6). Polymer viscosity during rotational moulding is reported to affect the degree of porosity in the final product, as highly viscous polymers tend to obstruct the passage of air molecules through the melt [138]. Therefore, improving polymer flow during the process allows the air trapped in the molten polymer to diffuse and be released. Likewise, previous research has reported reductions in the porosity of rotationally moulded products with the addition of mineral oil and glycerol monostearate to decrease melt viscosity and elasticity at a low shear rate [27].

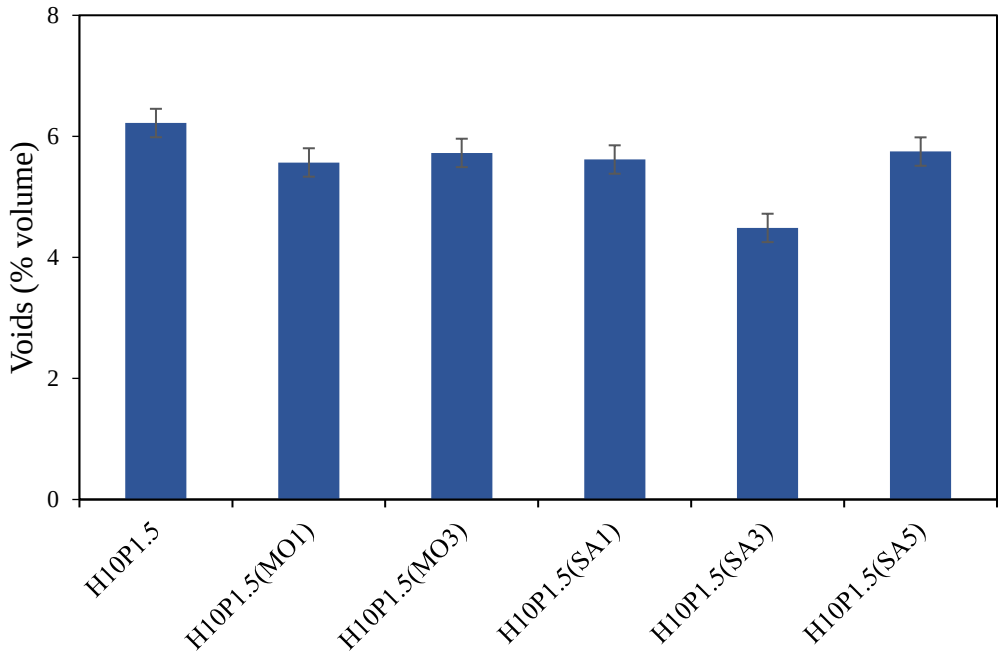

Figure 4-17: The porosity in rotationally moulded samples. Sample code: H = Hemp, fibre content (wt.%), P= pellet, followed by pellet size, MO= mineral oil, SA=stearic acid and their respective concentration (wt.%).

Table 4-6: Results of porosity analysis of rotationally moulded composites.

Sample	***Sample Size***	***Median (%)***
H10P1.5	5	6.4
H10P1.5(SA5)	5	5.7
H10P1.5 (MO3)	5	5.7
H10P1.5(SA1)	5	5.6
H10P1.5(MO1)	5	5.6
H10P1.5(SA3)	5	4.5

Sample code: H = Hemp, fibre content (wt.%), P= pellet followed by pellet size, MO= mineral oil, SA=stearic acid and their respective concentration (wt.%).

Rotationally moulded composites produced with 1.5 mm pellets and different proportions of mineral oil and stearic acid were tensile tested (Figure 4-18- Table 4-7). The addition of these processing aids did not significantly affect the tensile strength of rotationally moulded composites as confirmed by one-way ANOVA with a 95% confidence interval (Figure 4-19). This result was expected as the addition of processing aids was not supposed to increase the bonding between fibre and polymer matrix. Previous studies have suggested that the carboxyl groups of stearic acid can react with the hydroxyl (OH) groups available in cellulosic fibres by hydrogen bonding, improving tensile properties [6; 134]. However, those bonds are not as

strong as the covalent bonds between MAPE and hemp fibres. However, there was a significant reduction in the composite's Young's modulus with the addition of 3 wt.% of mineral oil, as shown in Figure 4-18. This reduction in Young's modulus indicates that mineral oil acted as a plasticiser. Plasticisers position themselves between polymer molecules, increasing flexibility and processability by interfering with polymer-polymer chain interactions, which also reduces Young's modulus [139].

In general, composites with 3 wt.% stearic acid presented the highest Young's modulus amongst the composites tested, as shown in Figure 4-18. This result was probably due to the reduction in composite porosity, as previously discussed (Item 4.2.2). Stearic acid prevents fibre agglomeration by reducing fibre-fibre interaction, thus improving fibre dispersion and wettability, resulting in a higher Young's modulus [134; 140-142]. Previous research reported tensile properties being increased by 23% with the use of treated sisal fibre with 3% stearic acid in polyethylene composites compared to untreated fibre composites [143]. On the other hand, the addition of 3 wt.% stearic acid did not increase the composite's Young's modulus compared to pure PE (Figure 4-20). This result was probably due to a combination of porosity, poor fibre-matrix adhesion and low fibre content.

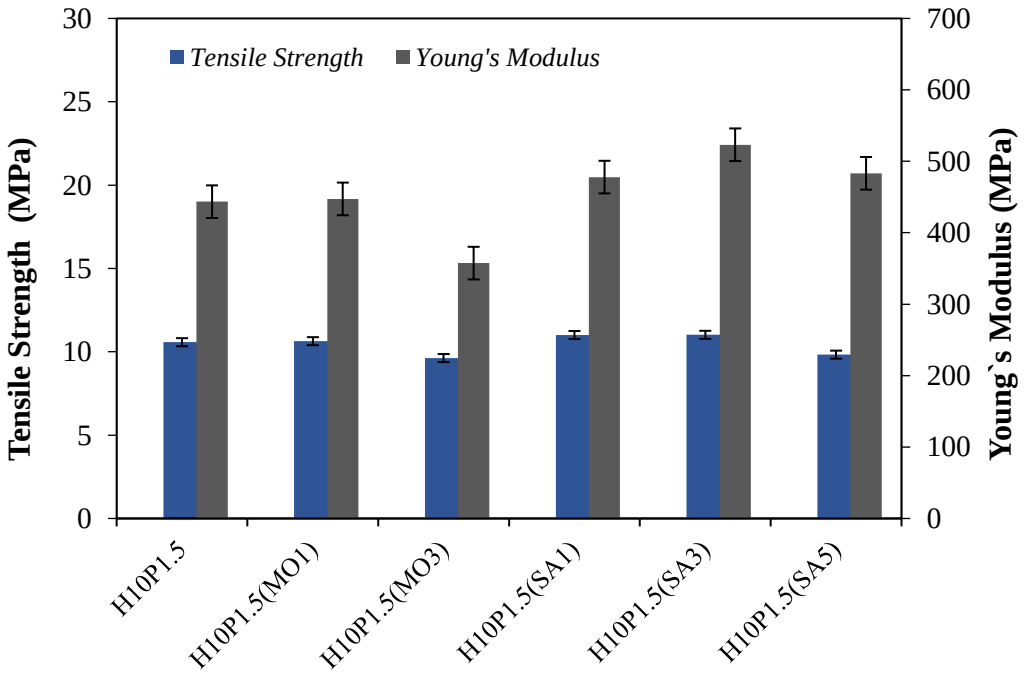

Figure 4-18.: Tensile strength and Young's modulus of rotationally moulded composites. Sample code: H = Hemp, fibre concentration, P= pellet, followed by pellet size, (MO= mineral oil), (SA=stearic acid) and their respective concentration.

Table 4-7: Statistical analysis of tensile strength and Young's modulus in composites with stearic acid (SA) and mineral oil (MO) in different proportions. P>0.05 (Gaussian distribution).

Samples	***Sample size***	***Tensile Strength (MPa)***	***SD***	***CV***	***Young's modulus (MPa)***	***SD***	***CV***
H10P1.5	5	10.70	0.40	3.35	443.5	14.4	03.16
H10P1.5(MO1)	5	10.6	0.26	2.33	447.3	32.4	06.77
H10P1.5(MO3)	5	09.62	0.81	8.45	357.4	58.6	16.39
H10P1.5(SA1)	5	11.00	0.26	2.33	477.9	32.4	06.77
H10P1.5(SA3)	5	11.01	0.28	2.51	523.2	42.5	07.83
H10P1.5(SA5)	5	9.83	0.35	3.35	483.2	61.8	12.78
PE	5	12.54	1.20	9.77	516.5	62.7	12.38

Sample code: H = Hemp, fibre content (wt.%), P= pellet followed by pellet size, MO= mineral oil, SA=stearic acid and their respective concentration (wt.%).

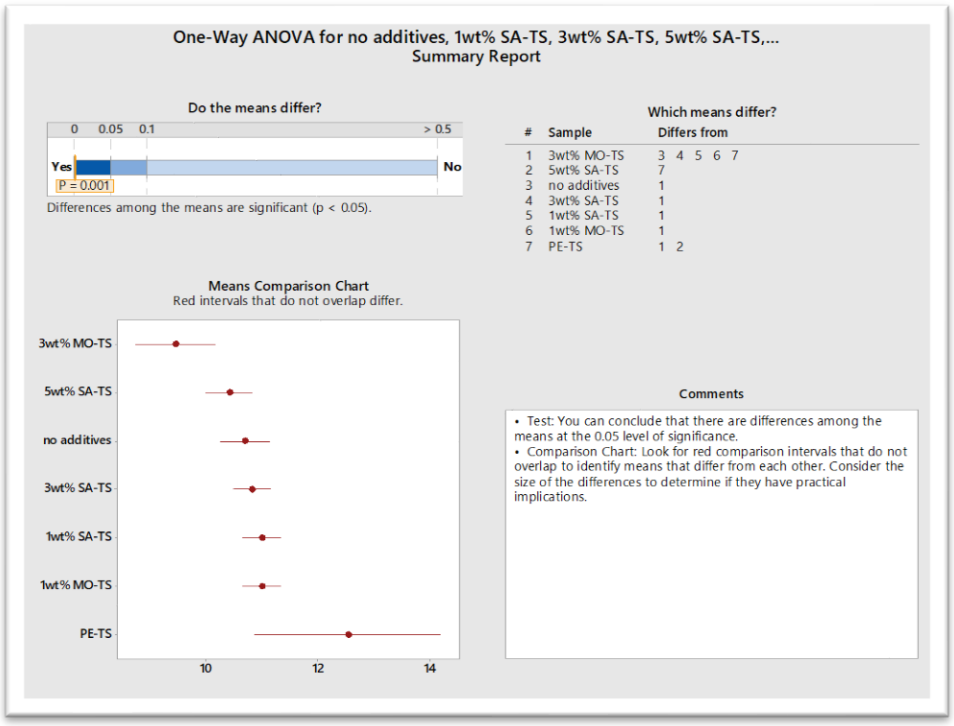

Figure 4-19: Result of one-way ANOVA hypothesis test of tensile strength (TS) of composites with stearic acid (SA) and mineral oil (MO) in different proportions.

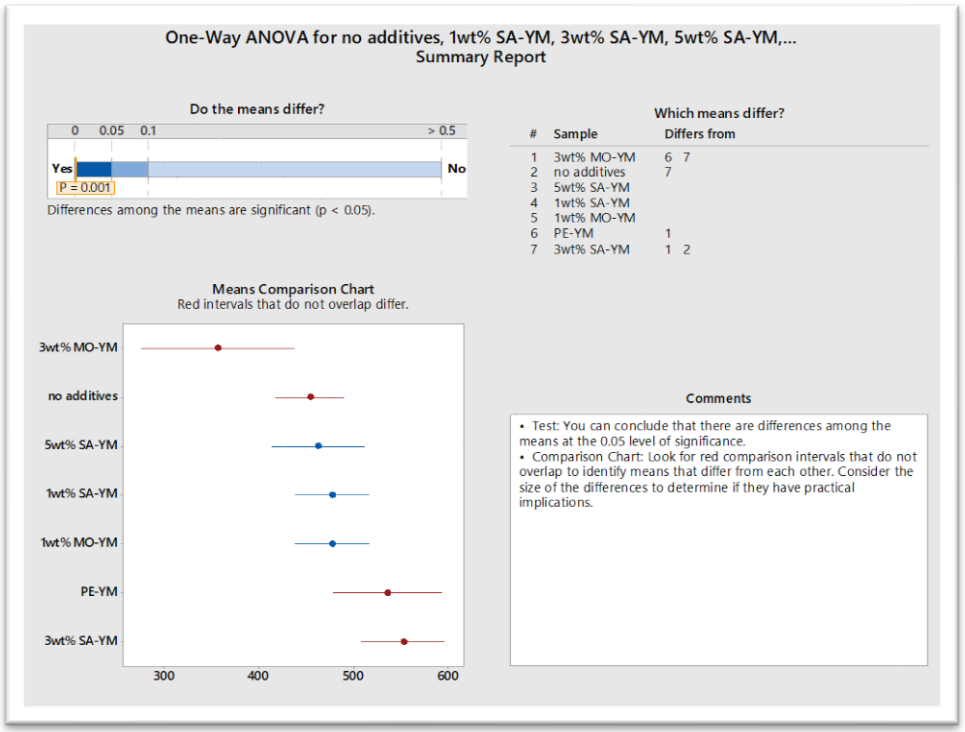

Figure 4-20: Result of one-way ANOVA hypothesis test of Young's Modulus (YM) of composites with stearic acid (SA) and mineral oil (MO) in different proportions.

4.4.8 The Influence of Fibre Content on Composites Produced with 1.5 mm Pellet Size

Rotationally moulded composites produced using a 1.5 mm pellet size with fibre contents of about 10, 12.5 and 15 wt.%, are shown in Figure 4-21. Composites with 10 and 12.5 wt.% fibre content showed satisfactory surface aesthetics with few voids and pinholes (Figure 4-21a). In contrast, the composite with 15 wt.% (Figure 4-21b) was very porous and had no consolidation for testing. This result means that 15 wt.% is beyond the optimal fibre content for this mixture to ensure that the polymer matrix fully covers the fibres during the process. Fibre wetting by the polymer matrix is more difficult at high fibre concentrations and can lead to fibre agglomeration [144].

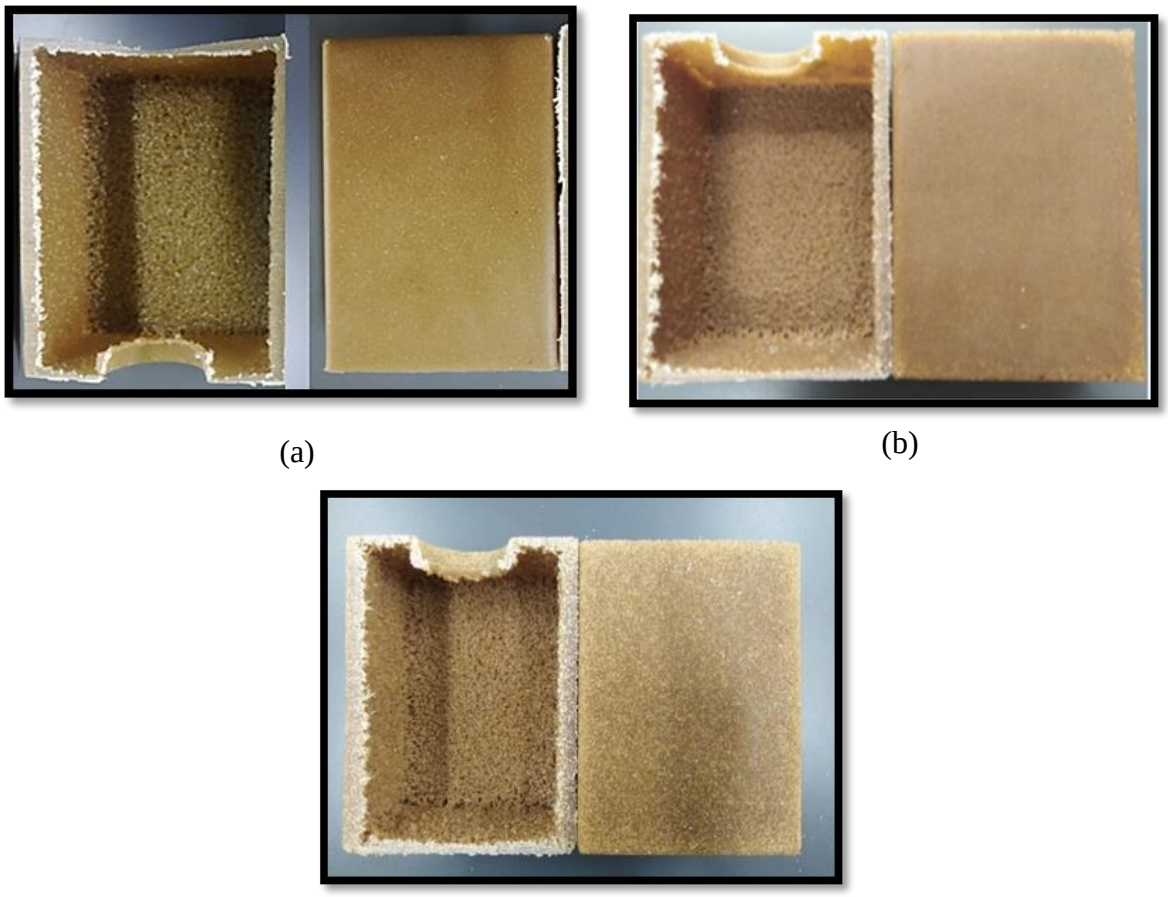

(a) (b)

(c)

Figure 4-21.: Rotationally moulded composites with fibre content of 10 (a), 12.5 (b) and 15 wt.% (c).

The successful composites were tensile tested, while the composite produced with 15 wt.% fibre did not have adequate consolidation for testing due to the saturation of fibre/matrix contact. Increasing the fibre content from 10 to 12.5 wt.% improved the tensile strength and Young's modulus of rotationally moulded composites, as shown in Figure 4-22. The composites with 12.5 wt.% fibre content had a Young's modulus that was approximately 24% higher than pure polyethylene (Figure 4-22 - Table 4-8). This result was confirmed to be statistically significant by ANOVA with a 95% confidence interval (Figure 4-24). However, no improvement in tensile strength was observed. Similarly, other studies with natural fibre-reinforced rotationally moulded composites have reported improvements in Young's modulus with the addition of fibre, with no increase in tensile strength [21; 120]. Young's modulus of composite materials increases with fibre content as the fibres are stiffer than the polymer matrix [6; 132]. Therefore, tensile strength depends on an efficient interfacial stress transfer from the matrix to the fibre. This is very challenging in rotational moulding due to the absence of external pressure characteristic of this process, which results in poor fibre/matrix compaction.

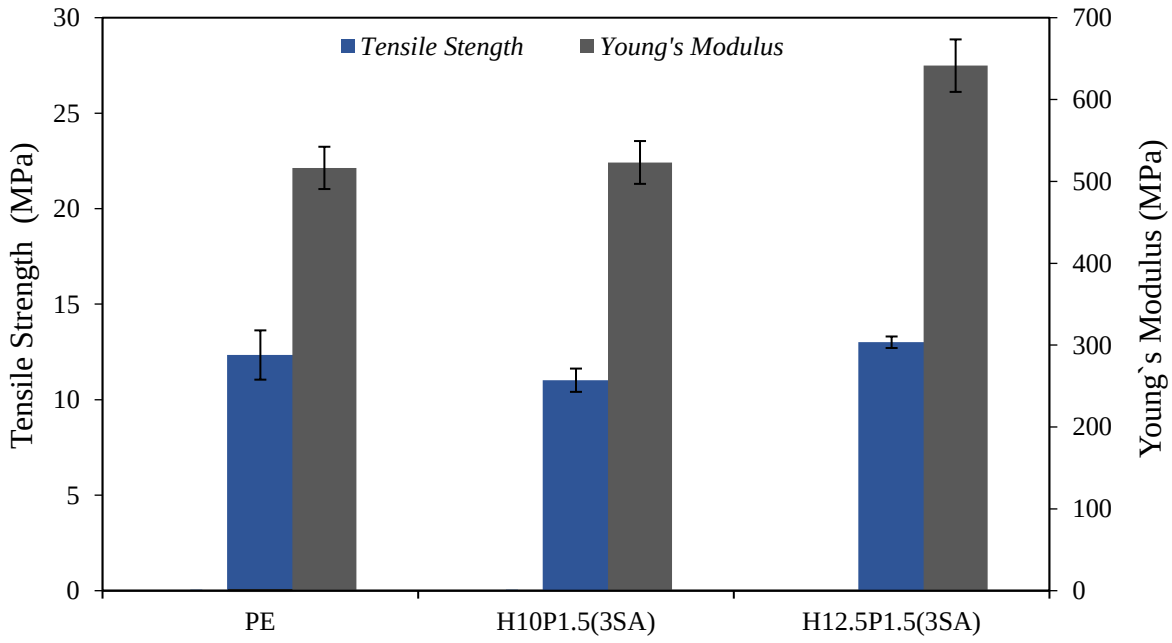

Figure 4-22: Tensile strength and Young's modulus of rotationally moulded composites Sample code: H = Hemp, fibre content (wt.%), P= pellet followed by pellet size, SA=stearic acid and concentration (wt.%).

Table 4-8: Statistical analysis of tensile strength and Young's modulus in composites with stearic acid and mineral oil in different proportions. P>0.05 (Gaussian distribution).

Sample	*Sample size*	*Tensile Strength (MPa)*	*SD*	*CV*	*Young's Modulus (MPa)*	*SD*	*CV*
PE	5	12.34	1.20	9.76	516.5	62.7	12.38
H10P1.5(SA3)	5	11.02	0.27	2.49	543.2	35	6.7
H12.5P1.5(SA3)	5	13.01	1.64	12.59	641.4	55.6	8.67
Sample code: H = Hemp, fibre content (wt.%), P= pellet followed by pellet size, SA=stearic acid and concentration (wt.%)							

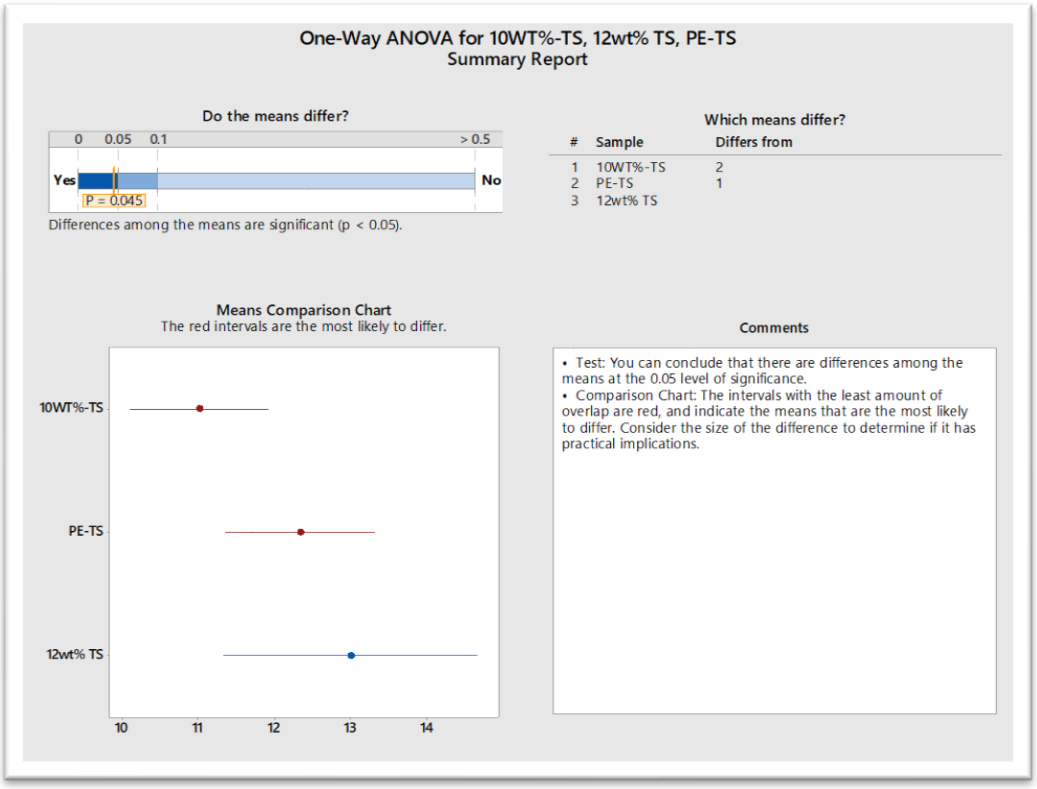

Figure 4-23: Result of one-way ANOVA hypothesis test of Tensile Strength (TS) of PE and composites with 10 and 12.5 wt.% fibre content.

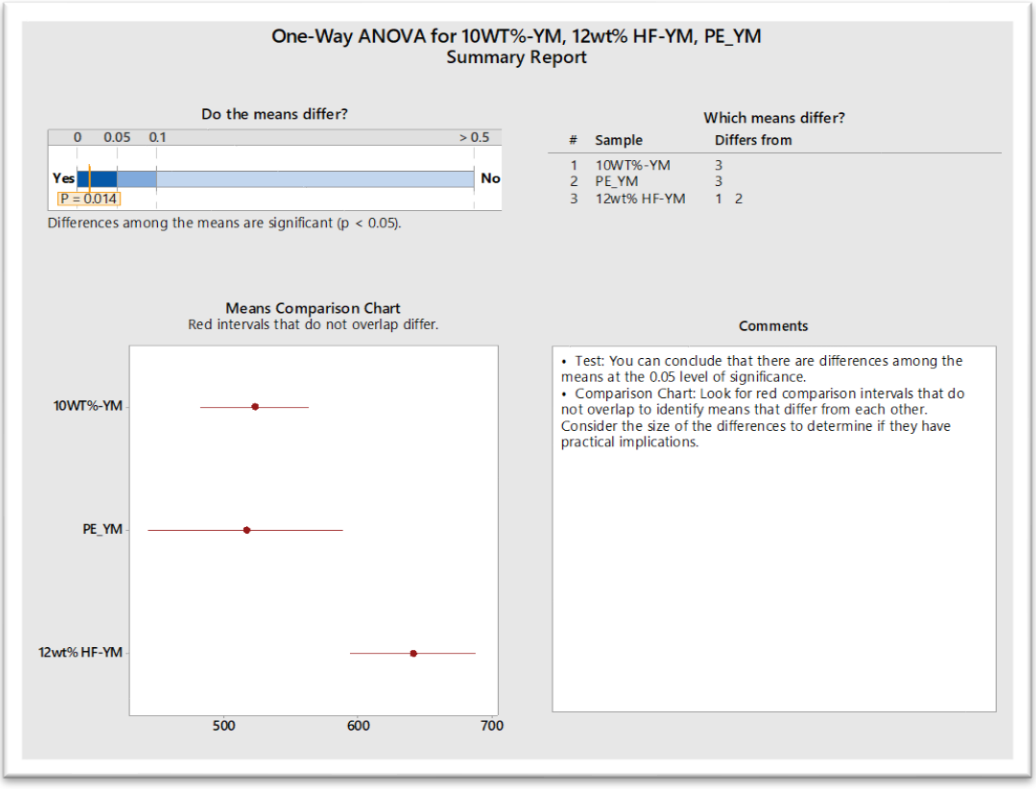

Figure 4-24: Result of one-way ANOVA hypothesis test of Young's Modulus (YM) of PE and composites with 10 and 12.5 wt.% fibre content.

4.5 Chapter Conclusions

It was concluded in Chapter 3 that the dry mixing technique results in fibre agglomeration and poor fibre dispersion within rotationally moulded composites. In this chapter, melt compounding of fibre and matrix by extrusion prior to rotational moulding improved fibre distribution, allowing higher fibre loads than the dry-mixing technique.

This chapter also showed that a 4 mm pellet size was not suitable for rotational moulding due to the inferior surface aesthetics of the composites produced. In contrast, composites produced with 1.5- and 0.5-mm pellet sizes had satisfactory surface aesthetics, with few voids and pinholes.

Porosity analysis by optical microscopy, Archimedes density test and micro-CT showed a trend toward larger voids with increased pellet size, which resulted in greater porosity in the final composites produced with a 1.5 mm pellet size. This behaviour was attributed to composite pellets of 1.5 mm size having not completely melted during the process.

Then, tensile testing showed that no reinforcement was obtained from the fibres in composites with a 0.5 mm pellet size. This result was probably a combination of poor fibre-matrix adhesion and inferior fibre length. However, there was a reduction in the tensile properties of composites prepared with a 1.5 mm pellet size compared to pure PE. Again, this was probably due to poor fibre-matrix adhesion but combined with porosity. It was also found that using 1.5 mm pellets was beneficial in maintaining the fibre length compared to composites produced with a 0.5 mm pellet size.

For this reason, processing aids were tested to mitigate porosity in composites prepared with a 1.5 mm pellet size. The best-performing processing aid was stearic acid at 3 wt.%. The addition of 3 wt.% stearic acid reduced polymer viscosity as shown by rheology analysis. This improved homogeneity and processability of the molten polymer resulted in lower porosity in the final composites. This is an innovative result as the use of stearic acid not been previously reported in any research with rotationally moulded composites.

The addition of stearic acid also allowed a maximum of 12.5 wt.% of fibre content to be incorporated in rotationally moulded composites. Consequently, increasing the fibre content from 10 to 12.5 wt.% improved the tensile strength and Young's modulus of rotationally moulded composites. In addition, composites produced with 12.5 wt.% of fibre had a Young's modulus that was improved by about 24% compared to pure polyethylene.

Chapter 5
Assessment of Fibre Orientation in Rotationally Moulded Composites

This chapter investigates the fibre orientation in rotationally moulded composites produced using pellets with an aspect ratio greater than 1. It is not likely that fibres could be aligned in a single direction in rotationally moulded composites due to the absence of external pressure and the low shear characteristics of this process. However, the hypothesis in this study was that large pellets might fall parallel to the mould wall (XY plane) during processing. Therefore, if there is any fibre alignment with the flow during extrusion, fibres within the pellets would also be parallel to the rotationally moulded composites' mould wall in a random direction.

First, fibre orientation was assessed from cross-sectional images of extruded filaments and rotationally moulded composites. Then, specimens from transversal and longitudinal directions of rotationally moulded composites were tensile tested. Finally, the effect of using pellets with a large aspect ratio on the final composite porosity was investigated via image analysis. The results showed that fibres in samples produced with composite pellets with aspect ratios larger than 1 were mostly oriented within 0 degrees (YZ plane), which means parallel to the mould wall. This probably contributed to the reinforcement obtained from the fibres in composites produced with 1.5 mm pellet sizes as it produced the highest tensile properties of all. In contrast, composites prepared with 2mm pellet size had inferior mechanical properties due to high porosity.

5.1 Materials

The industrial hemp fibre (*Cannabis Sativa L.*) used as reinforcement was grown in New Zealand. Hemp fibre was treated with an alkali solution of NaOH and Na_2SO_3; both were 98% purity and obtained from Merck. The coupling agent, polyethylene-grafted maleic anhydride, 456632, with viscosity 1,700–4,500 cP (140°C) and saponification value of 30–40 mg KOH/g, was obtained from Sigma Aldrich in powder form. A rotational moulding grade of low-medium-density polyethylene, VX567, with a melt flow index of 6.0 g/10 min (ASTM D 1238), and a density of 0.935 g/cm^3 (ASTM D 1505), was obtained from Vision Plastics (VPLAS) in powder form.

5.2 Methods for Composite Sample Preparation

5.2.1 Melt Compounding

A Labtech twin-screw extruder (L/D ratio 44:1, diameter 20 mm) was used to combine 10 wt.% HF, 3 wt.% MAPE and 3 wt.% stearic acid with polyethylene. The temperature control on the extruder was separated into five zones, which were set at T_1:140 °C (barrel entrance), T_2:140 °C, T_3:140 °C, T_4:140 °C and T_5:130 °C (barrel exit). A total of three extrusions were performed to improve the mixture homogeneity and reduce the diameter of the filaments produced. The first two extrusions were through a 3 mm diameter die at 80 rpm. The second extrusion was performed at 30 rpm through a 1.2 mm die using a filament winder to reduce the filament diameter to about 0.9 mm.

5.2.2 Pelletising

Pellets of composites with 0.9, 1.5 and 2 mm length and 0.9 mm diameter were uniformly chopped using a benchtop lab pelletiser SGS 25-E4 (Figure 5-1). The formulation and coding of the rotationally moulded composites produced using those pellets is described in Table 5-1.

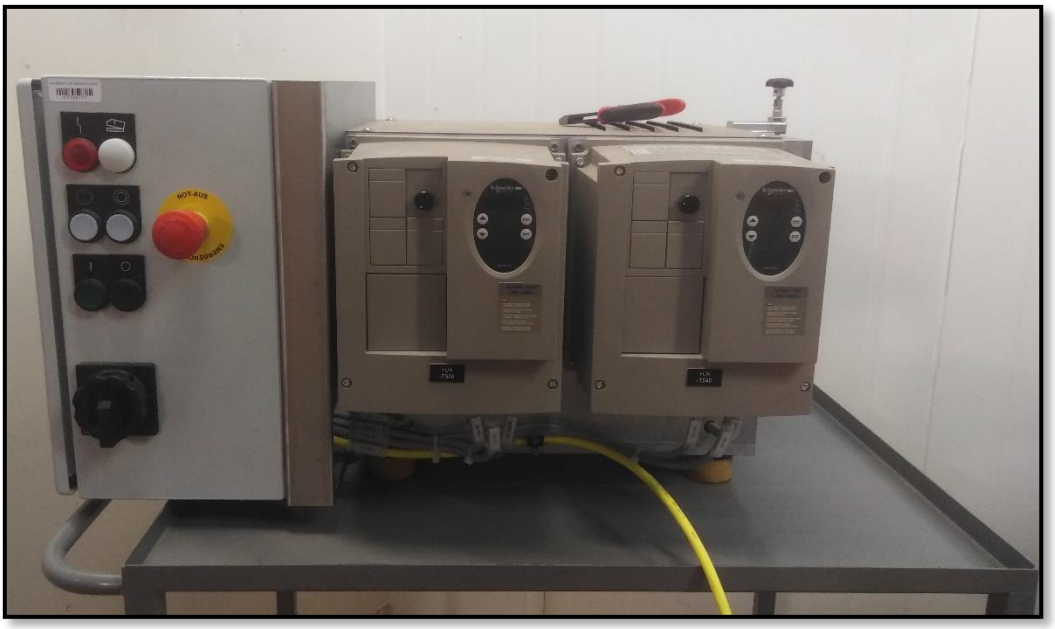

Figure 5-1: Benchtop lab pelletiser SGS 25-E4 – MAAG.

Table 5-1: Description of the composition of the composite pellets used in the rotational moulding.

Sample code	***Fibre Content (wt%)***	***MAPE (wt%)***	***Stearic acid (wt%)***	***Pellet size (mm)***
H10P0.9	10	3	3	0.9
H10P1.5	10	3	3	1.5
H10P2	10	3	3	2
PE	10	3	--------	Powder
Sample code: type of fibre (H = Hemp), fibre content, P= pellet followed by the size and PE=pure polyethylene.				

5.2.3 Rotational Moulding

Rotationally moulded composites were prepared as described in Chapter 3, Section 3.2.1.

5.2.4 Fibre Length Distribution

Approximately 2 g of each sample of the composite was dissolved in 200 mL of boiling xylene (135°C) for 30 min then filtered through a mesh with aperture dimensions of 120 µm x 120 µm to separate the fibres from the xylene filtrate. These fibres were dried and immersed in water with a small amount of dishwashing detergent to assist with fibre

dispersal. An FQA-360 electronic sequential fibre length analyser (Figure 5-2) was used to obtain a mean fibre length for each composite.

Figure 5-2: An FQA-360 electronic sequential fibre length analyser

5.2.5 Tensile Testing

Tensile testing specimens (sample V- ASTM D638-14) were placed in a conditioning chamber at 23 ± 3℃ and 50 ± 5% relative humidity for 48 h. The specimens were tested according to the ASTM D638-14 “Standard Method for Tensile Properties of Plastics”, using an INSTRON-4204 tensile testing machine fitted with a 10 KN load cell and operated at a rate of 1 mm/min. An Instron extensometer was used to measure the composite strain. Seven specimens of each type of composite were tested to failure.

5.2.6 Porosity Analysis by Optical Microscopy

Optical microscopy images of the surface of rotationally moulded composites were taken with 6.5x magnification, using a WILD M3B stereo microscope fitted with a Nikon camera (Digital Sight DSU1). The porosity in percentage per area was calculated using ImageJ. The pore analysis was adapted from a previous study where twelve optical microscopy images of the surfaces of rotationally moulded composites were used [123].

5.2.7 Particle Size Distribution by Optical Microscopy

Optical microscopic images of different sizes of composite pellets were obtained using a WILD M3B stereo microscope fitted with a Nikon camera (Digital Sight DSU1) at 6.5x magnification. The length and diameter of these pellets were measured from these optical microscopic images using the software ImageJ.

5.2.8 Fibre Orientation by Optical Microscopy

Specimens were cut from the cross-section (planes XY and YZ) of rotationally moulded composites as represented in Figure 5-3. These specimens were immersed in epoxy resin, ground and polished with a Struers Rotopol-21 machine to reveal the fibre orientations in different planes. Optical microscopic images of polished composite surfaces were taken using an Olympus BX53M fitted with a digital camera at 50x magnification.

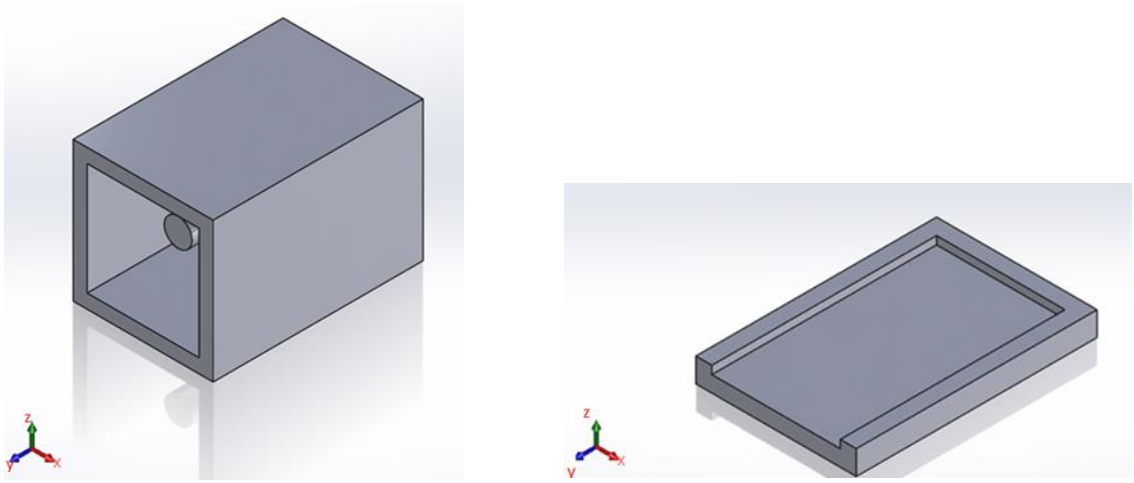

a) b)

Figure 5-3: a) Schematic of a composite in monoaxial rotational moulding (mould rotates about either the positive or negative Y axis), b) Composite cut plane XY.

5.3 Statistical Analysis

The software MINITAB version 18.1 was used for the statistical analysis of the results of tensile testing. First, the values of different parameters were expressed as mean values with standard deviation and coefficient of variation. Then, one-way ANOVA was applied to compare the differences in the mean of more than two population means with a 95% simultaneous confidence level. In some cases, a t-test was used to compare two population means with the same level of confidence. A hypothesis test that evaluates two mutually

exclusive statements about two or more population means was used to determine whether to reject the null hypothesis [106].

5.4 Results and Discussion

5.4.1 Production of Uniform Pellets of Composites for Use in Rotational Moulding

Hemp and polyethylene were melt compounded by extrusion and converted into pellets with an aspect ratio greater than 1 to be used in rotational moulding (Table 5-2). The minimum size of the pellet was limited by the filament diameter, which was about 0.9 mm (aspect ratio 1). Finally, the maximum size of the pellet was chosen to achieve a pellet aspect ratio of 2. Figure 5-4 shows the length distribution of these pellets.

Table 5-2: Dimensional characteristics of composite pellets

Sample Code	*Nominal Length (mm)*	*Diameter (mm)*	*Volume (mm^3)*	*Aspect ratio(L/D)*
P0.9	0.9	0.9	0.57	1
P1.5	1.5	0.9	0.95	1.7
P2	2.0	0.9	1.33	2.2

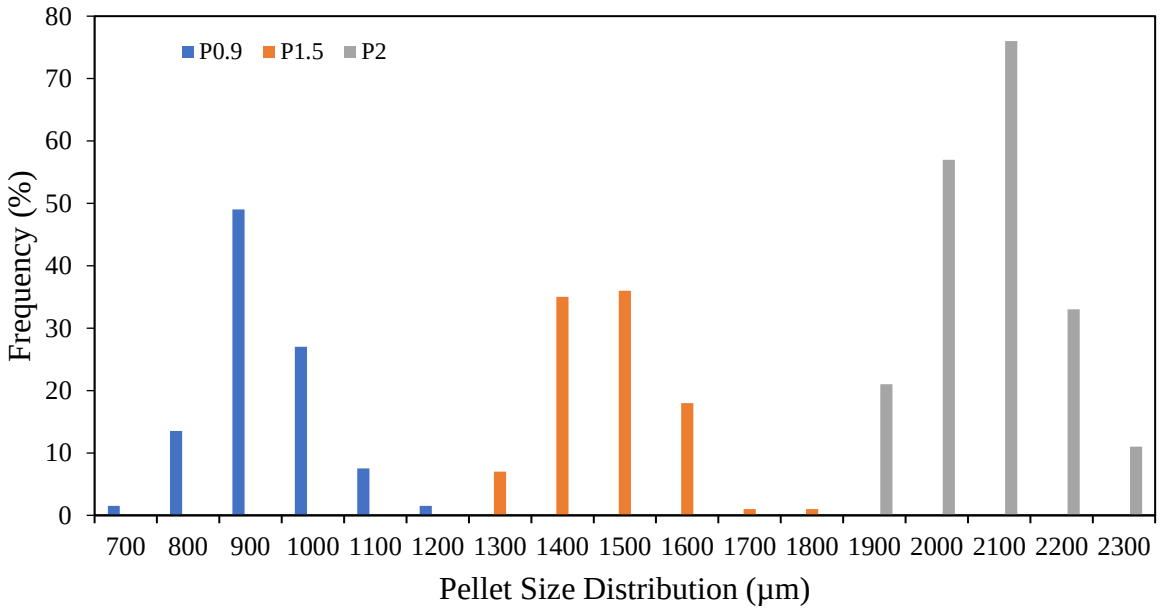

Figure 5-4: Size distribution of composite pellets.

5.4.2 Fibre Length Analysis

Fibre length is an important factor influencing the mechanical properties of reinforced composites. It is known that during processes such as extrusion, shear and elongation act on the fibre causing length reduction, which is detrimental to the composite's mechanical properties [145]. Therefore, multiple reprocessing cycles of fibre-reinforced composites can further reduce fibre length due to repeated exposure to high shear forces.

In this study, hemp fibre was subjected to three cycles of extrusion with polymer to improve the fibre-matrix mixing, hence reducing filament diameter to a maximum of 0.9 mm. The aim was to produce thin filaments of composites to assist polymer sintering during rotational moulding. However, multiple extrusions reduced the weighted fibre length from 1.2 mm to about 0.3 mm (Table 5-3). This reduction in fibre length after extrusion can compromise the stress transfer efficiency from matrix to fibre as the critical fibre length reported in the literature for hemp-polypropylene varies from 0.8 to 3.4 mm [23; 101].

For composites containing discontinuous fibres, the applied load is transferred from the matrix to the fibres using shear forces at the fibre-matrix interface, and high shear stresses are experienced at the fibre ends [23; 146]. Composite failure mechanisms are governed by fibre length, and sub-critical length fibres (L<Lc) cannot be fully stressed, so they will eventually debond and be pulled out of the matrix. Table 5-2 also shows that after pelletizing, there was no significant fibre length reduction. However, there was a slight reduction in fibre length with pellet size.

Table 5-3: Weighted fibre length and aspect ratio prior and after extrusion.

Fibre characteristics	***Fibres before extrusion***	***Fibres in extruded filaments***	***H10P0.9***	***H10P1.5***	***H10P2***
Median length (mm)	1.20	0.335	0.239	0.270	0.297
Aspect ratio	54	15	10	12	13

5.4.3 Porosity Analysis by Optical Microscopy

Optical microscopic images of the outer surface of rotationally moulded composites are shown in Figure 5-5. In general, larger voids can be seen in composites produced with pellets of 2 mm size. Analysis of the size of the voids shows a large number of pinholes of about 50

μm in all the samples, which increased with pellet size up to voids of 1.5 mm, Figure 5-6. The porosity per area was obtained from the analysis of different images of each composite using ImageJ. Table 5-4 shows that composites produced with a 2 mm pellet size were almost twice as porous as composites produced with a 0.9 mm pellet size. It also shows that increasing the pellet size from 0.9 to 1.5 mm did not increase the final composite porosity. Likewise, the results from Chapter 4 showed that the maximum particle size to produce rotationally moulded composites with moderate porosity is about 1.5 mm. The absence of pressure during rotational moulding does not favour the elimination of gases trapped between the particles during the process, particularly with large pellet sizes. The usual practice in the rotational moulding industry to mitigate composite porosity is increasing the processing time. However, natural fibres are prone to thermal degradation when subjected to long periods at high temperatures. This research showed that using 3 wt.% stearic acid is beneficial in mitigating porosity, as discussed in Chapter 4.

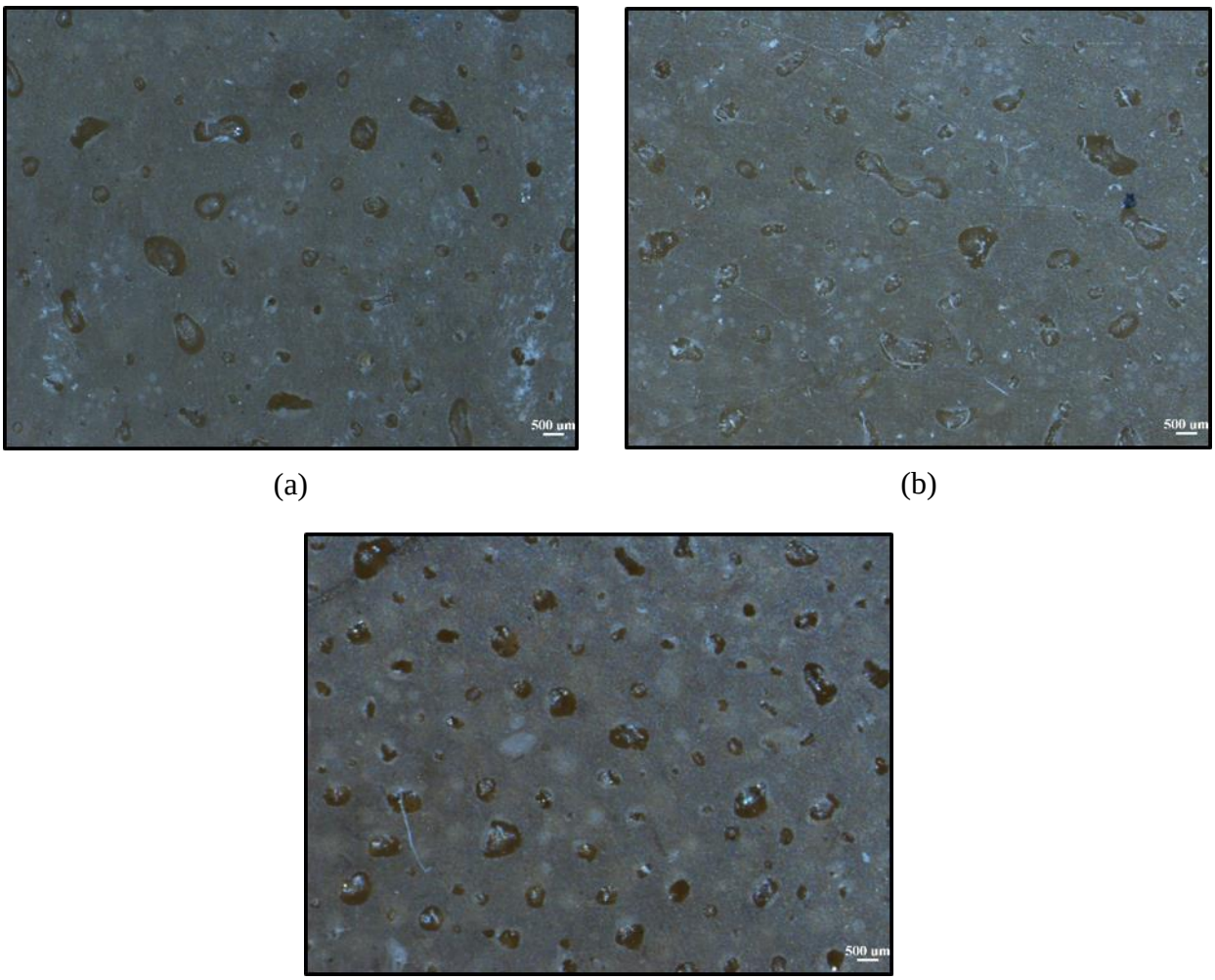

(a) (b)

(c)

Figure 5-5: Optical microscopic images of rotationally moulded composites: H10P0.9(a), H10P1.5(b) and H10P2(c). Scale bar 500 µm. Sample code: (H = Hemp), fibre content (wt.%), (P= pellet) followed by pellet size.

Table 5-4: Porosity in rotationally moulded composites by ImageJ.

Sample	***Sample Size***	***Porosity in area (%)***	***Median of Void size (µm)***
H10P0.9	12	6.2	75
H10P1.5	12	7.2	450
H10P2	12	11.2	600

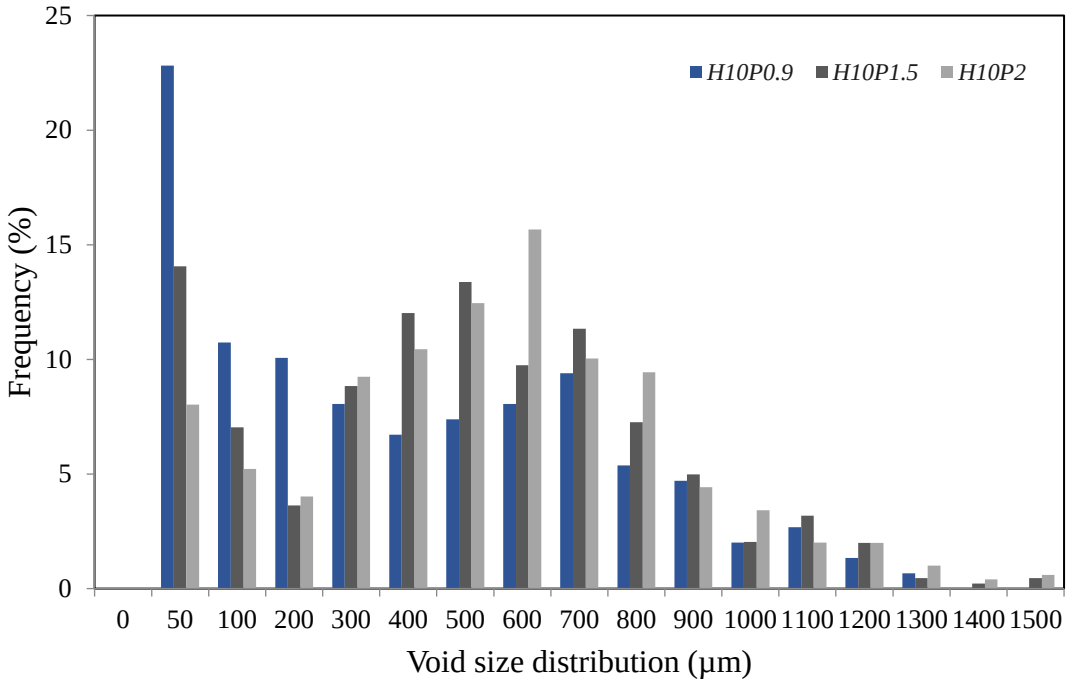

Figure 5-6: Void size distribution in rotationally moulded composites. Sample code: H = Hemp, fibre content (wt.%), P= pellet followed by pellet size.

5.4.4 Fibre Orientation

Initially, fibre orientations in cross-sectional microscopy images of extruded filaments of composite were analysed by ImageJ plugin "directionality". This method generates normalized histograms revealing the number of fibres present between 0° and 180° with a bin size of 1° using a Gaussian fit, as shown in Figure 5-8.

It is known that during extrusion, the polymer melt experiences both extensional and shear flow, which can result in the alignment of fibres in the flow direction [43]. For this reason, it was expected that hemp fibres would be mostly aligned with the flow direction in the extruded filaments of the composite. Figure 5-7-left shows the ends of the fibres, indicating that fibres were oriented primarily with the direction of polymer flow during extrusion. However, the vertical view of the filament (Figure 5-7-right) shows fibres oriented in random directions. In fact, most of these fibres were around 50° to the longitudinal axis (Figure 5-8).

The challenge of using this technique is that hemp fibre is a soft and curvy material, making it difficult to see its orientation in the longitudinal aspect. In addition, sample preparation is complex, as sanding and polishing are indicated for hard materials, not soft materials such as

polyethylene. This resulted in imperfections on the sample surface, which the software may misinterpret as fibres.

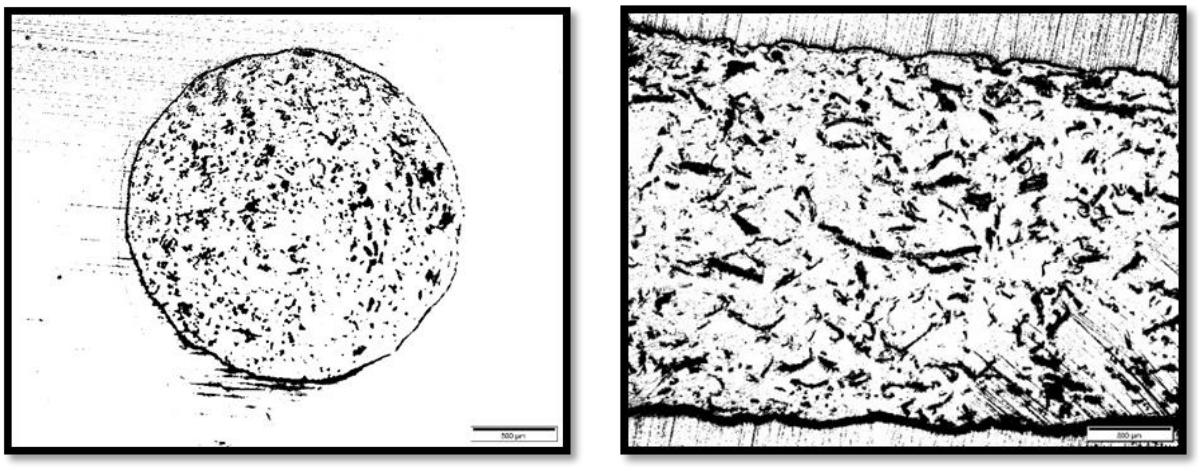

Figure 5-7: threshold image of vertical (left) and horizontal (right) cross-sessional view of the extruded filament of hemp-PE composite. scale 500µm.

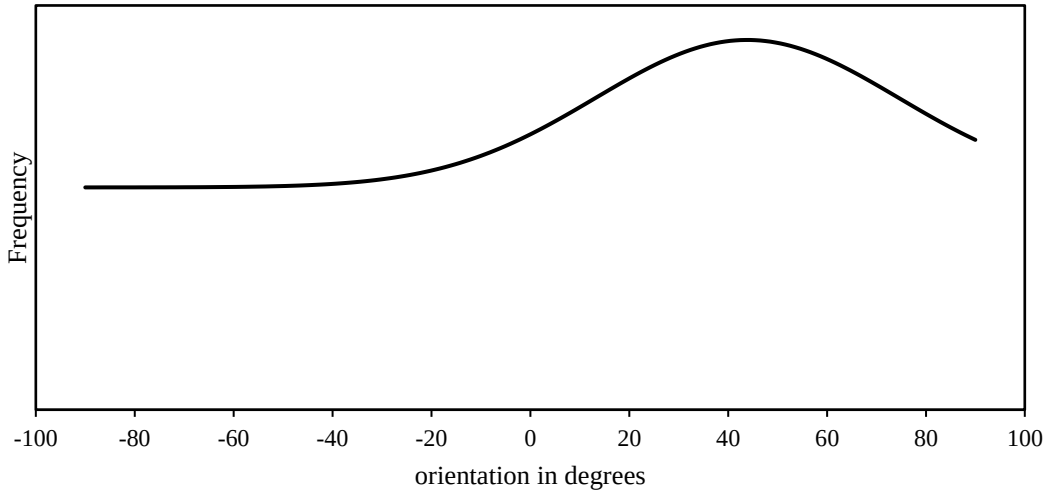

Figure 5-8: Fibre orientation in the horizontal section of the extruded filaments of hemp-PE composite.

The fibre orientation in rotationally moulded composites produced using composite pellets with different aspect ratios was assessed using optical microscopic images of the cross-sections (planes XY and YZ). Fibre orientation was quantified to measure the preferred orientation of fibres across X, Z and Y directions using the ImageJ. The X-direction corresponds to sample width, the Z-direction to sample thickness and the Y-direction to sample length (Figure 5-3). It was expected that using pellets with a high aspect ratio in rotational moulding would favour fibres being oriented parallel to the mould wall (XY plane) in random directions. This means that the fibres within the pellets would not be oriented

through the composite thickness. Figure 5-9 shows an undesirable fibre orientation in each plane with a cross ("x").

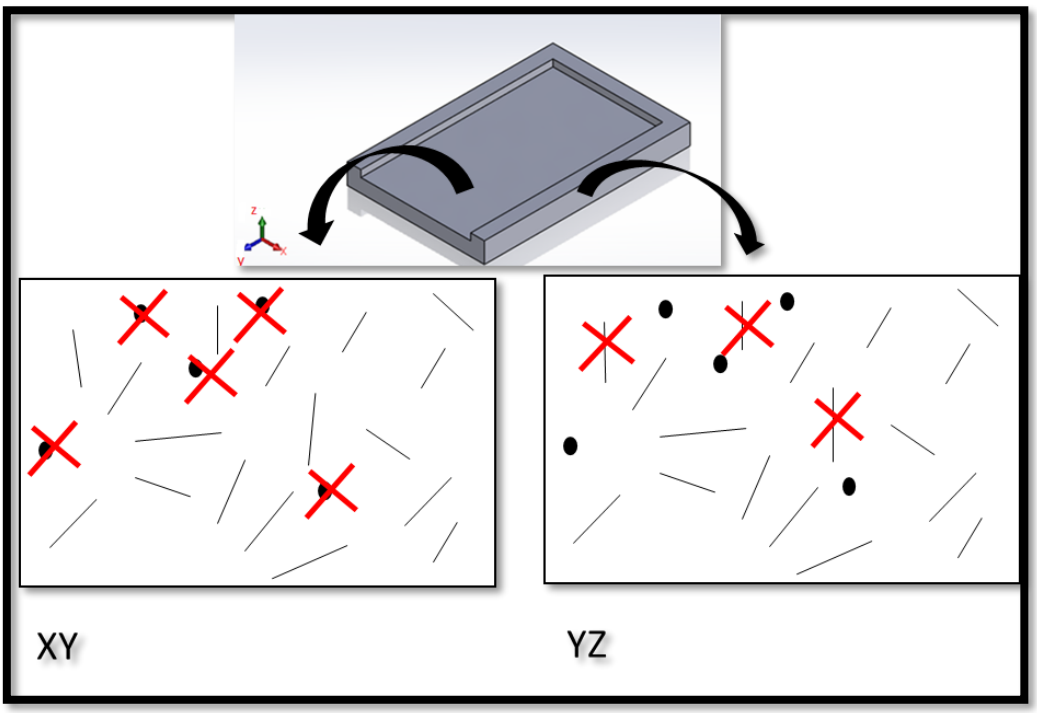

Figure 5-9: Schematic of undesirable fibre orientation (marked 'X') in the rotationally moulded composite (XY and YZ plane)

Polished cross-section images of rotationally moulded composites are shown in Figure 5-10. Previous research has analysed the elliptical shape of fibre cross-sections on a polished cutting plane to determine fibre orientation within composites [147; 148]. However, this method was not the most appropriate for this investigation due to the cross-sectional shape variations associated with hemp fibres, resulting in significant inaccuracies in fibre orientation assessment. Also, image analysis is a challenge as the imperfections on the composite surface, such as voids and scratches, cannot be distinguished from fibres by the software.

Samples with 0.9 mm pellet size

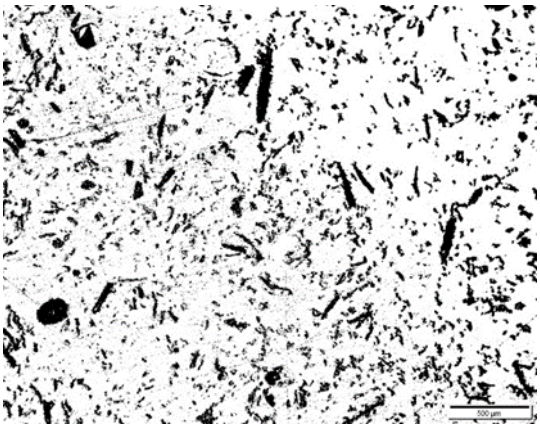

a) XY

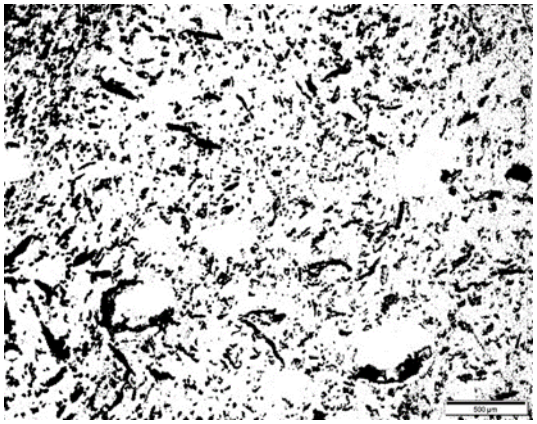

b) YZ

Samples with 1.5 mm pellet size

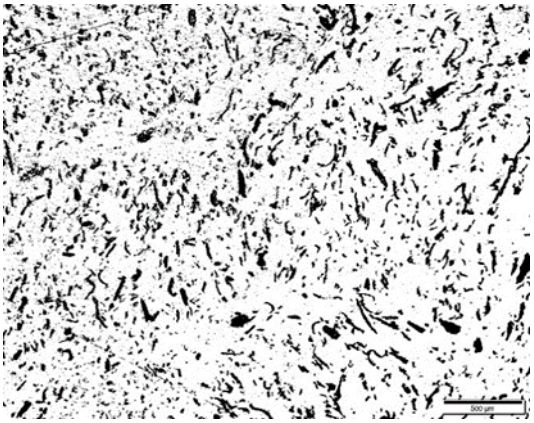

c) XY

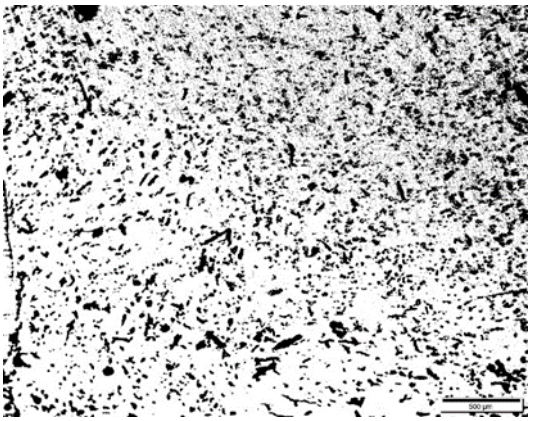

d) YZ

Samples with 2 mm pellet size

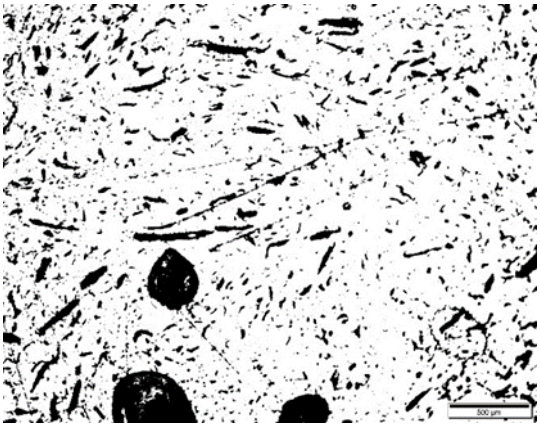

e) XY

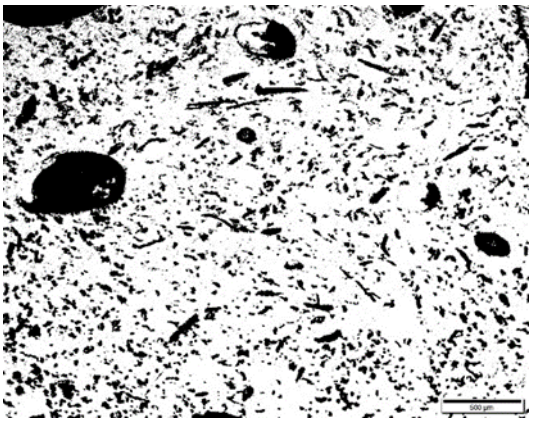

f) YZ

Figure 5-10: Example of images used to assess fibre orientation in rotationally moulded composites using ImageJ-directionality plugin.

Figure 5-11 shows the profile of fibre orientation distribution in the composite planes XY and YZ, obtained by ImageJ. The illustrations on the left side are representations of fibre orientation, as shown in the histograms. The results from the XY plane show that fibres were oriented in different directions, as expected. It is well known that maximum composite strength occurs when the reinforcing fibres are aligned and oriented parallel to the direction of the applied load. However, short fibre composites do not often consist of fibres oriented in a single direction. Figure 5-11 also shows the predominant fibre orientation in composites with 1.5- and 2-mm pellets is within ± 0° (YZ plane), represented by a peak.

In contrast, fibres within composites prepared with pellets of 0.9 mm were predominantly oriented through the mould thickness (90º at Z-direction). It can therefore be concluded that the fibre orientation within these composites is planar-random.

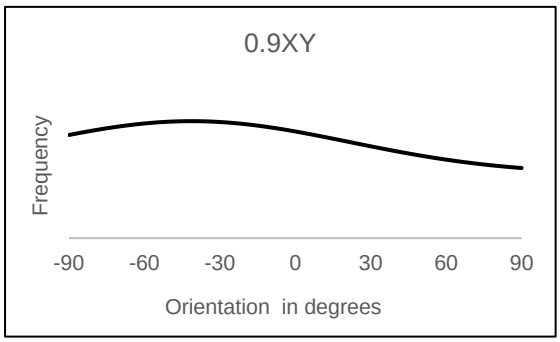

a) XY plane – sample H10P0.9

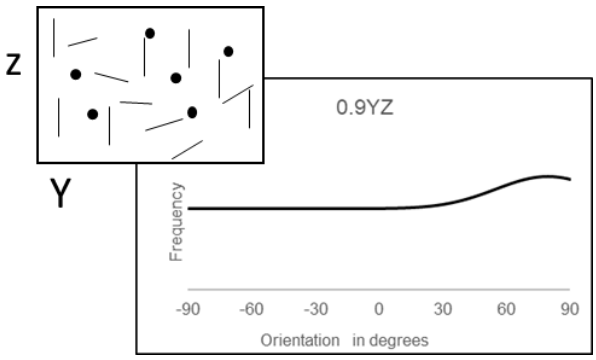

b) YZ plane – sample H10P0.9

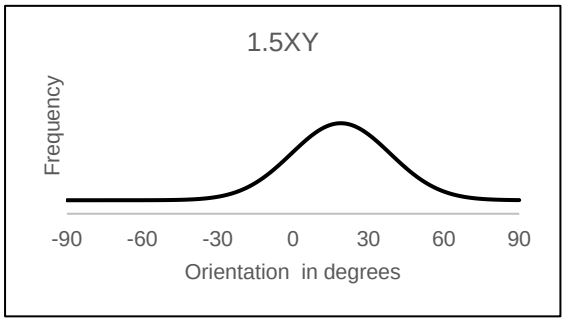

c) XY plane – sample H10P1.5

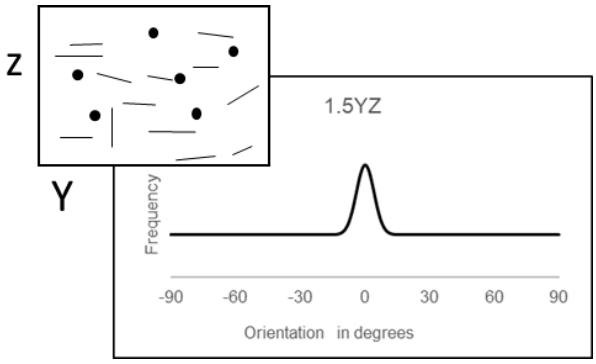

d) YZ plane – sample H10P1.5

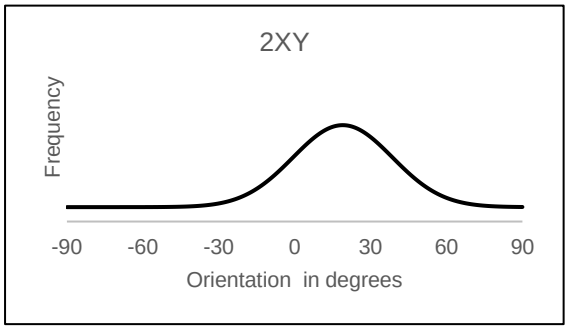

e) XY plane – sample H10P2

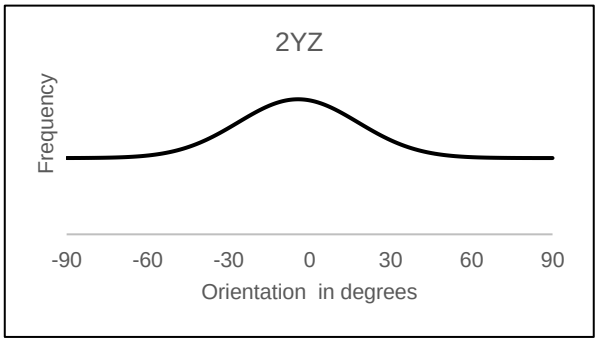

f) YZ plane – sample H10P2

Figure 5-11: Distribution of fibre orientation in rotationally moulded composites prepared with pellet sizes of 0.9, 1.5 and 2 mm.

5.4.5 Tensile Testing of Rotationally Moulded Composites

As the polymer flows transversely relative to the rotation direction during rotational moulding, any preferential fibre alignment with the flow during processing would favour the composite tensile strength in the transverse direction (X-axis). Fibre orientation was assessed by tensile testing rotationally moulded reinforced composites in both longitudinal and transverse directions. The ratio between transverse tensile strength (TTS) and longitudinal tensile strength (LTS) indicates the degree of fibre orientation; therefore, the lower the

TTS/LTS ratio, the higher the degree of fibre orientation along the longitudinal direction. Table 5-5 shows that the ratio of TTS/LTS for these composites was approximately 1. This indicates that fibres were almost equally oriented in both directions (isotropic), which was already expected.

Figure 5-12 shows that the composite produced with a 1.5 mm pellet size had the highest tensile strength of all samples tested. Its tensile strength was about 22% greater than pure PE (ANOVA in Figure 5-13). This is mostly likely due to the improvement in fibre orientation parallel to the mould wall observed in Item 5.4.4. A reduction in tensile strength was observed in composites prepared with a 2 mm pellet size (Figure 5-12 and Table 5-5). This result can be attributed to the increased porosity in composites produced with 2mm pellets compared to composites with 1.5 mm pellets, as shown in section 5.3.3.

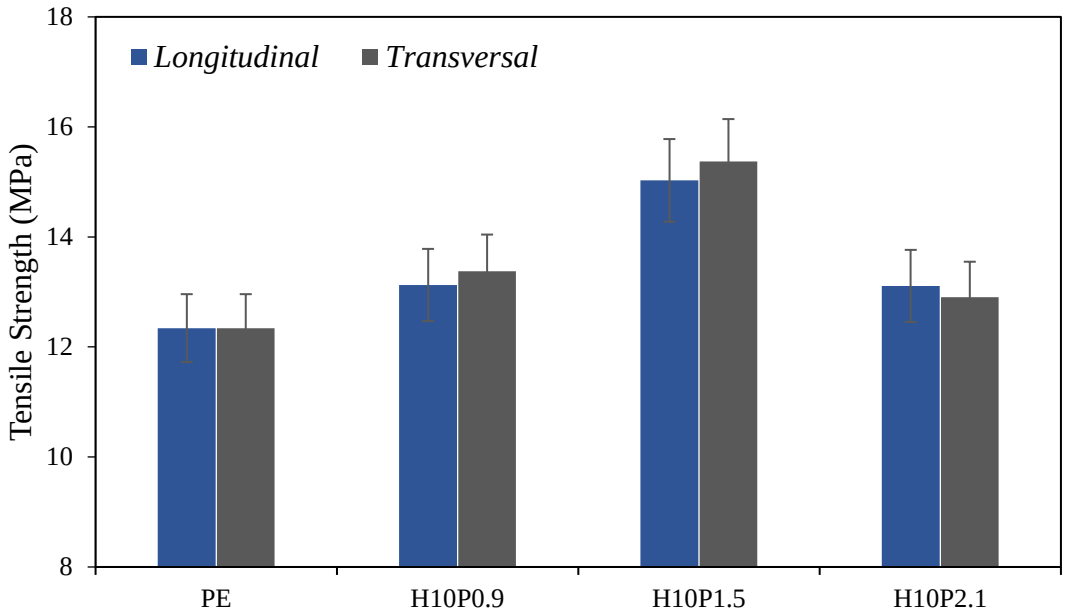

Figure 5-12: Tensile strength of rotationally moulded composites. Sample code: H = Hemp, fibre content (wt.%), P= pellet followed by pellet size.

Table 5-5:. Statistical analysis of tensile strength and Young's modulus in composites with stearic acid and mineral oil at different proportions. P>0.05 (Gaussian Distribution).

Sample code	*TTS/LTS*	*Sample Size*	*Tensile Strength (MPa) Longitudinal*	*SD*	*CV*	*Tensile Strength (MPa) Transversal*	*SD*	*CV*
PE	1	5	12.34	1.20	9.76	12.34	1.20	9.76
H10P0.9	1.02	5	13.13	0.84	6.37	13.37	0.47	3.49
H10P1.5	1.03	5	15.03	0.25	1.69	15.4	0.85	5.40
H10P2.0	0.98	5	13.11	1.38	10.62	12.9	0.55	4.24
Sample code: H = Hemp, fibre content (wt.%), and P= pellet, followed by its size.								

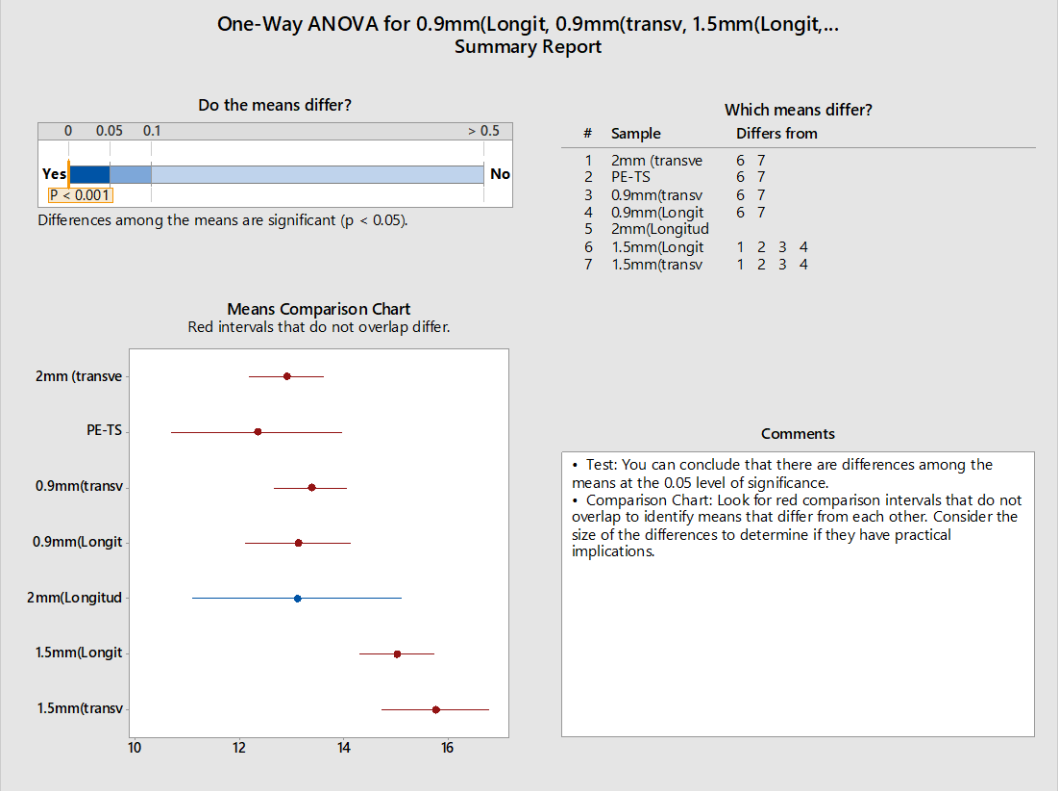

Figure 5-13: Result of one-way ANOVA hypothesis test of tensile strength of specimens obtained from transverse and longitudinal directions for rotationally moulded composites produced with pellet sizes of 0.9, 1.5 and 2 mm.

Composites produced with a pellet size of 1.5 mm had the highest Young's modulus among the tested samples, as shown in Figure 5-14. Figure 5-14 also shows that composites produced with a pellet size of 1.5 mm had a Young's modulus about 20% higher than pure polyethylene. This result was statistically significant by ANOVA with a 95% confidence interval, as shown in Figure 5-15.

Figure 5-14 shows that composites with a pellet size of 1.5 mm had a higher Young's modulus in the transverse direction. However, there was no statistical difference between composites produced with 1.5 mm samples cut in the transverse or horizontal direction with 95% confidence intervals using Student's t-test (Figure 5-16). As previously discussed, the reduction in Young's modulus with increasing pellet size was due to the increase in porosity found in composites with a pellet size of 2 mm.

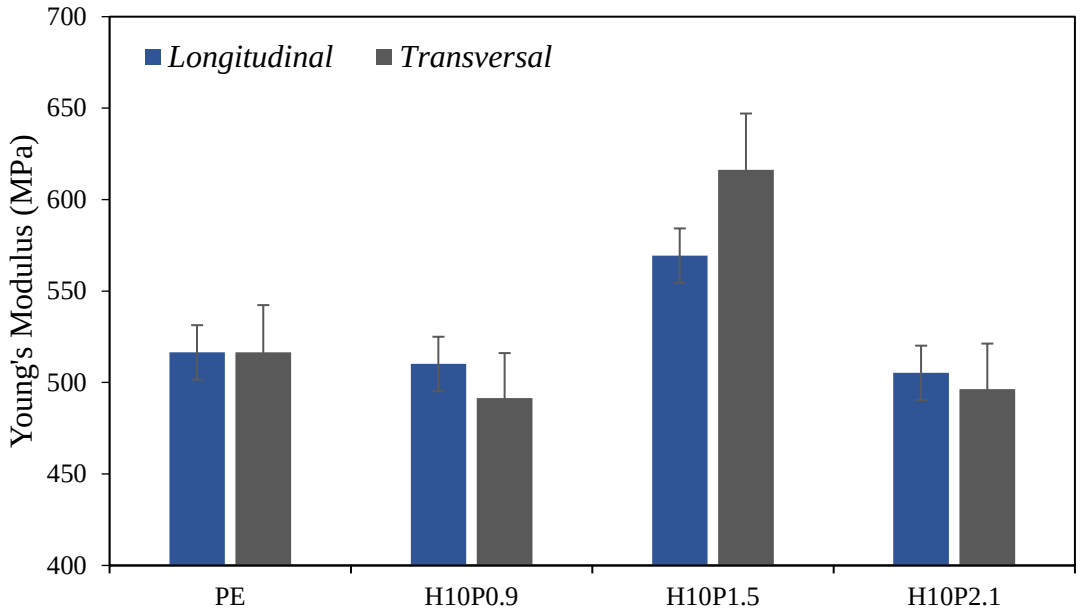

Figure 5-14: Young's Modulus of rotationally moulded composites.

Table 5-6: Statistical analysis of Young's modulus of rotationally moulded composites. P>0, Gaussean Distribution.

Sample code	***Sample Size***	***Young's Modulus (MPa) Horizontal***	***SD***	***CV***	***Young's Modulus (MPa) Transversal***	***SD***	***CV***
PE	5	536.5	46.1	8.60	516.5	62.7	12.38
H10P0.9	5	510.2	7.26	1.42	491.5	18.3	3.72
H10P1.5	5	569.5	29.8	5.24	616.2	56.3	9.12
H10P2.0	5	505.3	26.1	5.17	496.3	53.4	10.75
Sample code: H = Hemp, fibre content (wt.%), and P= pellet, followed by its size.							

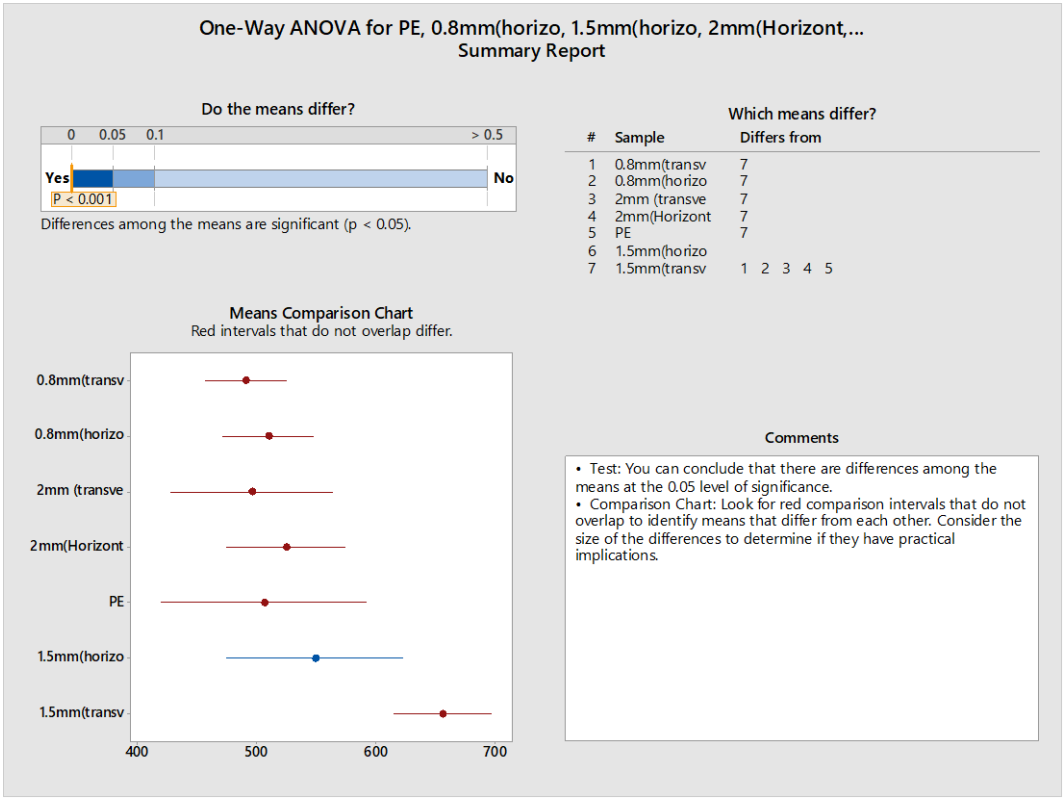

Figure 5-15 Result of one-way ANOVA hypothesis test of Young's modulus of specimens obtained from transversal and longitudinal direction of rotationally moulded composites produced with pellet sizes of 0.9, 1.5 and 2 mm.

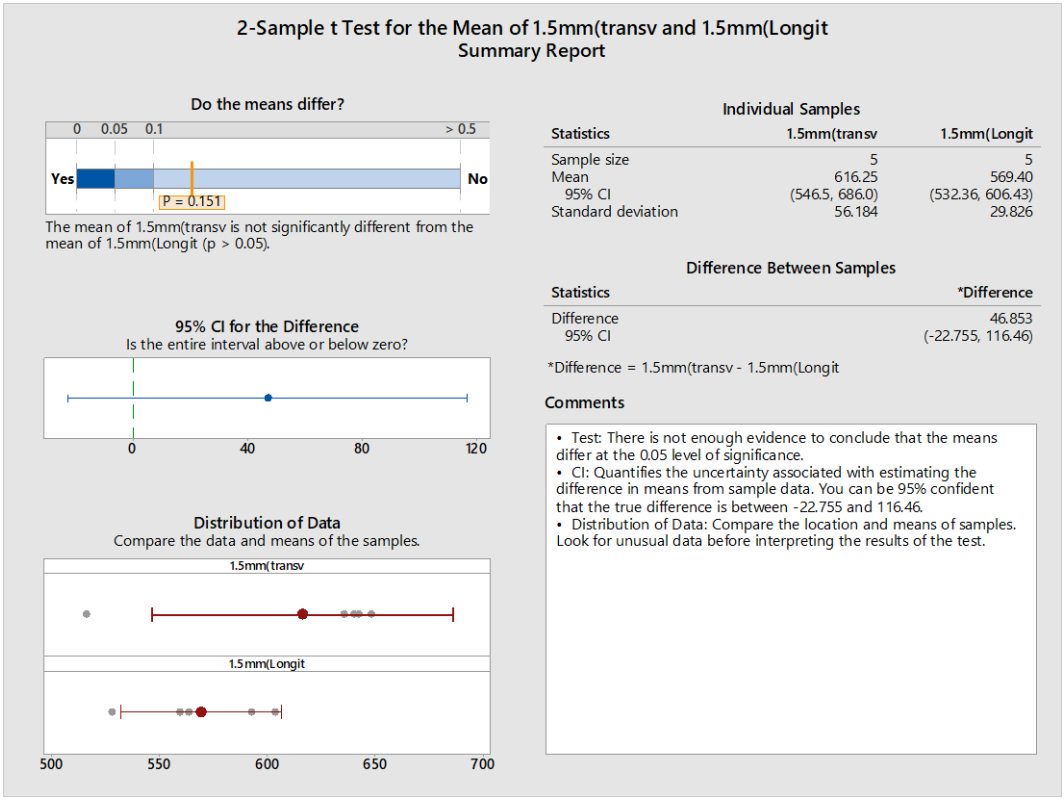

Figure 5-16: Result of 2-Sample t-test for the mean of Young's Modulus of transversal and longitudinal direction of rotationally moulded composites produced with a pellet size of 1.5 mm.

5.5 Conclusions

It was concluded in Chapter 4 that pellets with a maximum size of 1.5 mm can be used to produce rotationally moulded composites with moderate porosity by adding 3 wt.% of stearic acid. In this chapter, these pellet dimensions were controlled to assess the influence of the pellet aspect ratio on fibre orientation within rotationally moulded composites.

It was concluded from the analyses of the cross-sectional images of rotationally moulded composites that fibres were oriented in a planar-random direction. However, a predominant fibre orientation was observed in composites with 1.5- and 2-mm pellets within ± 0° (YZ plane), represented by a peak. This finding supports the hypothesis that using pellets with an increased aspect ratio (higher than 1) in rotational moulding could be beneficial in orienting the pellets, and consequently the fibres, parallel to the mould wall.

Composites produced with a 1.5 mm pellet size had superior tensile strength and Young's modulus compared to all other samples. This could be due to the predominant fibre orientation in composites using 1.5- and 2-mm pellets parallel to the XY plane. However, there was a reduction in tensile strength in composites prepared with 2 mm pellets compared to composites prepared using 1.5 mm pellets due to increased porosity.

Despite the results presented in this research, it is important to highlight that the cross-sectional shape variations of hemp fibres combined with the imperfections on the composite surface due to sample preparation could lead the software ImageJ to an inaccurate assessment of fibre orientation.

Chapter 6

Hybrids of Recycled Carbon Fibre with Hemp Fibre Produced by Rotational Moulding

Composites with two types of reinforcement fibres open a large field of opportunities and combined properties. Recycled carbon fibre leads to higher tensile and thermal properties, but these are petroleum-based. In contrast, hemp fibre has higher elongation-at-break, and is biodegradable. This study aimed to investigate the synergy of those two fibre types in a hybrid compound. Composites with an overall fibre content of 10 wt.% and different ratios of RCF and hemp fibre were prepared using a twin-screw extruder and rotational moulding.

It is well known that carbon fibre has a smooth and inert surface, which results in poor adhesion with thermoplastic matrices. To mitigate this problem, RCF was treated with HNO_3 at different times to increase the numbers of hydroxyl groups on the fibre surfaces. The coupling agent, grafted maleic anhydride polyethylene (MAPE), was used to bond recycled carbon fibre with polyethylene.

Filaments of the composites were randomly and uniformly chopped into pellets of 1.5 mm size to be used in rotational moulding. Composites produced with uniformly chopped pellets had longer fibres and the same porosity as composites produced with randomly chopped pellets. Consequently, hybrid composites were produced with uniformly chopped pellets.

Hybrid composites showed superior Young's modulus values compared to hemp-PE composites, regardless of whether treated or untreated recycled carbon fibre was used. It was also observed that the addition of carbon fibre reduced the voids in the final composites compared to hemp-PE composites, which probably contributed to the performance of hybrid composites. In addition, TGA analysis showed a slight improvement in the thermal resistance of hybrid composites compared to hemp-PE composites.

6.1 Materials and Methods

6.1.1 Materials

The industrial hemp fibre (*Cannabis Sativa L.)* used as reinforcement was grown in New Zealand. Treated hemp fibre had an average diameter of 22 µm, a real density of 1,500 kg/m^3, lengths ranging from 2 to 4 mm, tensile strength of 715 ± 471 MPa, and Young's modulus of 12 ± 7 GPa. Recycled carbon fibre (RCF) type Carbiso C (MSDS004) was obtained from ELG Carbon Fibre Ltd. The RCF had an average diameter of 7 µm, a real density of 1,800 kg/m^3, lengths ranging from 6 to 12 mm, tensile strength of 4150 MPa and Young's modulus of 230-255 GPa. The coupling agent used was polyethylene-grafted maleic anhydride Licocene PE MA 4351, viscosity 200-500 mPa.s (140°C) and acid value 42-49 mg KOH/g, obtained from Clariant in powder form. A rotational moulding grade of low-medium-density polyethylene, VX567, with a melt flow index of 6.0 g/10 min (ASTM D 1238), and density of 0.935 g/cm^3 (ASTM D 1505) was obtained in powder form from Vision Plastics (VPLAS).

6.2 Methods

6.2.1 Melt Compounding

Melt compounding was done as described in Chapter 4.

6.2.2 Pelletising

Extruded filaments were chopped into 1.5 mm pellets to be used in a rotational moulder. The granulators were fitted with 4 mm and 1.5 mm aperture screens, which provided control of the size of the pellets produced (Item 4.2.2). Uniformly chopped pellets with 1.5 mm length and diameter were produced using a benchtop lab pelletiser SGS 25-E4 (Item 5.2.2).

6.2.3 Rotational Moulding

Rotationally moulded composites were prepared as described in Chapter 3. The compositions used to produce rotationally moulded composites are shown in Table 6-1.

Table 6-1: Description of the composition of the composite pellets used in the rotational moulding.

Sample codes	*Type of Fibre*	*Fibre Content (wt.%)*	*MAPE (wt.%)*	*Stearic acid (wt.%)*	*Pellet size (mm)*
UCR1.5	Recycled carbon	10	3	3	1.5
UCU1.5	Recycled carbon	10	3	3	1.5
THU1.5	Hemp	10	3	3	1.5
80(THU1.5)/ 20(UCU1.5)	Recycled carbon + hemp	8 (HF) 2 (RCF)	3	3	1.5
50(THU1.5)/ 50(TCU1.5)	Recycled carbon + hemp	5 (HF) 5 (RCF)	3	3	1.5
50(THU1.5)/ 50(UCU1.5)	Recycled carbon + hemp	5 (HF) 5 (RCF)	3	3	1.5
Sample code: fibre treatment (U= untreated and T=treated), type of fibre (H = hemp and C=carbon fibre), R for randomly and U for uniformly chopped pellets, followed by their size					

6.2.4 Thermal Gravimetric Analysis

Three specimens of recycled carbon fibre/PE and hybrid/PE composites were analysed using a PerkinElmer STA 8000 analyser. This analysis was performed in a dynamic mode, heating from 50 °C to 800 °C at 10 °C/min and nitrogen-purged at 50 ml/min with an empty pan used as a reference. The initial weight of the samples was about 5–10 mg. The data from the test are displayed as TG (weight loss as a function of temperature) and DTG (derivative thermal gravimetry, weight loss rate as a function of temperature).

6.2.5 Fourier Transform Infrared Spectroscopy

FT-IR was used to evaluate the recycled carbon fibre surface chemistry after treatment with HNO_3. FT-IR measurements were performed using a PerkinElmer Spectrum One spectrometer with transmission mode from 4000 to 400 cm^{-1}. A total of 20 scans were taken for each sample with a resolution of 4 cm^{-1}. To prepare the samples, ground dried fibre and KBr (0.8 mg fibre per 400 mg KBr) were pressed into pellets.

6.2.6 Scanning Electron Microscopy

Scanning electron microscopy (SEM) micrographs of untreated and treated recycled carbon fibre were obtained using a Hitachi S-4100 field emission SEM. The same equipment was used to analyse cryogenic fractured filaments of RCF-PE composite.

The samples were previously mounted on aluminium stubs using carbon tape and then coated with platinum plasma. SEM observation was carried out at 5 kV.

6.2.7 Fibre Treatment with HNO_3

Recycled carbon fibres were immersed in 14 mol/L concentrated HNO_3 (65% volume) at 100 ℃. The content of nitric acid to RCF was 10 ml:1 g and the oxidation was performed for 60, 120 and 180 min. These fibres were washed in distilled water several times until a neutral pH was reached, and dried at 90 ℃ for 24 hours prior to being used. These conditions were adapted from previous research on acidic treatment applied to carbon fibres [77].

6.2.8 Tensile Testing of Rotationally Moulded Composites

The tensile strength and modulus of the hemp and hemp/recycled carbon fibre hybridised composites were measured using a universal testing machine. Tensile testing specimens (sample V- ASTM D638-14) were placed in a conditioning chamber at 23 ± 3℃ and 50 ± 5% relative humidity for 48 hours. The specimens were tested according to the ASTM D638-14 "Standard Method for Tensile Properties of Plastics", using an INSTRON-4204 tensile testing machine fitted with a 10 KN load cell and operated at a rate of 1 mm/min. An Instron extensometer was used to measure the composite strain. Five specimens of each type of composite were tested to failure.

6.2.9 Tensile Testing of Filaments of Composites

Extruded composite filaments with a diameter of about 3 mm, produced with and without MAPE, were tensile tested. The test was performed using an Instron-4204 machine fitted with a 5 KN load cell. A standard crosshead speed of 1 mm/min was applied to all filament specimens. The strain was measured using an Instron 2630-112 extensometer fitted to the samples, with a gauge length of 120 mm. All composite specimens were tested to maximum stress due to excessive necking. An average of five measurements was taken as the final experimental value.

6.2.10 Fibre Length Analysis by Optical Microscopy

Recycled carbon fibres were recovered from the degradation of the polymer matrix by heating the composites up to 600 ℃. These fibres' length was measured using optical microscopy.

6.2.11 Porosity by Optical Microscopy

The surface of rotationally moulded composites was examined using optical microscopy. The images were taken at 6.5x magnification, using a WILD M3B stereomicroscope fitted with a Nikon camera (Digital Sight DSU1). The porosity in percentage per area was obtained using ImageJ. The pore analysis was adapted from the studies of Spencer and Crawford [123]. These authors have also analysed the pores on the surface of rotationally moulded composites.

$$\text{Porosity (\%)} = \Sigma\text{pore area} / \Sigma\text{analysed area} \quad (6\text{-}1)$$

6.3 Statistical Analysis

The results of tensile testing were statistically analysed using the software MINITAB version 18. First, the values of different parameters were expressed as mean values with standard deviation and coefficient of variation. Then, one-way ANOVA was applied to compare the differences in the mean of more than two population means with a 95% simultaneous confidence level. In some cases, a t-test was used to compare two population means with the same level of confidence. A hypothesis test evaluates two mutually exclusive statements about two or more populations to determine whether to reject the null hypothesis [106].

6.4 Results and Discussion

6.4.1 Characterisation of Recycled Carbon Fibre

6.4.1.1 Thermal Gravimetric Analysis

Carbon fibres are stable at high temperatures and in inert environments [149; 150], making thermal gravimetric analysis practical for investigating the presence of sizing agents coating the fibre surface. More specifically for carbon fibres, the sizing often consists of a thin layer of epoxy that is coated onto the fibre surface. The TGA curve of recycled carbon fibre showed no mass reduction at 200–300°C, as shown in Figure 6-1. It confirms that the recycled carbon fibres were not sized. Furthermore, the thermal decomposition of the carbon fibre chain started at about 700°C, while less than 1% of mass loss was observed up to 900°C.

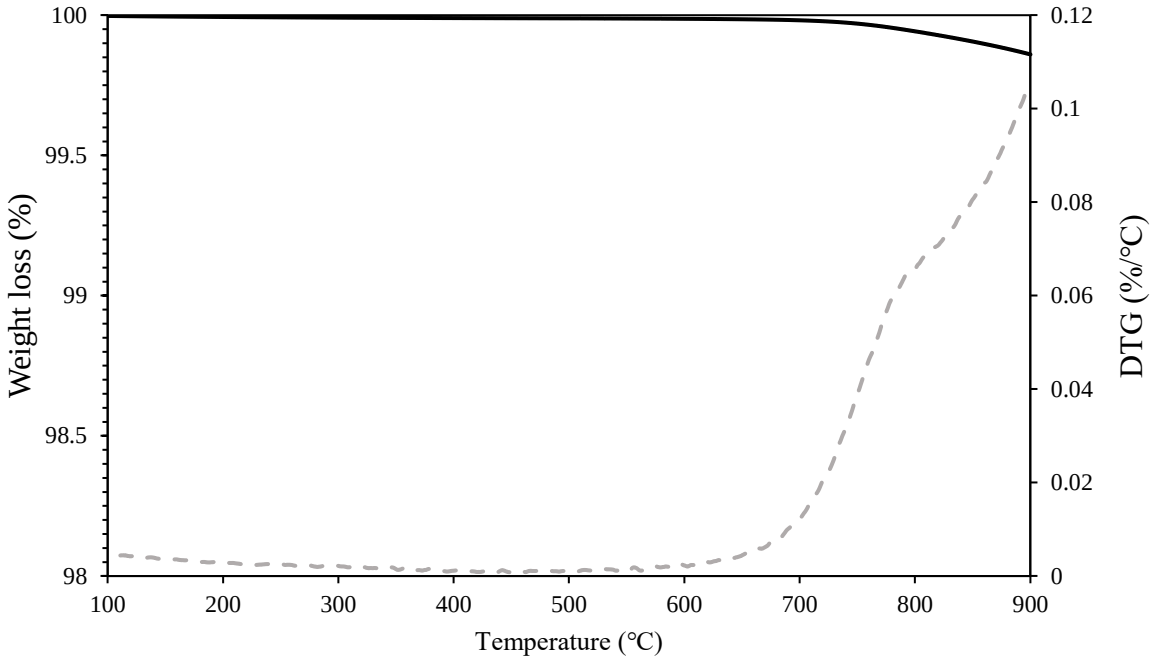

Figure 6-1: TGA analysis of recycled carbon fibre (RCF) under a nitrogen atmosphere.

6.4.1.2 Scanning Electron Microscopy (SEM)

SEM was used to identify differences between the surface morphology of virgin and recycled carbon fibre. The SEM images showed some impurities on the surface of the recycled carbon fibre (Figure 6-2b), which were not present on the virgin carbon fibre (Figure 6-2a). These impurities were reported in previous research to be the ash of the decomposed epoxy matrix from the recycling pyrolysis process [69]. This pyrolysate material on the fibre surface is reported to act as stress concentrator points, weakening the fibre during tensile load [76]. The SEM micrographs also showed that recycled carbon fibre had an average fibre diameter of 7 ± 0.4 µm, while virgin carbon fibre was about 8 ± 0.1 µm. This reduction in fibre diameter could be due to the loss of carbonaceous materials during the recycling process.

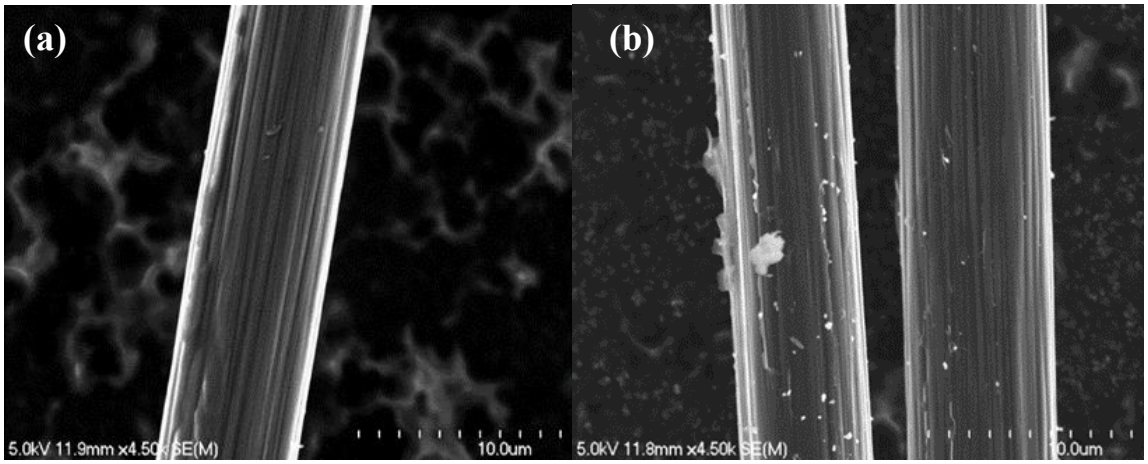

Figure 6-2: SEM images of virgin carbon fibre (a) and recycled carbon fibre (b).

6.4.2 Recycled Carbon Fibre Treatment with HNO_3

Carbon fibres have a chemically inert surface, which is incompatible with thermoplastic matrices. For this reason, fibre treatments are usually performed to incorporate oxygen groups on the fibre surface to react with coupling agents such as MAPE.

In this study, recycled carbon fibre was treated with HNO_3 for 60, 120 and 180 min at 130°C. The effect of the acidic treatment on recycled carbon fibre was evaluated using the following techniques.

6.4.2.1 Fourier Transform Infrared Spectroscopy (FT-IR)

FT-IR was used to investigate changes in the surface chemistry of recycled carbon fibres after treatment with HNO_3 (Figure 6-3). The description of the main peaks observed in treated recycled carbon fibre can be seen in Table 6-2. Figure 6-3 shows that the band at 1630 cm^{-1} corresponding to the H-bonded carbonyl group (C=O) conjugating with C=C in the graphene wall [151] appeared more intense after the treatment. Similarly, the band at 1385 cm^{-1} related to the carboxyl (COOH) group reached a maximum after 120 min of treatment. In addition, the band at 1052 cm^{-1}, corresponding to O-H stretching vibration, also increased in intensity with treatment time [152; 153]. These results indicate an increase in reactive functional groups on the fibre surface with treatment time. This introduction of reactive functional groups (OH) onto the carbon fibre surface is reported to improve fibre-polymer adhesion by creating chemical bonding with the assistance of a coupling agent [73; 77; 154].

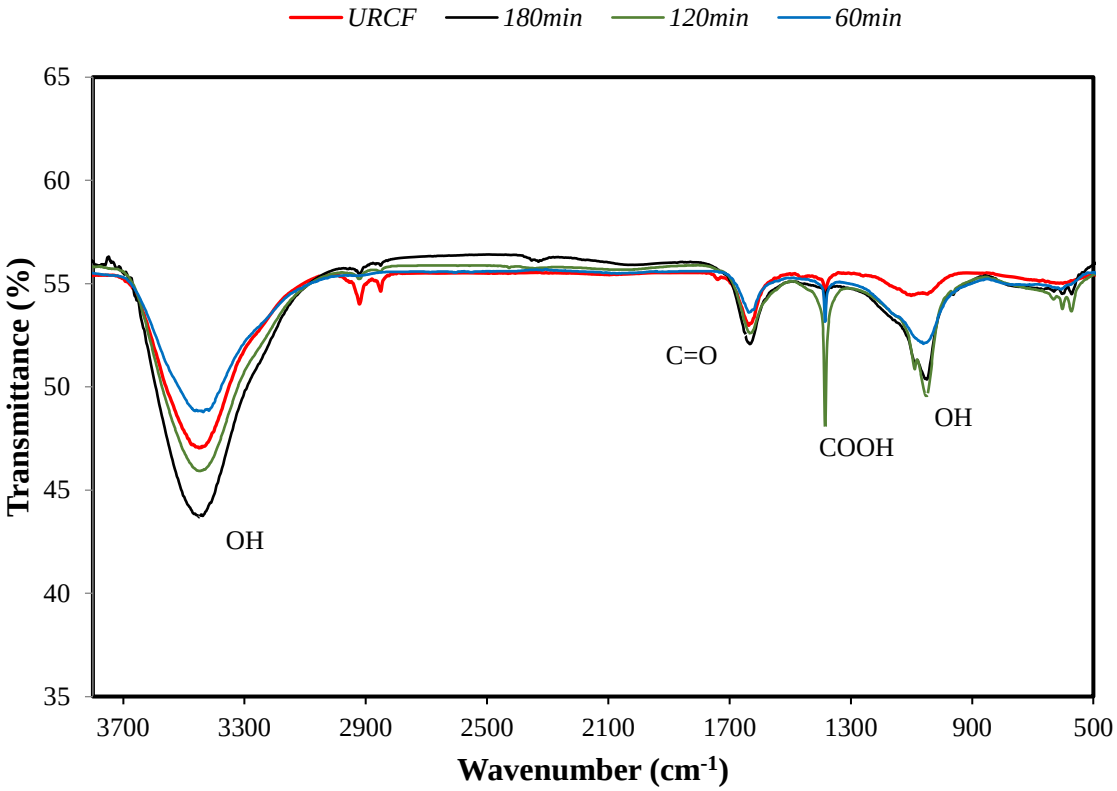

Figure 6-3: FT-IR spectra of untreated and treated recycled carbon fibre with different treatment periods.

Table 6-2: Assignment of the main functional groups found in the treated recycled carbon fibre spectrum [77; 155; 156].

Wavelength (cm^{-1})	***Functional Group***	***Band Assignment***
3384	OH	Water absorption and OH groups
2900	C=H, CH_2	Stretching of the methyl and methylene groups, hydrocarbon chains
1630	C=C and C = O	Stretching vibration in conjugated carbonyl (C=O) with C=C in the graphene wall
1385	COOH	carboxyl (COOH) group
1052	OH	O-H stretching vibration

6.4.2.2 Scanning Electron Microscopy

SEM images were used to compare the effects of nitric acid treatment on the surface of recycled carbon fibres. Figure 6-4 suggests an increase in fibre roughness with treatment time. At higher magnification, it can be seen that the parallel grooves distributed along the longitudinal direction of recycled carbon fibres were deepened in Figure 6-4d and Figure 6-4f compared to Figure 6-4b. This increased roughness benefits mechanical anchoring effects

between the fibre and the matrix [77]. It was also observed that some defects on the fibre surface appeared with 180 min treatment (Figure 6-4e), which indicates the beginning of severe oxidation [78].

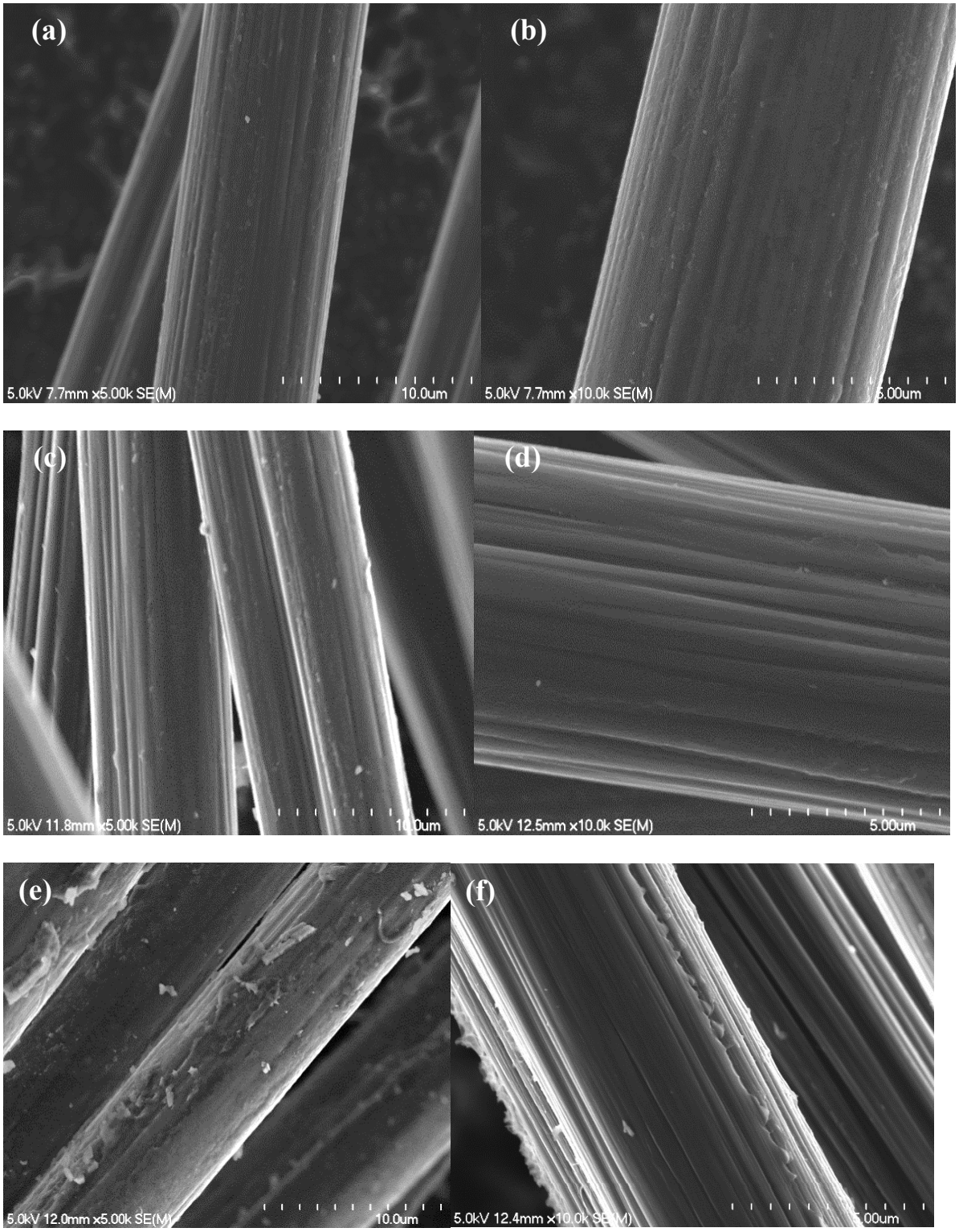

Figure 6-4: SEM images of treated RCFs after 60min (a and b), 120 min (c and d), and 180 min (e and f).

6.4.3 Evaluation of the Use of Maleic Anhydride Grafted Polyethylene (MAPE)

Figure 6-5 shows that adding 10 wt.% recycled carbon fibre improved the Young's modulus of composites compared to pure polyethylene due to the higher stiffness of recycled carbon fibre. The use of treated RCF also improved the composites' tensile strength and Young's modulus compared to composites with untreated RCF, regardless of MAPE addition (Figure 6-5). This result is probably due to the increased roughness on the RCF surface caused by the oxidation with nitric acid, leading to better bonding between fibre and matrix by mechanical interlocking. In addition, the fibre alignment obtained during the extrusion of these filaments probably contributed to an effective stress transfer during the tensile testing, which resulted in higher strength and stiffness.

The best-performing composite was produced with MAPE and treated RCF, improving tensile strength by about 45% and Young's modulus by 350% compared to pure PE (Figure 6-8). This is because the treatment of recycled carbon fibre with nitric acid increased fibre surface activity by introducing functional groups containing oxygen. As described in the literature, hydroxyl (OH) groups can form a chemical bond with the maleic anhydride groups on MAPE, while the main PE constituent of MAPE entangles with the polymeric matrix, improving the interfacial bond between fibre and matrix [77; 153; 154]. This improvement in interfacial bonding enhances the mechanical properties of reinforced composites [76; 153]. Previous studies have also reported an improvement in tensile strength using PE-g-MA to bond carbon fibre and thermoplastics [79-82]. Final tensile strength results were subjected to statistical analysis, as shown in Table 6-3, Figure 6-6 and Figure 6-7.

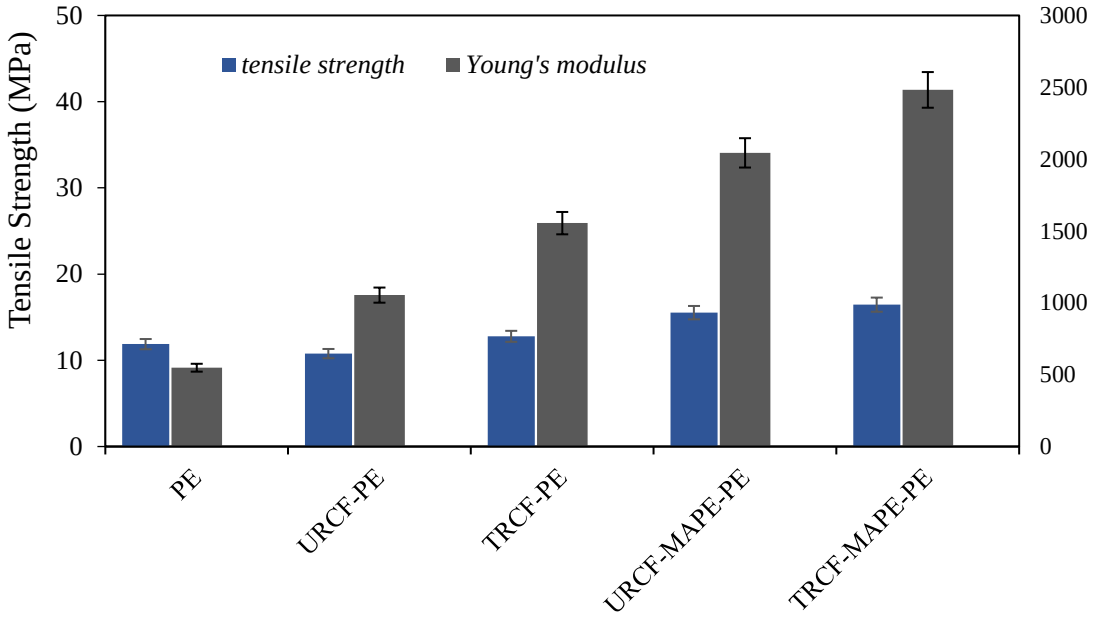

Figure 6-5: Tensile strength and Young's modulus of filaments of composites with untreated and treated recycled carbon fibre (URCF and TRCF) at 10wt% and PE with and without MAPE.

Table 6-3: Statistical analysis of tensile strength and Young's modulus of filaments of composites. P>0.05 (Gaussian Distribution).

Samples	***Sample Size***	***Tensile Strength (MPa)***	***SD***	***CV***	***Young's Modulus (MPa)***	***SD***	***CV***
URCF	5	9.03	1.22	13.47	1053.8	91.7	8.70
TRCF	5	13.23	1.50	11.35	1555	249	16.04
URCF-MAPE	5	15.53	1.61	10.36	2044	272	13.30
TRCF-MAPE	5	16.45	2.25	13.65	2481.9	197.8	7.97
Untreated (U) and Treated (T), Recycled carbon fibre (RCF) and MAPE							

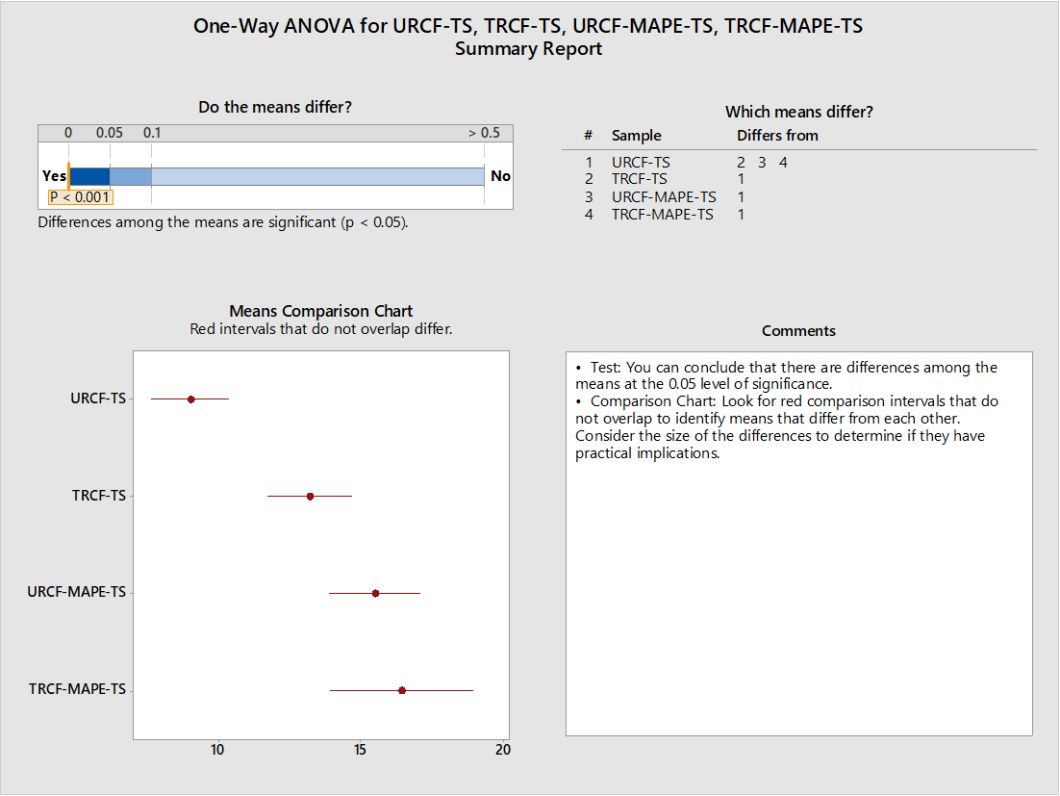

Figure 6-6: Result of one-way ANOVA hypothesis test of Tensile Strength of the following composite filaments: treated recycled carbon fibre with and without MAPE, untreated recycled carbon fibre with and without MAPE.

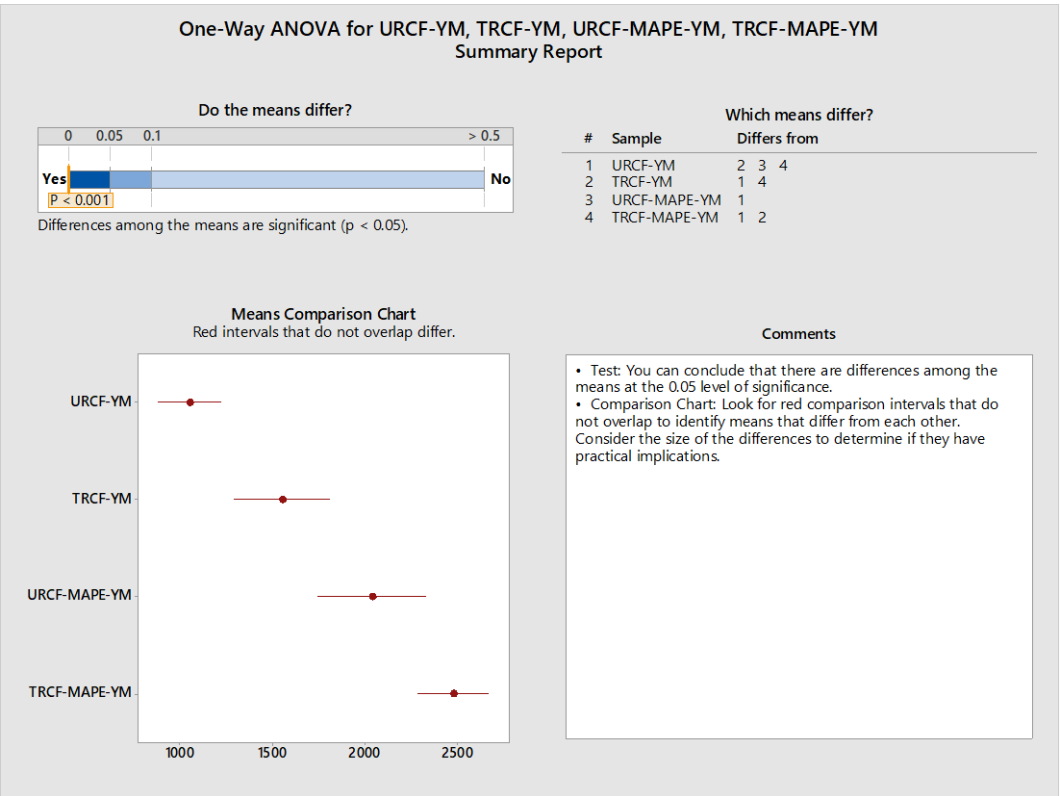

Figure 6-7: Result of one-way ANOVA hypothesis test of Young's Modulus of the following composite filaments: treated recycled carbon fibre with and without MAPE, untreated recycled carbon fibre with and without MAPE

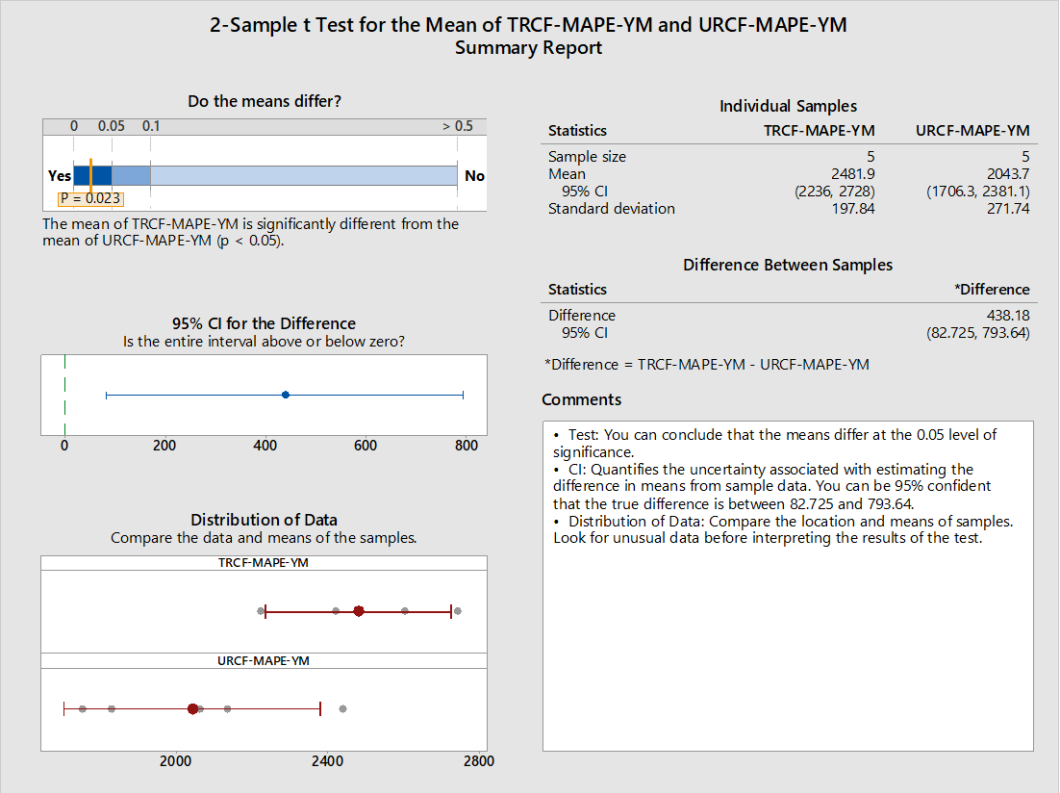

Figure 6-8: 2-sample t-test comparing Young's modulus of composite filaments of treated and untreated recycled carbon fibre with MAPE

SEM images of the fractured surfaces of composite filaments produced with treated RCF with and without MAPE at 3wt.% are shown in Figure 6-9. It was observed that there were more prominent fibre pull-outs in composites without MAPE (Figure 6-9a and b) compared to composites with MAPE (Figure 6-9c and d). This behaviour indicated fibre-matrix debonding and occurred less often in composites with MAPE, which showed more broken fibres embedded in the matrix or near-surface. However, the SEM images do not show a strong interface between the polymer matrix regardless of whether treated or untreated recycled carbon fibres were used, which means that some fibres were embedded in the matrix, while others were not.

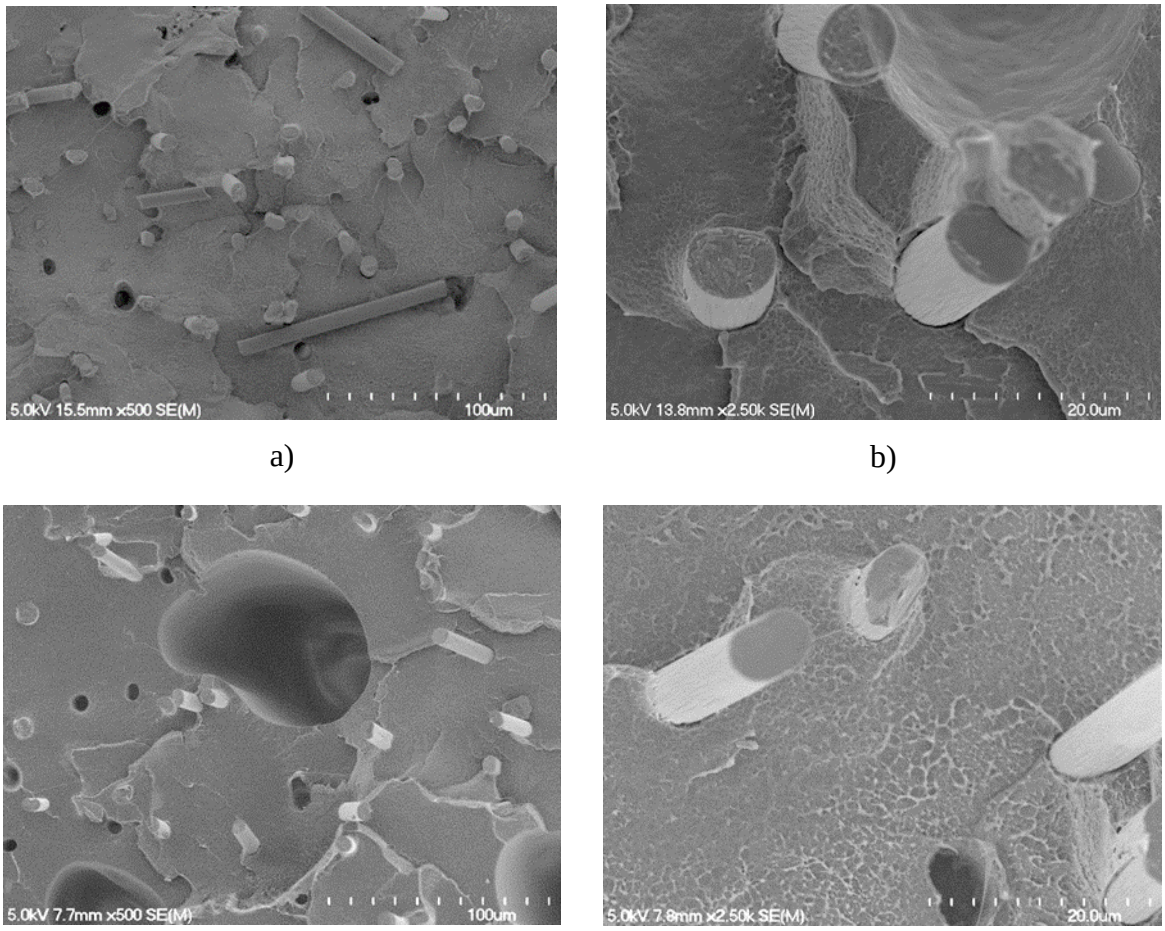

Figure 6-9: SEM images of composite filaments of treated RCF with MAPE (a and b) Untreated RCF and MAPE (c and d).

6.4.4 Study of Composite Pellet Shapes used to Produce Rotationally Moulded Composites

6.4.4.1 Analysis of Fibre Length Distribution

Recycled carbon fibre and polyethylene composites were randomly and uniformly chopped into 1.5 mm lengths to be used in rotational moulding. It is already known that significant length reductions occur during multiple processes such as extrusion and granulation. For this reason, this material was not extruded three times as in the previous chapter, but once. Recycled carbon fibres were recovered from composite pellets after the thermal degradation of the polymer matrix at 500°C, and their length distributions were analysed. Figure 6-10 shows that composites prepared with uniformly chopped pellets had a longer fibre length (230 µm) than composites prepared with randomly chopped pellets (173 µm) (see Table 6-4). This result means that recycled carbon fibres, initially 6-10 mm long, were significantly

shortened during extrusion and after granulation. It also shows that uniformly chopped pellets have the highest fibre aspect ratio, resulting in higher composite mechanical properties. Usually, a fibre aspect ratio above 10 is required to ensure adequate load transmission from a composite matrix to a reinforcing fibre [157]. However, the effectiveness of fibre length is determined by the strength of the fibre-matrix interfacial bond [146].

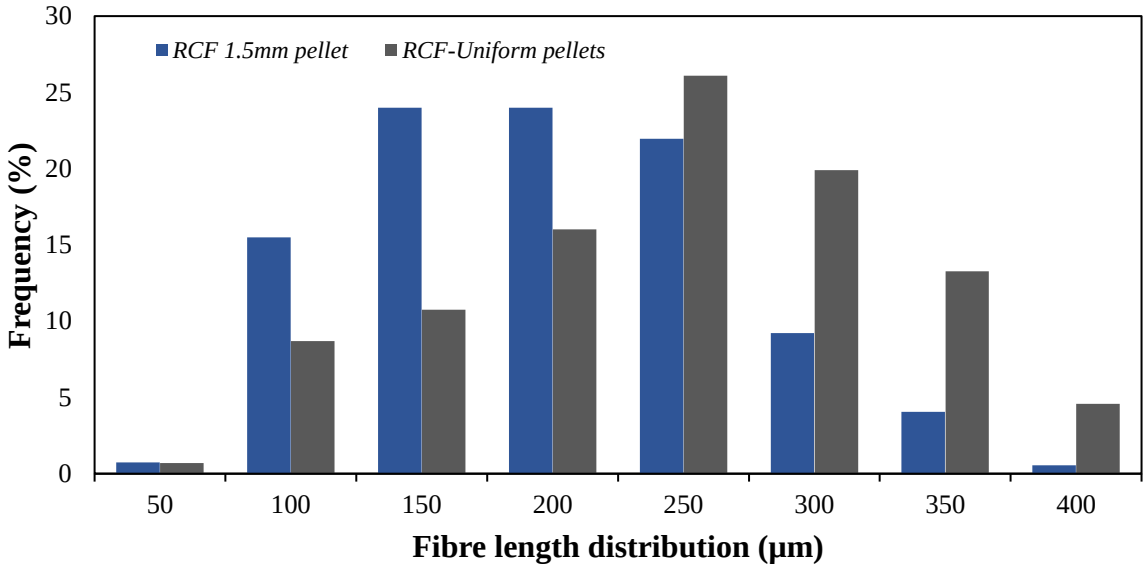

Figure 6-10: Fibre length distribution in composite pellets, randomly and uniformly chopped.

Table 6-4: Results of fibre length distribution in randomly and uniformly chopped composite pellets.

Factor	*Sample size*	*Median (µm)*	*Fibre aspect ratio*	*Minimum Length (µm)*	*Maximum Length (µm)*
RCF- randomly chopped pellets - 1.5mm	542	173	28	37	395
RCF-Uniform pellets (1.5 mm length and diameter)	542	230	38	33	439

6.4.4.2 Porosity in Rotationally Moulded Composite

Rotationally moulded polyethylene composites had their surfaces analysed by optical microscopy, as shown in Figure 6-11. It can be seen that composites produced with uniformly chopped pellets (Figure 6-11b) had fewer but larger voids than composites produced with randomly chopped pellets (Figure 6-11a). However, the analysis of these images by ImageJ showed no significant difference in porosity between them, as shown in Table 6-5. Porosity has long been known to influence the mechanical properties of composites significantly. It arises due to the inclusion of air during processing, the limited wettability of fibres, fibre bundles, and the low ability of fibres to compact.

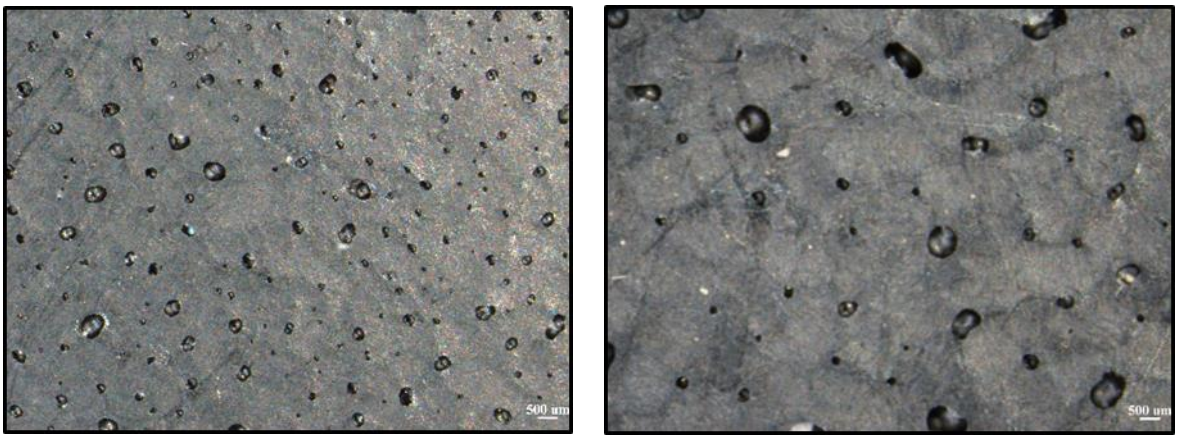

a) b)

Figure 6-11: Optical microscopy images of the surface of rotationally moulded composites produced with (a) randomly chopped 1.5 mm pellets and (c) uniformly chopped 1.5 mm pellets.

Table 6-5: Porosity analysis of rotationally moulded composites with recycled carbon fibre.

Sample	***Sample Size***	***Randomly chopped 1.5mm pellets***	***Uniformly chopped 1.5mm pellets***
Porosity in % area	12	3.91	4.3

6.4.4.3 Tensile Testing of Rotationally Moulded Composite

Figure 6-12 shows that composites produced with randomly chopped pellets of 1.5 mm size had a lower tensile strength and Young's modulus than pure polyethylene. However, the composites prepared with uniformly chopped 1.5 mm pellets showed a Young's modulus that was improved by approximately 22%. This result was probably due to the difference in fibre aspect ratio between these composites. Fibre length has an important role in composites'

reinforcement once the load applied is transferred from the matrix to the fibre by shear. If fibre length (L) > Lc, fibre reinforcement becomes more effective, and the fibre can be fully loaded over a greater length before fibre fracture occurs [8].

Another factor that might have contributed to this difference in mechanical properties is that uniformly chopped pellets might have contributed to the fibres' orientation parallel to the mould wall, as found in the previous chapter. The low tensile strength of these composites is due to the moderate interface between recycled carbon fibres and polyethylene, as discussed in Item 5.3.3. The use of carbon fibres as reinforcement for polyethylene composites is challenging because of their unreactive surfaces, which leads to poor interface adhesion [74; 164; 165]. As already discussed, a good interfacial bonding ensures an efficient load transfer from the matrix to the fibre, improving the overall mechanical properties.

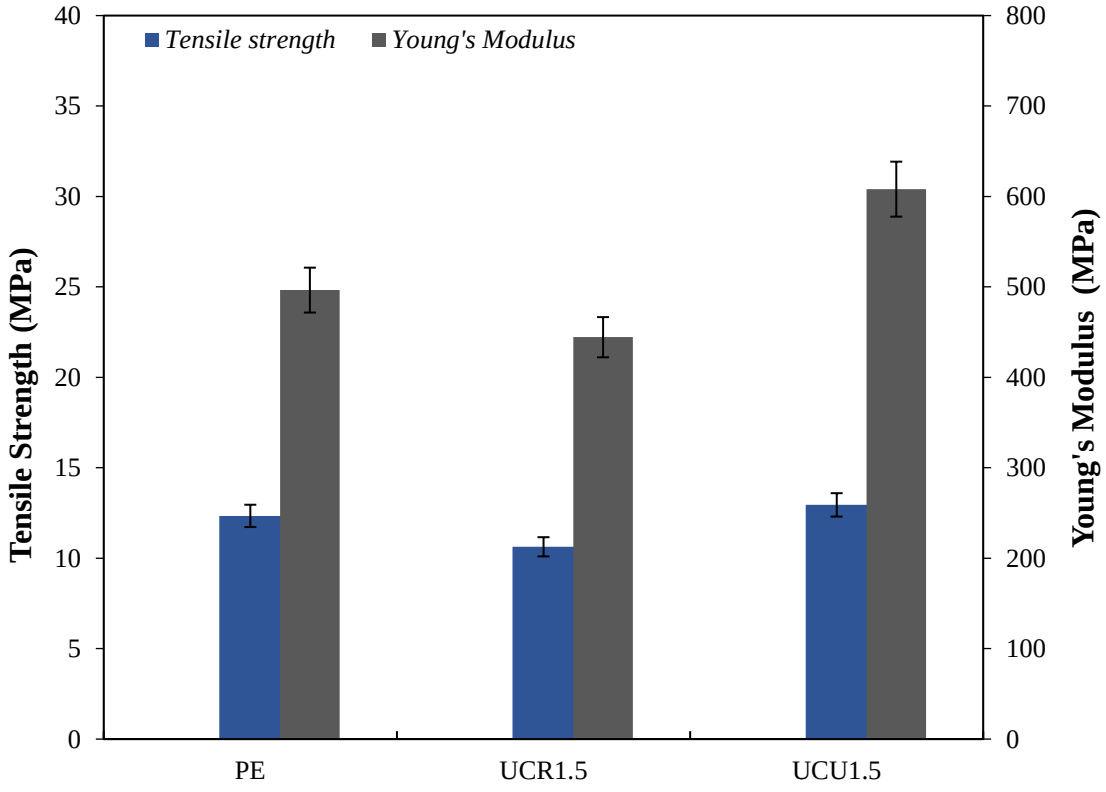

Figure 6-12: Tensile strength of rotationally moulded composites. UC = untreated recycled carbon fibre, U = uniformly chopped pellets with 1.5 mm diameter and length, R = randomly chopped pellets with 1.5 mm diameter and length.

Table 6-6: Statistical analysis of tensile strength and Young's modulus of rotationally moulded composites. P>0.05 (Gaussian Distribution).

Sample code	*Sample size*	*Tensile Strength (MPa)*	*SD*	*CV*	*Young's Modulus (MPa)*	*SD*	*CV*
PE	5	12.34	1.25	9.77	506.5	62.7	12.37
UCR1.5	5	12.30	1.20	10.5	516.5	73.7	13.35
UCU1.5	5	12.95	0.85	8.23	608.1	48.5	10.21

6.4.5 Effect of Hybridisation on the Mechanical Properties of Rotationally Moulded Composites

Hybrid composites were prepared by mixing composite pellets of hemp and recycled carbon fibre. Filaments of hemp and recycled carbon fibre were extruded separately, and their composition is described in Item 6.2.1. In general, the hybridisation of hemp with recycled carbon fibre resulted in a stiffer and stronger composite compared to natural fibre counterparts, as shown in Figure 6-13. However, it was found that there was not a statistically significant difference between the tensile strength of the hybrid composites and pure PE. This indicates that the RCF treatment was not efficient in improving the adhesion between RCF and PE in rotationally moulded composites. PE has a nonpolar nature and therefore would be non-reactive with the inert surface of the RCF [80; 158].

Similarly, there was no difference in tensile strength and Young's modulus in hybrid composites produced with untreated and treated recycled carbon fibre (Figure 6-13). It was expected that treated RCF would improve the interface between fibre and matrix, and thus the composites' mechanical properties. Previously, this research showed that composite filaments with treated recycled carbon fibre had superior mechanical properties than those with untreated fibre (Item 5.3.3). However, the low shear and absence of pressure characteristics of rotational moulding do not contribute to a good polymer-matrix interface and polymer consolidation. As a result, porosity within the final composites probably contributed to a reduction in the mechanical properties, tensile strength and Young's modulus compared to tensile properties of filaments of composite. Therefore, it was concluded that treating RCF with HNO_3 was not advantageous, considering that it is a hazard chemical and no gain in the composite's mechanical properties was observed.

Hybrid composites had superior Young's modulus values (about 20%) compared to pure polyethylene, as shown in Figure 6-13. This result was confirmed to be statistically significant by a 2-sample t-test, 95% confidence interval (Figure 6-16). Similarly, a previous study showed that the hybridization of flax fibre with carbon fibre resulted in greater stiffness in the hybrid material compared to its natural fibre counterparts [159]. In addition, the Young's modulus of hybrid composites increased with recycled carbon fibre content (from 20 to 50%). A probable explanation is the reinforcement obtained due to the high stiffness of RCF along with the reduced porosity in the final composites.

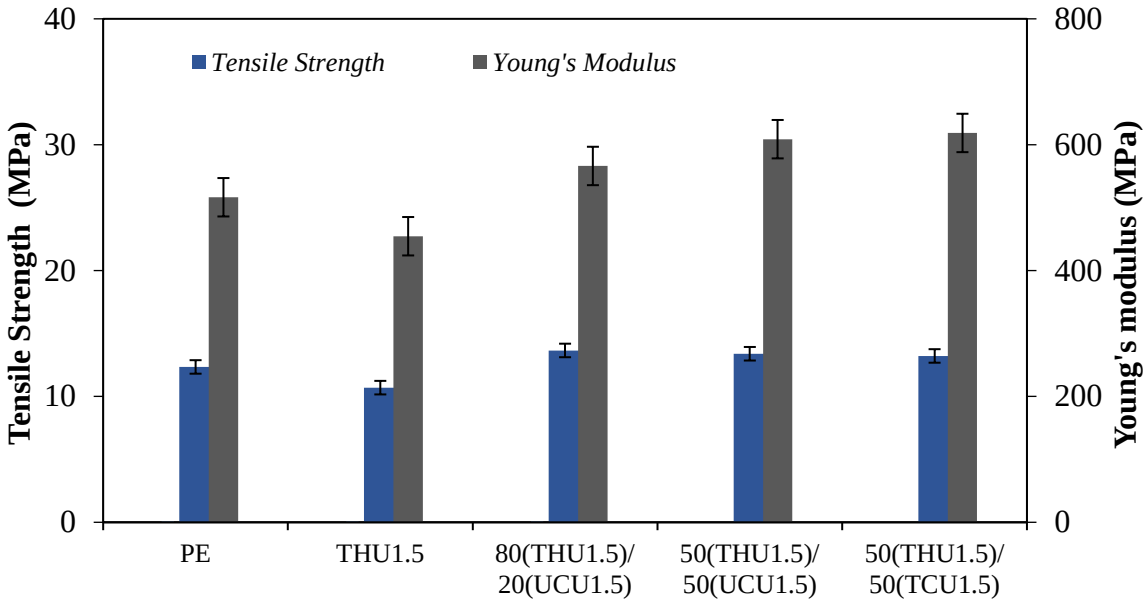

Figure 6-13: Tensile strength of pure PE, hemp fibre composites and hybrid composites of hemp and untreated recycled carbon fibre. TH= treated hemp, TC = treated carbon, UC= untreated carbon, U = uniformly chopped pellets with 1.5 mm diameter and length.

Table 6-7: Statistical analysis of tensile strength and Young's modulus of rotationally moulded composites. P>0.05 (Gaussian Distribution).

Sample Code	*Sample Size*	*Tensile Strength (MPa)*	*SD*	*CV*	*Young's Modulus (MPa)*	*SD*	*CV*
PE	5	12.34	1.25	9.77	516.5	62.7	12.37
THU1.5	5	10.68	0.37	3.53	454.54	14.38	3.16
80(THU1.5)/ 20(TCU1.5)	5	13.65	1.49	10.89	566.2	68.4	12.07
50(THU1.5)/ 50(UCU1.5)	5	13.39	0.48	3.58	608.8	22.7	3.73
50(THU1.5)/ 50(TCU1.5)	5	13.22	0.64	4.80	618.7	72.0	11.63

TH= treated hemp, TC = treated recycled carbon, UC= untreated recycled carbon, U = uniformly chopped pellets with 1.5 mm diameter and length.

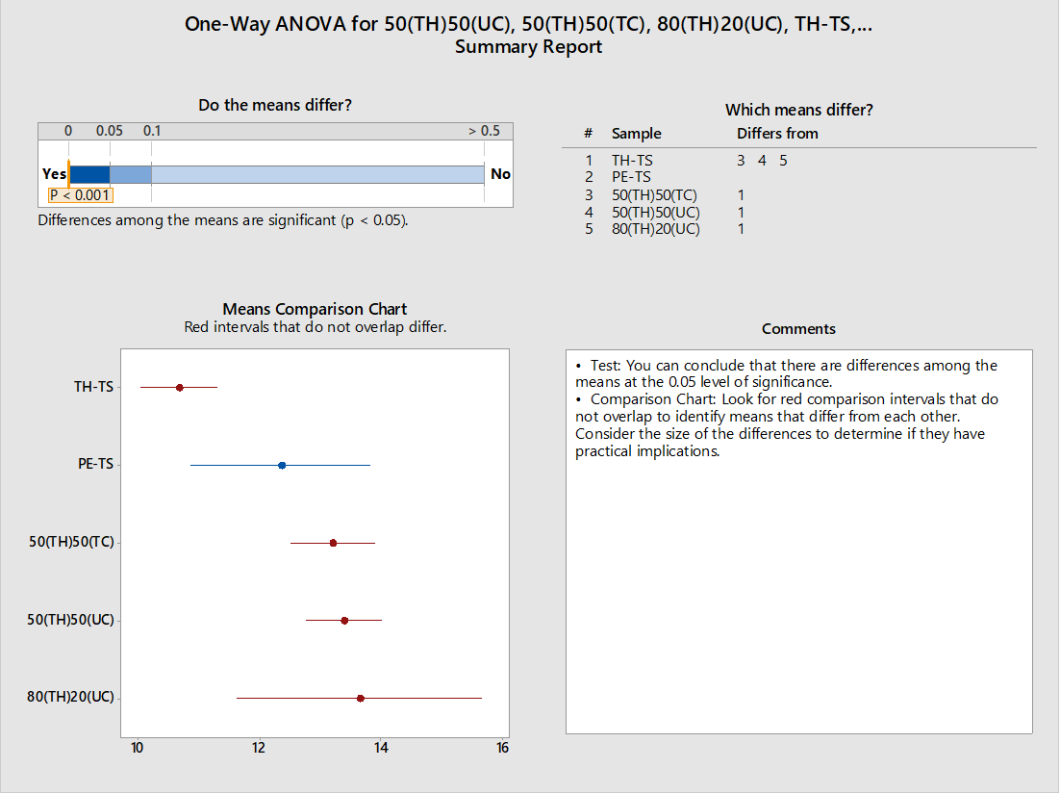

Figure 6-14: Result of one-way ANOVA hypothesis test of tensile strength of the following composite samples: pure PE, treated HF, hybrid (50%treated HF/50%untreated RCF), hybrid (50%treated HF/50%treated RCF), hybrid (20%treated HF/80%untreated RCF).

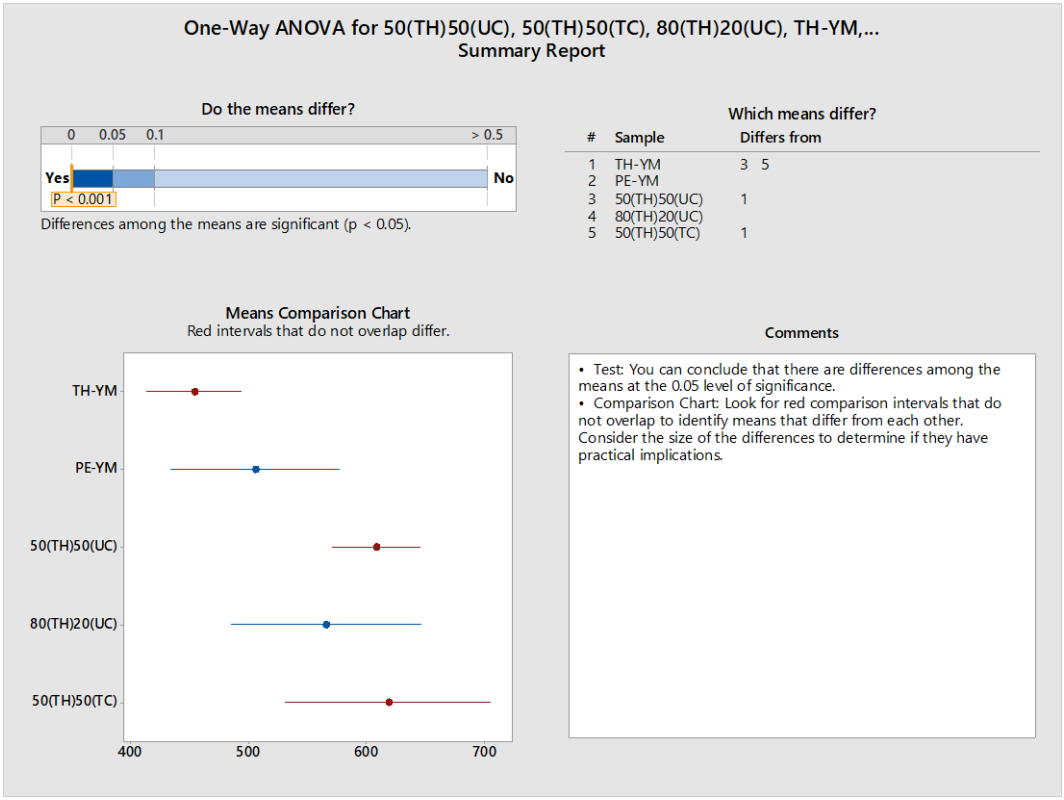

Figure 6-15: Result of one-way ANOVA hypothesis test of Young's modulus of the following composite samples: pure PE, treated HF, hybrid (50%treated HF/50%untreated RCF), hybrid (50%treated HF/50%treated RCF), hybrid (20%treated HF/80%untreated RCF).

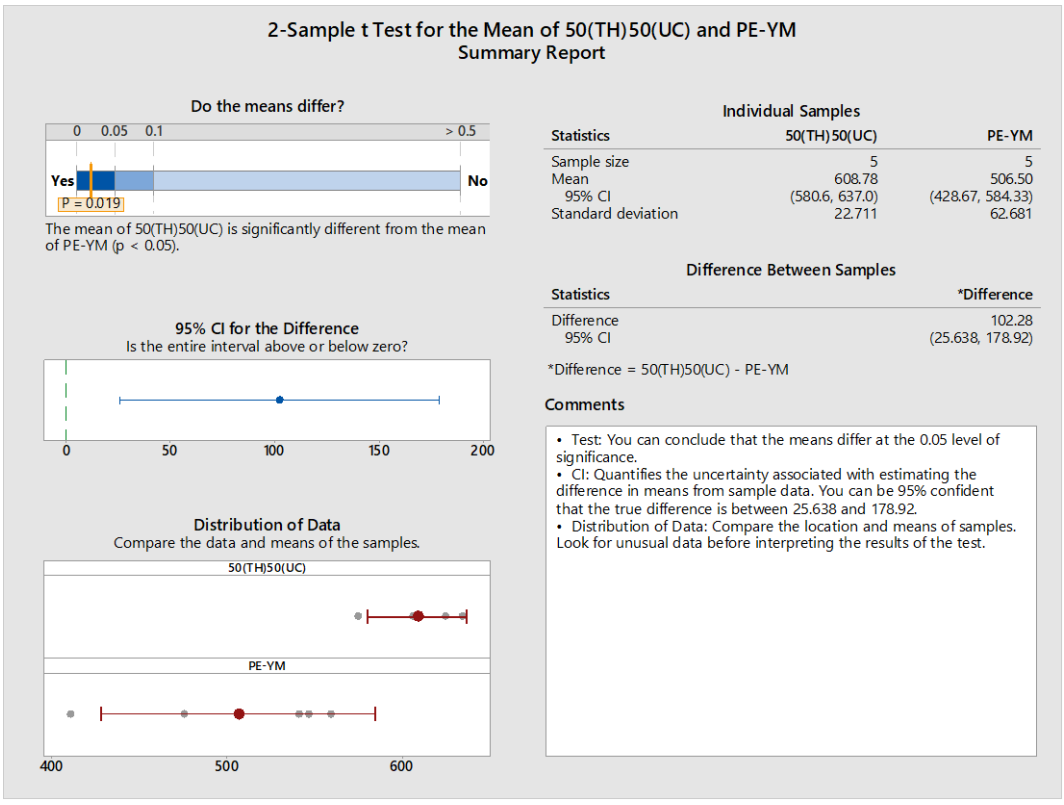

Figure 6-16: Result of 2-sample t-test of Young's modulus of pure PE and hybrid (50%treated HF/50%untreated RCF).

6.4.6 Effect of Hybridisation on the Porosity of Rotationally Moulded Composites

The hybridisation of hemp with recycled carbon fibre improved the surface aesthetics of rotationally moulded composites, as shown in Figure 6-17. Image analysis showed that hybrid composites had more but smaller voids on their surface than hemp-PE composites (Figure 6-18). The higher thermal conductivity of carbon fibres probably assisted the sintering of hemp-PE composite pellets during the process, thus reducing the porosity of the final composites (Table 6-8). Hybrid composites had many pinholes on their surfaces, which are related to the release of air trapped during the process. Usually, using external pressure minimizes gas inclusions in composites, even those that occur within the filling structure. However, the lack of pressure and shear forces during rotational moulding can lead to a significant number of internal voids [160; 161].

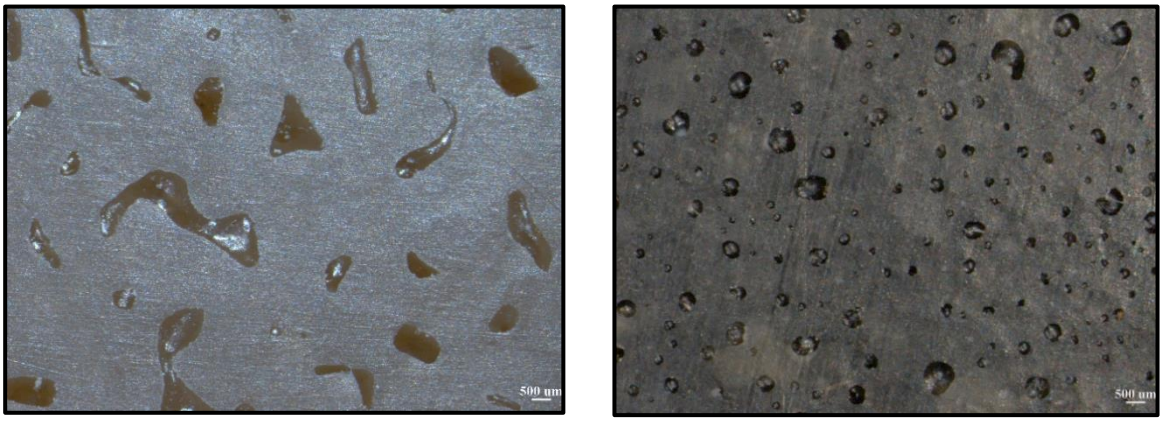

a) b)

Figure 6-17: Optical microscopy images of hemp fibre-PE composite (a) and a hybrid composite of hemp and recycled carbon fibre and PE (50% RCF-50%HF) (b).

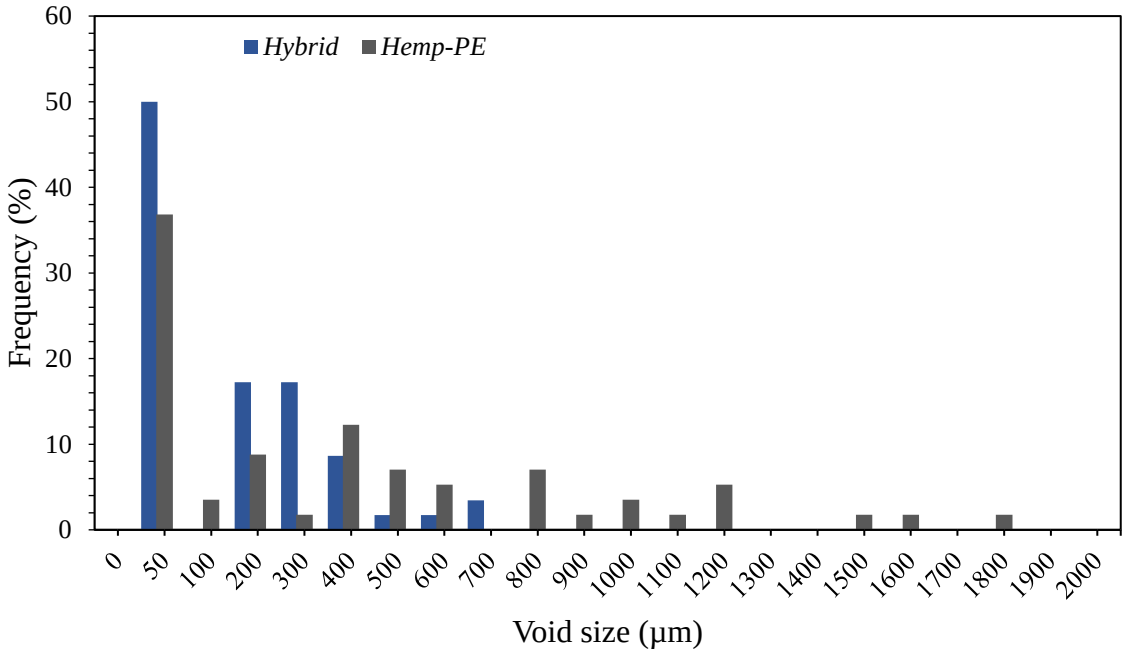

Figure 6-18: Void size distribution in HF-PE and hybrid composites.

Table 6-8: Porosity analysis of hemp-PE and hybrid composites.

Sample code	***Sample size***	***Porosity (area %)***
THU1.5	12	7.7
50(THU1.5) / 50(UCU1.5)	12	6.8

6.4.7 Effect of Hybridisation on Thermal Behaviour of Composites

Figure 6-19 shows a two-stage degradation process between 300 and 500 ℃ in the TG and DTG curves of hybrid and hemp-PE composites. The first stage (250–400℃) is due to the decomposition of hemicellulose and cellulose, whereas the second stage, at about 500 ℃, is due to cellulose and lignin decomposition. The main events observed in the TG and DTG curves are summarised in Table 6-9, which shows that the addition of recycled carbon fibre increased the onset temperature of decomposition of the composite and the temperature at the main decomposition peak. It also shows that the residual charcoal increased from 2.9 to 4.7% with the hybridisation of the hemp composite. These results indicate an increase in thermal

stability due to the addition of recycled carbon fibre, which is more resistant to heat than hemp fibre.

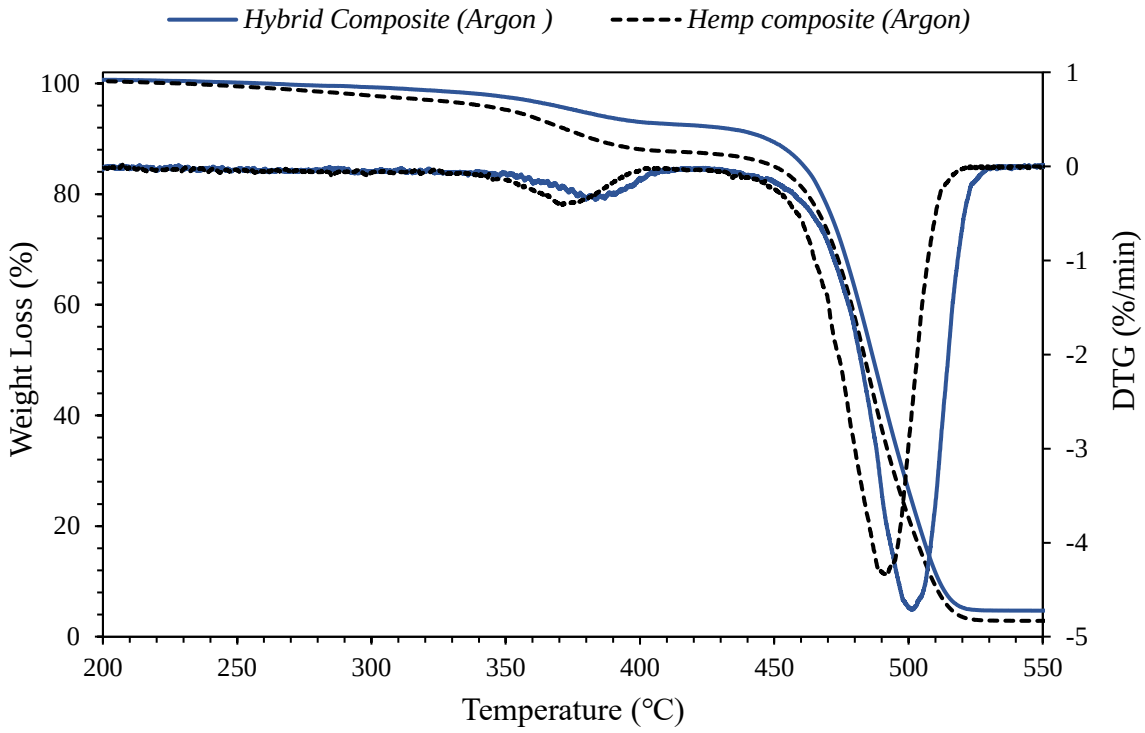

Figure 6-19: Thermograms of hemp-PE and hemp-recycled carbon fibre-PE composites.

Table 6-9 Summarised thermal analysis data for various specimens.

Sample code	***Onset decomposition temperature (℃)***	***Temperature at the main decomposition peak (℃)***	***Residual char yield (%)***
50(THU1.5) / 50(UCU1.5)	385	500	4.7
THU1.5	370	490	2.9

6.5 Conclusions

The previous chapters showed improvements with the addition of 3 wt.% of stearic acid to reduce the final porosity within rotationally moulded composites. However, there is still room for improvement as just modest tensile properties were obtained for fibre reinforced composites, compared to pure PE, due to porosity. For this reason, in this chapter recycled carbon fibre was assessed to reduce porosity within hybrid composites produced by rotational moulding.

Filaments of composite with treated RCF had superior tensile properties compared to composites with untreated fibre, regardless of the addition of MAPE. This result was attributed to an increase in fibre roughness, which contributed to mechanical interlocking. The best-performing composite was prepared with treated RCF and MAPE, which probably resulted in a superior interface between fibre and matrix.

The hybridisation of hemp fibre with recycled carbon fibre resulted in composites with superior tensile strength and Young's modulus, regardless of recycled carbon fibre treatment. Additionally, there was no difference between the tensile properties of rotationally moulded composites with untreated and treated recycled carbon fibre. In conclusion, these results showed that treating recycled carbon fibre with HNO_3 prior to rotational moulding is not advantageous, considering the time consumed and the hazardous residues generated.

The addition of carbon fibre reduced the size of the voids on the hybrid composites' surface compared to hemp-PE composites. The combination of low porosity and the high stiffness of recycled carbon fibre contributed to an increase of 20% in the Young's modulus in hybrid composites with 50% RCF compared to pure polyethylene.

Chapter 7
General Conclusions

This research showed that alkali-treated hemp fibre could be used for increasing the strength and stiffness of rotationally moulded products. It also showed that:

- Treated hemp fibre is an environmentally friendly alternative to reduce the use of petrol-based thermoplastics in rotationally moulded products.
- Alkali treatment must be used to improve both fibre resistance to thermal degradation and fibre separation from their bundles.
- MAPE must be used to improve the adhesion between alkali-treated hemp fibre and polyethylene.
- Fibre and matrix must be melt-compounded prior to rotational moulding to improve fibre dispersion.
- Stearic acid at 3wt.% can successfully mitigate porosity in hemp fibre-reinforced rotationally moulded PE composites.
- Composite pellets up to 1.5 mm in size (with an aspect ratio higher than 1) can be used to produce rotationally moulded composites with increased fibre length and fibre orientation parallel to the mould wall. In addition, using large pellets in rotational moulding would reduce processing costs related to micronizing.
- The hybridisation of natural fibres with recycled carbon fibre would be beneficial to reduce void size and increase stiffness within the final composites.
- The modest tensile properties encountered in this research resulted from a combination of poor fibre-matrix interfaces and high porosity due to the lack of pressure and shear forces during rotational moulding. As a result, potential applications certainly could not include demanding structural applications. Instead, the application area is more likely to be consumer products, such as furniture accessories or garden equipment.

Chapter 8

Recommendations and Future Work

This research has provided important outcomes for improving the mechanical properties of rotationally moulded polyethylene composites reinforced with alkali-treated hemp fibre. Some suggestions for further research, considering the findings presented, are as follows:

- This research showed that melt compounding fibres before rotational moulding is an efficient method to improve fibre dispersion within the matrix. However, there was a significant fibre length reduction after extrusion. Perhaps studying other mixing methods to avoid this fibre reduction during the process would be beneficial in increasing mechanical properties in the final composites.
- In this research, PE was used, as it is the most common polymer applied in the rotational moulding industry. However, other polymers with lower density might improve fibre wettability, thus reducing composite porosity, which might be beneficial with regard to mechanical properties.
- This research showed that the major issue when using reinforcement in rotational moulding is void formation. Therefore, further study on void reduction could be done with different additives and fine pellets.
- The research showed that 2D image analysis to study fibre orientation gives limited results. Using a different technique to study fibre orientation, such as X-ray microcomputer tomography followed by image analysis, would be more accurate.

References

1. Crawford, R. J. (1996). *Rotational moulding of plastics*. (2nd ed.). Research Studies Press.

2. Oliveira, M. A., Pickering, K. L., Sunny, T., & Lin, R. J. (2021). Treatment of hemp fibres for use in rotational moulding. *Journal of Polymer Research, 28*(2), 1-9.

3. Crawford, R. J., Crawford, R. J., & Throne, J. L. (2001). *Rotational molding technology*. William Andrew.

4. Greco, A., Romano, G., & Maffezzoli, A. (2014). Selective reinforcement of LLDPE components produced by rotational molding with thermoplastic matrix pultruded profiles. *Composites Part B: Engineering, 56*, 157-162.

5. Torres, F. G., & Aragon, C. L. (2006). Final product testing of rotational moulded natural fibre-reinforced polyethylene. *Polymer Testing, 25*(4), 568-577.

6. Pickering, K. L., Efendy, M. G. A., & Le, T. M. (2016). A review of recent developments in natural fibre composites and their mechanical performance. *Composites Part A: Applied Science and Manufacturing, 83*, 98-112.

7. Faruk, O., Bledzki, A. K., Fink, H. P., & Sain, M. (2014). Progress report on natural fiber reinforced composites. *Macromolecular Materials and Engineering, 299*(1), 9-26.

8. Lei, Y., Wu, Q., Yao, F., & Xu, Y. (2007). Preparation and properties of recycled HDPE/natural fiber composites. *Composites Part A: Applied Science and Manufacturing, 38*(7), 1664-1674.

9. Sanadi, A., Young, R., Clemons, C., & Rowell, R. (1994). Recycled newspaper fibers as reinforcing fillers in thermoplastics: Part I-Analysis of tensile and impact properties in polypropylene. *Journal of Reinforced Plastics and Composites, 13*(1), 54-67.

10. Kabir, M., Wang, H., Lau, K., & Cardona, F. (2012). Chemical treatments on plant-based natural fibre reinforced polymer composites: An overview. *Composites Part B: Engineering, 43*(7), 2883-2892.

11. Sawpan, M. A., Pickering, K. L., & Fernyhough, A. J. (2011). Effect of various chemical treatments on the fibre structure and tensile properties of industrial hemp fibres. *Composites Part A: Applied Science and Manufacturing, 42*(8), 888-895.

12. Xie, Y., Hill, C. A. S., Xiao, Z., Militz, H., & Mai, C. (2010). Silane coupling agents used for natural fiber/polymer composites: A review. *Composites Part A: Applied Science and Manufacturing, 41*(7), 806-819.

13. Liu, H., You, L., Jin, H., & Yu, W. (2013). Influence of alkali treatment on the structure and properties of hemp fibers. *Fibers and polymers, 14*(3), 389-395.

14. Chandrasekar, M., Ishak, M. R., Sapuan, S. M., Leman, Z., & Jawaid, M. (2017). A review on the characterisation of natural fibres and their composites after alkali treatment and water absorption. *Plastics, Rubber and Composites, 46*(3), 119-136.

15. Keener, T., Stuart, R., & Brown, T. (2004). Maleated coupling agents for natural fibre composites. *Composites Part A: Applied Science and Manufacturing, 35*(3), 357-362.

16. Prachayawarakorn, J., Khunsumled, S., Thongpin, C., Kositchaiyong, A., & Sombatsompop, N. (2008). Effects of silane and MAPE coupling agents on the properties and interfacial adhesion of wood-filled PVC/LDPE blend. *Journal of Applied Polymer Science, 108*(6), 3523-3530.

17. Cisneros-López, E. O., González-López, M. E., Pérez-Fonseca, A. A., González-Núñez, R., Rodrigue, D., & Robledo-Ortíz, J. R. (2017). Effect of fiber content and surface treatment on the mechanical properties of natural fiber composites produced by rotomolding. *Composite Interfaces, 24*(1), 35-53.

18. Hanana, F. E., Chimeni, D. Y., & Rodrigue, D. J. (2018). Morphology and mechanical properties of maple reinforced LLDPE produced by rotational moulding: Effect of fibre content and surface treatment. *Polymer Composites 26*(4), 299-308.

19. Cisneros-López, E., Pérez-Fonseca, A., Ramírez-Arreola, D., González-Núñez, R., González-García, Y., Robledo-Ortíz, J., & Rodrigue, D. (2018). Polylactic acid–agave fiber biocomposites produced by rotational molding: A comparative study with compression molding. *Advances in Polymer Technology, 37*, 2528-2540.

20. González-López, M. E., Pérez-Fonseca, A. A., Cisneros-López, E. O., Manríquez-González, R., Ramírez-Arreola, D. E., Rodrigue, D., & Robledo-Ortíz, J. R. (2019). Effect of maleated PLA on the properties of rotomolded PLA-agave fiber biocomposites. *Journal of Polymers and the Environment, 27*(1), 61-73.

21. López-Bañuelos, R. H., Moscoso, F. J., Ortega-Gudiño, P., Mendizabal, E., Rodrigue, D., & González-Núñez, R. (2012). Rotational molding of polyethylene composites based on agave fibers. *Polymer Engineering & Science, 52*(12), 2489-2497.

22. Höfler, G., Lin, R. J., & Jayaraman, K. (2018). Rotational moulding and mechanical characterisation of halloysite reinforced polyethylenes. *Journal of Polymer Research, 25*(6), 132.

23. Pervaiz, M., Sain, M., & Ghosh, A. (2006). Evaluation of the influence of fibre length and concentration on mechanical performance of hemp fibre reinforced polypropylene composite. *Journal of Natural Fibers, 2*(4), 67-84.

24. Greco, A., Maffezzoli, A., & Forleo, S. (2014). Sintering of PLLA powders for rotational molding. *Thermochimica Acta, 582*, 59-67.

25. Xu, L., & Crawford, R. (1993). Analysis of the formation and removal of gas bubbles in rotationally moulded thermoplastics. *Journal of Materials Science, 28*(8), 2067-2074.

26. Crawford, R. J. (2012). *Practical guide to rotational moulding*. Smithers Rapra.

27. Chaudhary, B. I., Takacs, E., & Vlachopoulos, J. (2001). Processing enhancers for rotational molding of polyethylene. *Polymer Engineering and Science, 41*(10), 1731-1742.

28. Kulikov, O., Hornung, K., & Wagner, M. (2009). Novel processing additives for rotational molding of polyethylene. *International Polymer Processing 24*(5), 452-462.

29. Zampaloni, M., Pourboghrat, F., Yankovich, S., Rodgers, B., Moore, J., Drzal, L., Mohanty, A., & Misra, M. (2007). Kenaf natural fiber reinforced polypropylene composites: A discussion on manufacturing problems and solutions. *Composites Part A: Applied Science and Manufacturing, 38*(6), 1569-1580.

30. Milner, K. C., Anacker, R. L., Fukushi, K., Haskins, W. T., Landy, M., Malmgren, B., & Ribi, E. (1963). Symposium on relationship of structure of microorganisms to their immunological properties: III. Structure and biological properties of surface antigens from gram-negative bacteria. *Bacteriological Reviews, 27*(4), 352.

31. Beckermann, G. (2007). *Performance of hemp-fibre reinforced polypropylene composite materials.* PhD thesis, University of Waikato, Hamilton, New Zealand.

32. Bledzki, A., & Gassan, J. (1999). Composites reinforced with cellulose based fibres. *Progress in Polymer Science, 24*(2), 221-274.

33. Kumar, A., Kumar, J., & Bhaskar, T. (2020). Utilization of lignin: A sustainable and eco-friendly approach. *Journal of the Energy Institute, 93*(1), 235-271.

34. Shahzad, A. (2012). Hemp fiber and its composites–A review. *Journal of Composite Materials, 46*(8), 973-986.

35. Pickering, K. (2008). *Properties and Performance of Natural-Fibre Composites*. Cambridge, England: Elsevier.

36. Rehman, M., Fahad, S., Du, G., Cheng, X., Yang, Y., Tang, K., Liu, L., Liu, F.-H., & Deng, G. (2021). Evaluation of hemp (*Cannabis sativa L.*) as an industrial crop: A review. *Environmental Science and Pollution Research, 28*(38), 52832-52843.

37. Le Duigou, A., Pillin, I., Bourmaud, A., Davies, P., & Baley, C. (2008). Effect of recycling on mechanical behaviour of biocompostable flax/poly(l-lactide) composites. *Composites Part A: Applied Science and Manufacturing, 39*(9), 1471-1478.

38. Moran, J., Alvarez, V., Petrucci, R., Kenny, J., & Vazquez, A. (2007). Mechanical properties of polypropylene composites based on natural fibers subjected to multiple extrusion cycles. *Journal of Applied Polymer Science, 103*(1), 228-237.

39. Wambua, P., Ivens, J., & Verpoest, I. (2003). Natural fibres: Can they replace glass in fibre reinforced plastics? *Composites Science and Technology, 63*(9), 1259-1264.

40. Monteiro, S. N., Calado, V., Rodriguez, R. J., & Margem, F. M. (2012). Thermogravimetric stability of polymer composites reinforced with less common lignocellulosic fibers–An overview. *Journal of Materials Research and Technology, 1*(2), 117-126.

41. Ghazali Mohd, A. E. (2016). *Bio-composites materials from engineered natural fibres for structural applications.* Doctoral thesis, University of Waikato.

42. Salit, M. S., Jawaid, M., Yusoff, N. B., & Hoque, M. E. (2015). *Manufacturing of Natural Fibre Reinforced Polymer Composites*. (Vol. 1). Springer, Cham.

43. Fu, S.-Y., & Lauke, B. (1996). Effects of fiber length and fiber orientation distributions on the tensile strength of short-fiber-reinforced polymers. *Composites Science and Technology, 56*(10), 1179-1190.

44. Le Troedec, M., Sedan, D., Peyratout, C., Bonnet, J. P., Smith, A., Guinebretiere, R., Gloaguen, V., & Krausz, P. J. (2008). Influence of various chemical treatments on the composition and structure of hemp fibres. *Composites Part A: Applied Science and Manufacturing, 39*(3), 514-522.

45. Efendy, M. A., & Pickering, K. L. J. (2014). *Comparison of Harakeke with hemp fibre as a potential reinforcement in composites*. *Composites Part A: Applied Science and Manufacturing, 67*, 259-267.

46. Matthews, F. L., & Rawlings, R. D. (1999). *Composite Materials: Engineering and Science*. Boca Raton, FL: CRC press.

47. Walker, J. C. (2006). Basic wood chemistry and cell wall ultrastructure. In *Primary Wood Processing* (pp. 23-67). Springer.

48. Pérez, J., Munoz-Dorado, J., de la Rubia, T., & Martinez, J. (2002). Biodegradation and biological treatments of cellulose, hemicellulose and lignin: an overview. *International Microbiology, 5*(2), 53-63.

49. Gassan, J., & Bledzki, A. (2000). Possibilities to improve the properties of natural fiber reinforced plastics by fiber modification–Jute polypropylene composites. *Applied Composite Materials, 7*(5-6), 373-385.

50. Sinha, E., & Panigrahi, S. (2009). Effect of plasma treatment on structure, wettability of jute fiber and flexural strength of its composite. *Journal of Composite Materials, 43*(17), 1791-1802.

51. Clarke, A., Davidson, N., & Archenhold, G. (1993). Measurements of fibre direction in reinforced polymer composites. *Journal of Microscopy, 171*(1), 69-79.

52. Lu, J. Z., Wu, Q., & McNabb, H. S. (2007). Chemical coupling in wood fiber and polymer composites: A review of coupling agents and treatments. *Wood and Fiber Science, 32*(1), 88-104.

53. Li, X., Tabil, L. G., & Panigrahi, S. (2007). Chemical treatments of natural fiber for use in natural fiber-reinforced composites: A review. *Journal of Polymers and the Environment, 15*(1), 25-33.

54. Kabir, M., Wang, H., Lau, K., & Cardona, F. (2013). Effects of chemical treatments on hemp fibre structure. *Applied Surface Science 276*, 13-23.

55. Le Troëdec, M., Peyratout, C. S., Smith, A., & Chotard, T. (2009). Influence of various chemical treatments on the interactions between hemp fibres and a lime matrix. *Journal of the European Ceramic Society, 29*(10), 1861-1868.

56. Li, Y., Mai, Y.-W., & Ye, L. (2000). Sisal fibre and its composites: A review of recent developments. *Composites Science and Technology, 60*(11), 2037-2055.

57. Lu, J. Z., Wu, Q., & Negulescu, I. I. (2007). The influence of maleation on polymer adsorption and fixation, wood surface wettability, and interfacial bonding strength in wood-pvc composites. *Wood and Fiber Science, 34*(3), 434-459.

58. Kelm, G. R., & Wickett, R. R. (2017). The role of fatty acids in cosmetic technology. In *Fatty Acids* (pp. 385-404). Elsevier.

59. Ahmad, M. U. (2017). *Fatty acids: Chemistry, synthesis, and applications*. Elsevier.

60. Patti, A., Lecocq, H., Serghei, A., Acierno, D., & Cassagnau, P. (2021). The universal usefulness of stearic acid as surface modifier: applications to the polymer formulations and composite processing. *Journal of Industrial and Engineering Chemistry, 96*, 1-33.

61. Rueda, M. M., Auscher, M.-C., Fulchiron, R., Perie, T., Martin, G., Sonntag, P., & Cassagnau, P. (2017). Rheology and applications of highly filled polymers: A review of current understanding. *Progress in Polymer Science, 66*, 22-53.

62. Broda, J., Slusarczyk, C., Fabia, J., & Demsar, A. (2016). Formation and properties of polypropylene/stearic acid composite fibers. *Textile Research Journal, 86*(1), 64-71.

63. Moret, S., Marega, M., Conte, L., & Purcaro, G. (2012). *Sample preparation techniques for the determination of some food contaminants (polycyclic aromatic hydrocarbons, mineral oils and phthalates).* AGRIS. 313-356p.

64. Taynton, P., Ni, H., Zhu, C., Yu, K., Loob, S., Jin, Y., Qi, H. J., & Zhang, W. (2016). Repairable woven carbon fiber composites with full recyclability enabled by malleable polyimine networks. *Advanced Materials, 28*(15), 2904-2909.

65. Marsh, G. (2008). Reclaiming value from post-use carbon composite. *Reinforced Plastics, 52*(7), 36-39.

66. Pimenta, S., & Pinho, S. T. (2011). Recycling carbon fibre reinforced polymers for structural applications: Technology review and market outlook. *Waste management, 31*(2), 378-392.

67. Yu, K., Shi, Q., Dunn, M. L., Wang, T., & Qi, H. J. (2016). Carbon fiber reinforced thermoset composite with near 100% recyclability. *Advanced Functional Materials, 26*(33), 6098-6106.

68. Pickering, S. J. (2006). Recycling technologies for thermoset composite materials—Current status. *Composites Part A: Applied Science Manufacturing, 37*(8), 1206-1215.

69. Meyer, L. O., Schulte, K., & Grove-Nielsen, E. (2009). CFRP-recycling following a pyrolysis route: process optimization and potentials. *Journal of Composite Materials, 43*(9), 1121-1132.

70. Marsh, G. (2009). Carbon recycling: A soluble problem. *Reinforced Plastics, 53*(4), 22-27.

71. Yip, H., Pickering, S., & Rudd, C. (2002). Characterisation of carbon fibres recycled from scrap composites using fluidised bed process. *Plastics, Rubber and Composites, 31*(6), 278-282.

72. Chen, Y.-M., & Ting, J.-M. (2002). Ultra high thermal conductivity polymer composites. *Carbon, 40*(3), 359-362.

73. Tiwari, S., & Bijwe, J. (2014). Surface treatment of carbon fibers: A review. *Procedia Technology, 14*, 505-512.

74. Tang, L. G., & Kardos, J. L. (1997). A review of methods for improving the interfacial adhesion between carbon fiber and polymer matrix. *Polymer Composites, 18*(1), 100-113.

75. Pickering, S. J. (2011). Recycling thermoset composite materials. In L. Nicolais (Ed.), *Wiley Encyclopedia of Composites* (pp. 1-17). Wiley.

76. Sharma, M., Gao, S., Mäder, E., Sharma, H., Wei, L. Y., & Bijwe, J. (2014). Carbon fiber surfaces and composite interphases. *Composites Science and Technology, 102*, 35-50.

77. Tiwari, S., Bijwe, J., & Panier, S. (2011). Tribological studies on polyetherimide composites based on carbon fabric with optimized oxidation treatment. *Wear, 271*(9-10), 2252-2260.

78. Tian, H., Yao, Y., Liu, D., Li, Y., Jv, R., Xiang, G., & Xiang, A. (2019). Enhanced Interfacial Adhesion and Properties of Polypropylene/Carbon Fiber Composites by Fiber Surface Oxidation in Presence of a Compatibilizer. *Polymer Composites, 40*(S1), E654-E662.

79. Savas, L. A., Tayfun, U., & Dogan, M. (2016). The use of polyethylene copolymers as compatibilizers in carbon fiber reinforced high density polyethylene composites. *Composites Part B: Engineering, 99*, 188-195.

80. Karsli, N. G., & Aytac, A. (2011). Effects of maleated polypropylene on the morphology, thermal and mechanical properties of short carbon fiber reinforced polypropylene composites. *Materials Design, 32*(7), 4069-4073.

81. Zhou, Z., Xu, M., Yang, Z., Li, X., & Shao, D. (2014). Effect of maleic anhydride grafted polyethylene on the properties of chopped carbon fiber/wood plastic composites. *Journal of Reinforced Plastics Composites, 33*(13), 1216-1225.

82. Wong, K., Mohammed, D. S., Pickering, S., & Brooks, R. (2012). Effect of coupling agents on reinforcing potential of recycled carbon fibre for polypropylene composite. *Composites Science and Technology, 72*(7), 835-844.

83. Jawaid, M., & Khalil, H. A. (2011). Cellulosic/synthetic fibre reinforced polymer hybrid composites: A review. *Carbohydrate Polymers, 86*(1), 1-18.

84. Fu, S.-Y., Lauke, B., Mäder, E., Yue, C.-Y., Hu, X., & Mai, Y.-W. (2001). Hybrid effects on tensile properties of hybrid short-glass-fiber and short-carbon-fiber-reinforced polypropylene composites. *Journal of Materials Science, 36*(5), 1243-1251.

85. Bunsell, A., & Harris, B. (1974). Hybrid carbon and glass fibre composites. *Composites, 5*(4), 157-164.

86. Venkateshwaran, N., ElayaPerumal, A., Alavudeen, A., & Thiruchitrambalam, M. (2011). Mechanical and water absorption behaviour of banana/sisal reinforced hybrid composites. *Materials Design, 32*(7), 4017-4021.

87. Luyt, A., & Malunka, M. (2005). Composites of low-density polyethylene and short sisal fibres: the effect of wax addition and peroxide treatment on thermal properties. *Thermochimica Acta, 426*(1-2), 101-107.

88. Sreekala, M., George, J., Kumaran, M., & Thomas, S. (2002). The mechanical performance of hybrid phenol-formaldehyde-based composites reinforced with glass and oil palm fibres. *Composites Science and Technology, 62*(3), 339-353.

89. Velmurugan, R., & Manikandan, V. (2007). Mechanical properties of palmyra/glass fiber hybrid composites. *Composites Part A: Applied Science Manufacturing, 38*(10), 2216-2226.

90. Ahmed, K. S., & Vijayarangan, S. (2008). Tensile, flexural and interlaminar shear properties of woven jute and jute-glass fabric reinforced polyester composites. *Journal of Materials Processing and Technology, 207*(1-3), 330-335.

91. Crawford, R. J. (1996). Recent advances in the manufacture of plastic products by rotomoulding. *Journal of Materials Processing Technology, 56*(1), 263-271.

92. Biron, M. (2012). *Thermoplastics and Thermoplastic Composites*. William Andrew.

93. Igumenov, M., & Lavrov, N. (2017). Features of the rotational moulding of thermoplastics. *International Polymer Science Technology, 44*(10), 39-46.

94. Yan, W., Lin, R. J. T., & Bhattacharyya, D. (2006). Particulate reinforced rotationally moulded polyethylene composites – Mixing methods and mechanical properties. *Composites Science and Technology, 66*(13), 2080-2088.

95. Michaeli, W., Greif, H., & Vosseburger, F.-J. (2000). *Training in Plastics Technology: A Text and Workbook*. Munich, Germany: Hanser Verlag.

96. Wilson, K. (1994). Patent No. 2275473. Improvements in or relating to rotational moulding.

97. Spence, A., & Crawford, R. (1996). Removal of pinholes and bubbles from rotationally moulded products. *Proceedings of the Institution of Mechanical Engineers, Part B: Journal of Engineering Manufacture, 210*(6), 521-533.

98. Gogos, G. (2004). Bubble removal in rotational molding. *Polymer Engineering and Science, 44*(2), 388-394.

99. Evans, K. (1998). Rotomolding works better in a vacuum. *Plastics Technology, 44*(7), 56-57.

100. Tinevez, J. Y. (2010). Directionality plugin for ImageJ [Software].

101. Sunny, T. (2021). *Improving the performance of polypropylene matrix composite materials using engineered hemp fibre mats.* PhD thesis, University of Waikato, Hamilton, New Zealand.

102. Sabuncuoglu, B., Tanabi, H., Soete, J., & Lomov, S. V. (2020). Micro-CT analysis of deviations in fiber orientation and composite stiffness near the microvascular channels embedded in glass-fiber reinforced composites. *Composite Structures, 237*, 111896.

103. Karamov, R., Martulli, L. M., Kerschbaum, M., Sergeichev, I., Swolfs, Y., & Lomov, S. V. (2020). Micro-CT based structure tensor analysis of fibre orientation in random fibre composites versus high-fidelity fibre identification methods. *Composite Structures, 235*(111818).

104. Segal, L., Creely, J., Martin Jr, A., & Conrad, C. (1959). An empirical method for estimating the degree of crystallinity of native cellulose using the X-ray diffractometer. *Textile Research Journal, 29*(10), 786-794.

105. Stoof, D., & Pickering, K. (2018). Sustainable composite fused deposition modelling filament using recycled pre-consumer polypropylene. *Composites Part B: Engineering, 135*, 110-118.

106. Minitab "Method table for One-Way ANOVA" (2021). [Software].

107. Manalo, A. C., Wani, E., Zukarnain, N. A., Karunasena, W., & Lau, K.-t. J. (2015). Effects of alkali treatment and elevated temperature on the mechanical properties of bamboo fibre–polyester composites. *Composites Part B: Engineering, 80*, 73-83.

108. Wang, H., Postle, R., Kessler, R., & Kessler, W. (2003). Removing pectin and lignin during chemical processing of hemp for textile applications. *Textile Research Journal, 73*(8), 664-669.

109. Mishra, M. (2018). *Encyclopedia of Polymer Applications*. [3v]. Boca Raton, FL: CRC Press.

110. Kabir, M., Wang, H., Lau, K., Cardona, F., & Aravinthan, T. (2012). Mechanical properties of chemically-treated hemp fibre reinforced sandwich composites. *Composites Part B: Engineering, 43*(2), 159-169.

111. Nishiyama, Y., Johnson, G. P., & French, A. D. (2012). Diffraction from nonperiodic models of cellulose crystals. *Cellulose, 19*(2), 319-336.

112. Tserki, V., Zafeiropoulos, N., Simon, F., & Panayiotou, C. (2005). A study of the effect of acetylation and propionylation surface treatments on natural fibres. *Composites Part A: Applied Science and Manufacturing, 36*(8), 1110-1118.

113. Ouajai, S., & Shanks, R. A. (2005). Composition, structure and thermal degradation of hemp cellulose after chemical treatments. *Polymer Degradation and Stability, 89*(2), 327-335.

114. Islam, M., Pickering, K., & Foreman, N. (2010). Influence of alkali treatment on the interfacial and physico-mechanical properties of industrial hemp fibre reinforced polylactic acid composites. *Composites Part A: Applied Science, 41*(5), 596-603.

115. Prime, R. B., Bair, H. E., Vyazovkin, S., Gallagher, P. K., & Riga, A. (2009). Thermogravimetric analysis (TGA). In *Thermal Analysis of Polymers: Fundamentals and Applications* (pp. 241-317). Hoboken, NJ: John Wiley & Sons.

116. Rana, A., Mandal, A., Mitra, B., Jacobson, R., Rowell, R., & Banerjee, A. (1998). Short jute fiber-reinforced polypropylene composites: Effect of compatibilizer. *Journal of Applied Polymer Science, 69*(2), 329-338.

117. Mohanty, S., Verma, S. K., & Nayak, S. K. (2006). Dynamic mechanical and thermal properties of MAPE treated jute/HDPE composites. *Composites Science Technology, 66*(3-4), 538-547.

118. Hanana, F. E., & Rodrigue, D. (2021). Effect of particle size, fiber content, and surface treatment on the mechanical properties of maple-reinforced LLDPE produced by rotational molding. *Polymers and Polymer Composites*, *29*(5), 343-353.

119. Saheb, D. N., & Jog, J. P. (1999). Natural fiber polymer composites: A review. *Advances in Polymer Technology: Journal of the Polymer Processing Institute, 18*(4), 351-363.

120. Ortega, Z., Monzón, M., Benítez, A., Kearns, M., McCourt, M., & Hornsby, P. J. (2013). Banana and abaca fiber-reinforced plastic composites obtained by rotational molding process. *Materials and Manufacturing Processes 28*(8), 879-883.

121. Verdaguer, A., & Rodrigue, D. (2014) Effect of surface treatment on the mechanical properties of wood-plastics composites produced by dry-blending. *Proceedings of the 72nd Annual Technical Conference & Exhibition, Society of Plastics Engineers, Las Vegas NV* (pp. 28-30).

122. Yang, H.-S., Wolcott, M. P., Kim, H.-S., Kim, S., & Kim, H.-J. (2007). Effect of different compatibilizing agents on the mechanical properties of lignocellulosic material filled polyethylene bio-composites. *Composite Structures, 79*(3), 369-375.

123. Spence, A., & Crawford, R. (1996). The effect of processing variables on the formation and removal of bubbles in rotationally molded products. *Polymer Engineering and Science, 36*(7), 993-1009.

124. Little, J. E., Yuan, X., & Jones, M. I. (2012). Characterisation of voids in fibre reinforced composite materials. *NDT E International, 46*, 122-127.

125. Castellanos, D., Martin, P. J., Butterfield, J., McCourt, Kearns, M., & Cassidy, P. (2020). Sintering and densification of fibre reinforcement in polymers during rotational moulding. *Procedia Manufacturing, 47*, 980-986.

126. Rao, M. A., & Throne, J. L. (1972). Principles of rotational molding. *Polymer Engineering and Science, 12*(4), 237-264.

127. Ogila, K., Shao, M., Yang, W., & Tan, J. J. E. P. L. (2017). Rotational molding: A review of the models and materials. *Express Polymer Letters, 11*(10), 778-798.

128. Greco, A., & Maffezzoli, A. (2004). Powder-shape analysis and sintering behavior of high-density polyethylene powders for rotational molding. *Journal of Applied Polymer Science, 92*(1), 449-460.

129. Mehdikhani, M., Gorbatikh, L., Verpoest, I., & Lomov, S. V. (2019). Voids in fiber-reinforced polymer composites: A review on their formation, characteristics, and effects on mechanical performance. *Journal of Composite Materials, 53*(12), 1579-1669.

130. Weber, E., Fernandez, M., Wapner, P., & Hoffman, W. (2010). Comparison of X-ray micro-tomography measurements of densities and porosity principally to values measured by mercury porosimetry for carbon–carbon composites. *Carbon 48*, 2151-2158.

131. Berzin, F., Beaugrand, J., Dobosz, S., Budtova, T., & Vergnes, B. (2017). Lignocellulosic fiber breakage in a molten polymer. Part 3. Modeling of the dimensional change of the fibers during compounding by twin screw extrusion. *Composites Part A: Applied Science Manufacturing, 101*, 422-431.

132. Ku, H., Wang, H., Pattarachaiyakoop, N., & Trada, M. (2011). A review on the tensile properties of natural fiber reinforced polymer composites. *Composites Part B: Engineering, 42*(4), 856-873.

133. Del Angel, C., Morales, A. B., Navarro-Pardo, F., Lozano, T., Lafleur, P. G., Sanchez-Valdes, S., Martinez-Colunga, G., Ramirez-Vargas, E., Alonso, S., & Zitzumbo, R. (2015). Mechanical and rheological properties of polypropylene/bentonite composites with stearic acid as an interface modifier. *Journal of Applied Polymer Science, 132*(30), 42264.

134. Dányádi, L., Móczó, J., & Pukánszky, B. (2010). Effect of various surface modifications of wood flour on the properties of PP/wood composites. *Composites Part A: Applied Science and Manufacturing, 41*(2), 199-206.

135. Samsudin, M., Ishak, Z. M., Jikan, S., Ariff, Z., & Ariffin, A. (2006). Effect of filler treatments on rheological behavior of calcium carbonate and talc-filled polypropylene hybrid composites. *Journal of Applied Polymer Science, 102*(6), 5421-5426.

136. Hernández, Y., Lozano, T., Morales-Cepeda, A. B., Navarro-Pardo, F., Angeles, M. E., Morales-Zamudio, L., Melo-Banda, J. A., Sánchez-Valdes, S., Martínez-Colunga, G., & Rodríguez, F. (2019). Stearic acid as interface modifier and lubricant agent of the system: Polypropylene/calcium carbonate nanoparticles. *Polymer Engineering & Science, 59*(s2), E279-E285.

137. Gorjan, L., Galusca, C., Sami, M., Sebastian, T., & Clemens, F. (2020). Effect of stearic acid on rheological properties and printability of ethylene vinyl acetate based feedstocks for fused filament fabrication of alumina. *Additive Manufacturing, 36*(101391).

138. Liu, S.-J., & Chen, C.-F. (2000). Optimisation of bubble size in qc rotationally moulded parts. *Plastics, Rubber and Composites, 29*(8), 411-416.

139. Oliveira Santos, R. P., Castro, D. O., Ruvolo-Filho, A. C., & Frollini, E. (2014). Processing and thermal properties of composites based on recycled PET, sisal fibers, and renewable plasticizers. *Journal of Applied Polymer Science, 131*(12), https://doi.org/10.1002/app.40386.

140. Baumer, M. I., Leite, J. L., & Becker, D. (2014). Influence of calcium carbonate and slip agent addition on linear medium density polyethylene processed by rotational molding. *Materials Research, 17*(1), 130-137.

141. Paul, S. A., Oommen, C., Joseph, K., Mathew, G., & Thomas, S. (2010). The role of interface modification on thermal degradation and crystallization behavior of composites from commingled polypropylene fiber and banana fiber. *Polymer Composites, 31*(6), 1113-1123.

142. Paul, S. A., Joseph, K., Mathew, G. G., Pothen, L. A., & Thomas, S. (2010). Influence of polarity parameters on the mechanical properties of composites from polypropylene fiber and short banana fiber. *Composites Part A: Applied Science and Manufacturing, 41*(10), 1380-1387.

143. Torres, F., & Cubillas, M. (2005). Study of the interfacial properties of natural fibre reinforced polyethylene. *Polymer Testing, 24*(6), 694-698.

144. León, L. D. V. E., Escocio, V. A., Visconte, L. L. Y., Junior, J. C. J., & Pacheco, E. B. A. V. (2020). Rotomolding and polyethylene composites with rotomolded lignocellulosic materials: A review. *Journal of Reinforced Plastics and Composites, 39*(11-12), 459-472.

145. Dickson, A. R., Even, D., Warnes, J. M., & Fernyhough, A. (2014). The effect of reprocessing on the mechanical properties of polypropylene reinforced with wood pulp, flax or glass fibre. *Composites Part A: Applied Science and Manufacturing, 61*, 258-267.

146. Harper, L., Turner, T., Warrior, N., & Rudd, C. (2006). Characterisation of random carbon fibre composites from a directed fibre preforming process: The effect of fibre length. *Composites Part A: Applied Science Manufacturing, 37*(11), 1863-1878.

147. Silva, C. A., Viana, J. C., van Hattum, F. W., & Cunha, A. M. (2008). Fiber orientation in injection molding with rotating flow. *Polymer Engineering & Science, 48*(2), 395-404.

148. Sun, X., Lasecki, J., Zeng, D., Gan, Y., Su, X., & Tao, J. (2015). Measurement and quantitative analysis of fiber orientation distribution in long fiber reinforced part by injection molding. *Polymer Testing, 42*, 168-174.

149. Donnet, J.-B., & Bansal, R. C. (1998). *Carbon Fibers*. (3rd ed.). New York: CRC Press.

150. Rahaman, M. S. A., Ismail, A. F., & Mustafa, A. (2007). A review of heat treatment on polyacrylonitrile fiber. *Polymer Degradation and Stability, 92*(8), 1421-1432.

151. Tamburri, E., Orlanducci, S., Terranova, M., Valentini, F., Palleschi, G., Curulli, A., Brunetti, F., Passeri, D., Alippi, A., & Rossi, M. (2005). Modulation of electrical properties in single-walled carbon nanotube/conducting polymer composites. *Carbon, 43*(6), 1213-1221.

152. Shin, S., Jang, J., Yoon, S.-H., & Mochida, I. (1997). A study on the effect of heat treatment on functional groups of pitch based activated carbon fiber using FTIR. *Carbon, 35*(12), 1739-1743.

153. Moreno-Castilla, C., López-Ramón, M., & Carrasco-Marın, F. (2000). Changes in surface chemistry of activated carbons by wet oxidation. *Carbon, 38*(14), 1995-2001.

154. Zhang, Y., Zhu, S., Liu, Y., Yang, B., & Wang, X. (2015). The mechanical and tribological properties of nitric acid-treated carbon fiber-reinforced polyoxymethylene composites. *Journal of Applied Polymer Science, 132*(15), https://doi.org/10.1002/app.41812.

155. Feng, N., Wang, X., & Wu, D. (2013). Surface modification of recycled carbon fiber and its reinforcement effect on nylon 6 composites: Mechanical properties, morphology and crystallization behaviors. *Current Applied Physics, 13*(9), 2038-2050.

156. Su, F.-h., Zhang, Z.-z., Wang, K., Jiang, W., & Liu, W.-m. (2005). Tribological and mechanical properties of the composites made of carbon fabrics modified with various methods. *Composites Part A: Applied Science and Manufacturing, 36*(12), 1601-1607.

157. Mutje, P., Lopez, A., Vallejos, M., Lopez, J., & Vilaseca, F. (2007). Full exploitation of *Cannabis sativa* as reinforcement/filler of thermoplastic composite materials. *Composites Part A: Applied Science Manufacturing, 38*(2), 369-377.

158. Akonda, M. H., Lawrence, C. A., & Weager, B. M. (2012). Recycled carbon fibre-reinforced polypropylene thermoplastic composites. *Composites Part A: Applied Science and Manufacturing, 43*(1), 79-86.

159. Dhakal, H., Zhang, Z., Guthrie, R., MacMullen, J., & Bennett, N. (2013). Development of flax/carbon fibre hybrid composites for enhanced properties. *Carbohydrate Polymers, 96*(1), 1-8.

160. Andrzejewski, J., Krawczak, A., Wesoły, K., & Szostak, M. (2020). Rotational molding of biocomposites with addition of buckwheat husk filler. Structure-property correlation assessment for materials based on polyethylene (PE) and poly (lactic acid) PLA. *Composites Part B: Engineering, 202*, 108410.

161. Arribasplata-Seguin, A., Quispe-Dominguez, R., Tupia-Anticona, W., & Acosta-Sullcahuamán, J. (2021). Rotational molding parameters of wood-plastic composite materials made of recycled high density polyethylene and wood particles. *Composites Part B: Engineering, 217*, 108876.